36th Annual Condensed Matter and Materials Meeting

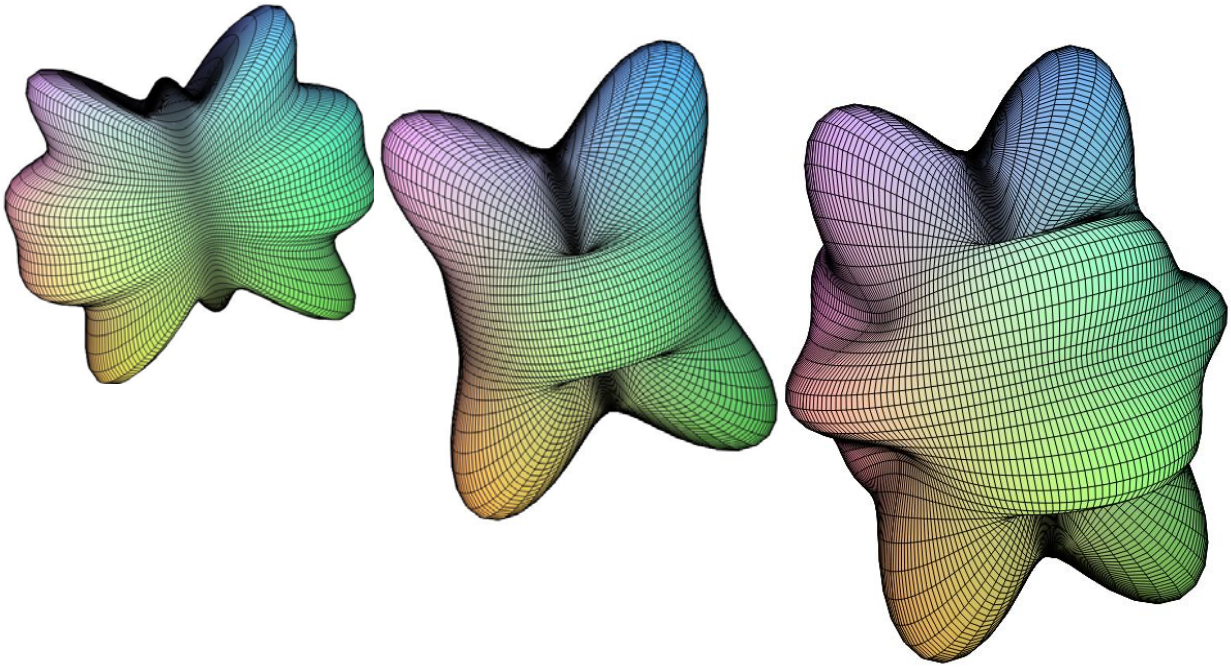

Wagga 2012

Charles Sturt University, Wagga Wagga, NSW
31st January – 3rd February, 2012

Australian and New Zealand Institutes of Physics

36th Annual Condensed Matter and Materials Meeting

Charles Sturt University, Wagga Wagga, NSW

31st January – 3rd February, 2012

CONFERENCE HANDBOOK

ISBN: 978-0-646-57071-6

WW2012 Organising Committee

Wayne Hutchison
Annemieke Mulders
Hans Riesen
Heiko Timmers
Stewart Campbell
Glen Stewart

School of Physical, Environmental and Mathematical Sciences
The University of New South Wales, Canberra

http://pems.unsw.adfa.edu.au/cmm/2012

2012 SPONSORS

ammrf
Australian Microscopy & Microanalysis Research Facility

ammrf.org.au

CRYOGENIC
CRYOGENIC LIMITED

cryogenicaus.com

scitek
total vacuum solutions

www.scitek.com.au

Australian Government

ansto

www.ansto.gov.au

John Morris Scientific
Service plus Solutions

www.johnmorris.com.au

UNSW
THE UNIVERSITY OF NEW SOUTH WALES

CANBERRA

www.unsw.adfa.edu.au

DOMO TECHNICA

www.domotech.com.au

Nucletron

rob.saunders@au.nucletron.com

WWTZ

pems.unsw.adfa.edu.au/staff/profiles/campbell

WW2012 CONTENTS

Cover
Meet the "Wagga-poles"! The magnetic *dipole* and electric *quadrupole* are relatively familiar to us. However, resonant (soft) x-ray diffraction is introducing us to the extended family of higher order multipoles with their much less pronounceable names (such as the *hexadecapole* and the *hexacontatetrapole*). From left to right, the images show the anisotropy of the 4*f* electron density for rare earth ions of the borocarbide series (RB_2C_2) with R = dysprosium, holmium and terbium. As reported by Andrew Princep and collaborators, the higher order multipoles are vitally important in the description of the physics exhibited by these compounds (J Physics: Condensed Matter, 2011 & 2012)

WW2012 MAPS

Wagga Wagga and the location of the Charles Sturt University campus

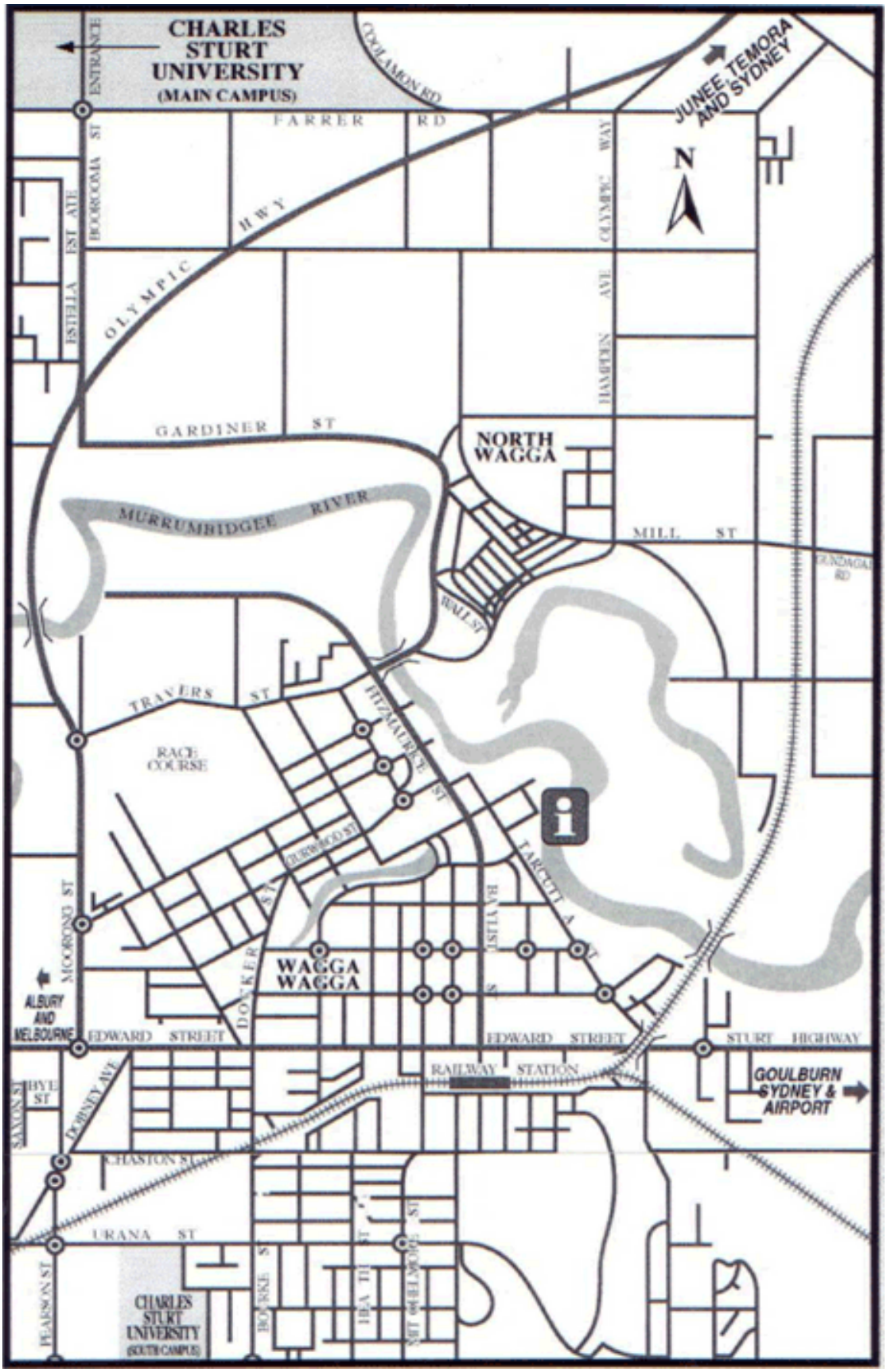

Charles Sturt University

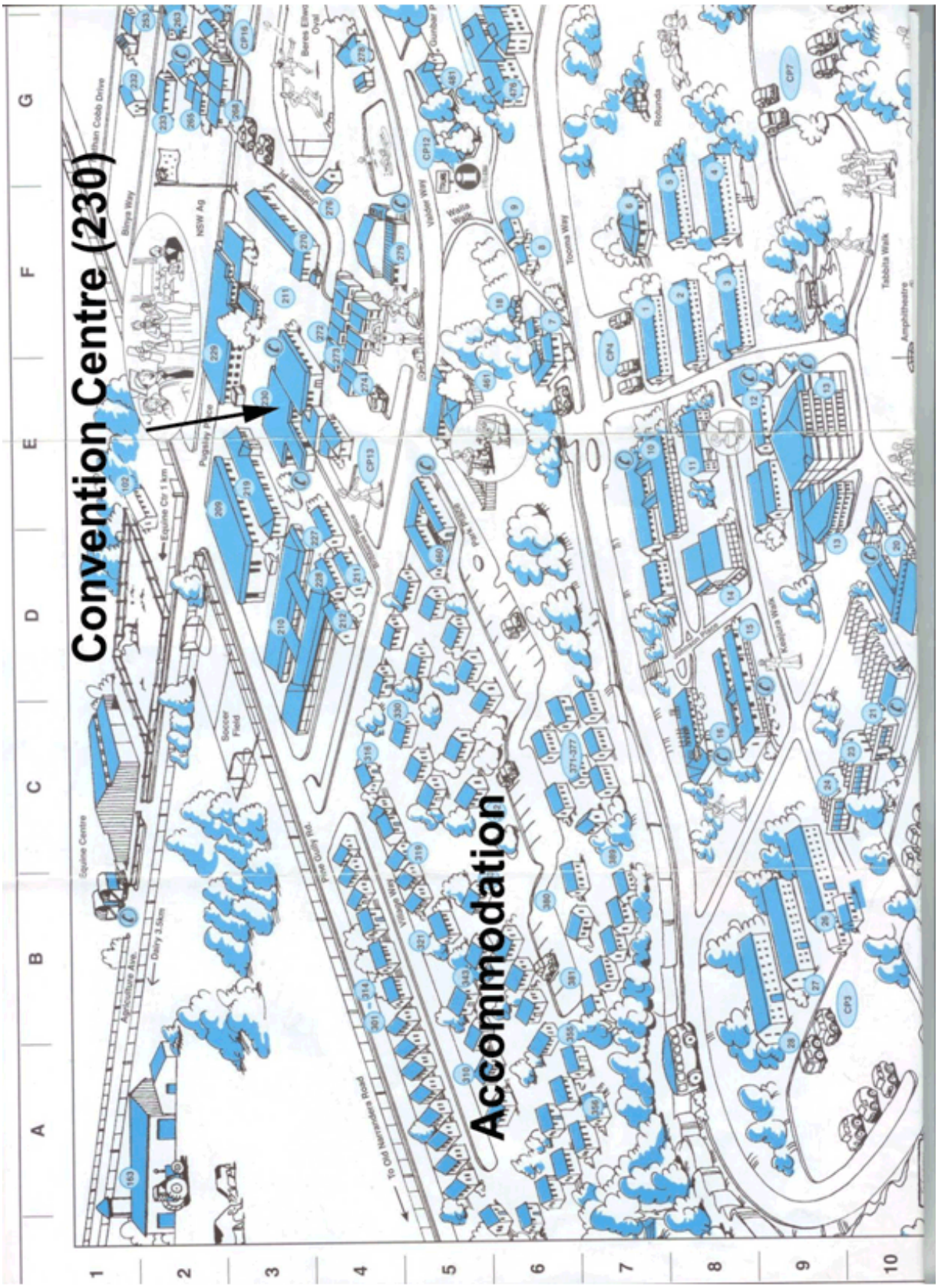

WW2012 THE CMM GROUP WEB SITE

Welcome to the "Wagga" community

Just by attending the annual Condensed Matter and Materials (CMM) Meeting you are a member of the CMM topical group of the Australian Institute of Physics (AIP). There are no forms or membership fees involved.

Take a look at the CMM Group web site

It can be accessed from the AIP national web site (**www.aip.org.au**) by clicking on **AIP Groups** listed under "Related Groups" in the column at the left of the home page and then selecting **Condensed Matter and Materials Group (CMM)**. Alternatively, you can go directly to **pems.unsw.adfa.edu.au/cmm**.

Please share your favourite "Wagga" experiences

If you have some special group images of you and colleagues, interesting events and stories from previous "Waggas", please share them with us by passing them on to Glen Stewart (**g.stewart@adfa.edu.au**) who will have them incorporated into the history section of the CMM Group web site. Please include in your e-mail the year of the meeting and the names of those "Waggarites" you are able to identify in the images.

Wagga 1978 (taken by John Collins)

Wagga 2009

Perhaps you go all the way back to the good old days of sweltering lecture theatres without air conditioning when the blokes loved their beards, floral body shirts and Bermuda socks. There must be some great yarns and photographs lying around in the backs of minds and desk drawers, respectively.

WW2012 INFORMATION FOR PARTICIPANTS

Scientific Program:

All poster sessions and lectures will be held at the Convention Centre. Chairpersons and speakers are asked to adhere closely to the schedule for the oral program. A PC laptop computer and data projector, overhead projector, pointer and microphone will be available. Please check that your presentation is compatible with the facilities provided as early as possible. Posters should be mounted as early as possible. Please remove your Wednesday session posters by early Thursday morning and your Thursday session posters by the close of the program on Friday.

Logistics:

Please wear your name tag at all times. Registration and all other administrative matters should be addressed to the registration desk or a committee member. For lost keys or if locked out of your room from 0900 to 1700, contact Shiralee Hillam at the Events Office for assistance 6933 4974; after hours, contact the Accommodation and Security Office near the corner of Valder Way and Park Way or phone them at 6933 2288. Delegates must check out of their rooms on Friday morning, before 10:00.

Meals, Refreshments and Recreational Facilities:

All meals will be served in the dining room, except the Conference Dinner on Wednesday 7 February, which will be held in the Convention Centre. You will receive a dining room pass on registration and a ticket to the Conference Dinner. The dining room pass must be produced at every meal. It may also be required as identification for use of all other campus facilities, which are at your disposal.

Morning and afternoon tea will be served each day, as indicated in the timetable. Coffee and tea-making facilities are also available in the Common Room of each residence. In addition, on arrival on Tuesday afternoon and for the poster sessions, drinks will be available from the Conference Bar.

The swimming pool is open on weekdays from 06:00 until 21:00, as are the adjacent gymnasium and squash courts. Tennis courts opposite the oval are also available. A wide range of facilities such as exercise bikes, weight training, table tennis and basketball are available in the gymnasium. All of the facilities are free, i.e. covered by your registration fee.

Convention Centre Contact Numbers:

Registration Desk Phone	(02) 6933 4989
Convention Centre Office	Phone (02) 6933 2606 Fax (02) 6933 2643
Events Office Phone	(02) 6933 4974
After hours Emergencies, Accommodation and Security Office Phone	(02) 6933 2288

Internet access: wireless internet access will be available within the Convention Centre (see http://www.csu.edu.au/division/dit/wireless/index.htm)

Nucletron Pty Ltd
16 Little Commodore Street
Newtown, NSW 2042

Nucletron

Rob Saunders
email: rob.saunders@au.nucletron.com
ph.: +61 2 9517 1300
fax: +61 2 9517 1311

rob.saunders@au.nucletron.com

Domo-Technica
PO Box 7077
Silverwater, NSW 2128

DOMO TECHNICA

Michael Anderson
email: Michael@domotech.com.au
ph.: +61 2 9748 6955
fax: +61 2 9748 7855

www.domotech.com.au

John Morris Scientific
PO Box 447
Willoughby, NSW 2068

John Morris Scientific
Service plus Solutions

Vitali Polonski
email: vitalip@johnmorris.com.au
ph.: 1800 251 799
fax: 1800 446926

www.johnmorris.com.au

WW2012 EXHIBITORS

Scitek Australia Pty Limited
Unit 4/12 Chaplin Drive
Lane Cove West
Sydney, NSW 2066

scitek
total vacuum solutions

Craig MARSHALL
email: craig@scitek.com.au
ph.: +61 2 9420 0477
mobile: 0413 756 226
fax.:+61 2 9418 3540

www.scitek.com.au

Cryogenic Limited
5/187 Bourke Street
Darlinghurst, NSW 2010

CRYOGENIC
CRYOGENIC LIMITED

Jack Clements
email: Jack@cryogenicaus.com
ph.: 0403 940 823

cryogenicaus.com

UNSW CANBERRA

Wagga2012 – Shirt*

Stewart Campbell, UNSW, Canberra (Sponsor)

Never Stand Still

With Grateful Thanks to Andrew Princep - Help with Graphic Designer, Shirt Supplier

- Wagga Wagga 1977 – Inaugural Meeting
- Wagga2012 - Shirt
  - Mark the Continuing Series
- Emblem
  - WW77 with Arrows
    - Search all Directions
    - Echo of AIP Logo
  - Green and Gold

- *Wagga2012 - Shirt
  - Available for Purchase
  - Registration Desk - Limited Numbers

2012 PARTICIPANTS (at 20th Jan 2012)

	participant		affiliation	email
1	Adura	**Abiona**	UNSW Canberra	Adurafimihan.Abiona@student.adfa.edu.au
2	Rose	**Ahlefeldt**	ANU	rla111@physics.anu.edu.au
3	Muhammad	**Ahmed**	RMIT	hamiid_9@yahoo.com
4	Zakiya	**Al-Azri**	Auckland	zala006@aucklanduni.ac.nz
5	Michael	**Anderson**	Domo-Technica	michael@domotech.com.au
6	Bakir	**Babic**	NMI	Bakir.Babic@measurement.gov.au
7	Frederik	**Bachhuber**	Auckland	frederik.bachhuber@gmail.com
8	Wei	**Bao**	Renmin (China)	w.bao22@gmail.com
9	John	**Bartholomew**	ANU	jgb111@physics.anu.edu.au
10	Tim	**Bastow**	CSIRO	Tim.Bastow@csiro.au
11	Sarah	**Beaven**	ANU	sarah.beavan@anu.edu.au
12	Joel	**Bertinshaw**	UNSW	joelbertinshaw@gmail.com
13	Graham	**Bowden**	Southampton	G.Bowden@soton.ac.uk
14	Jodie	**Bradby**	ANU	jodie.bradby@anu.edu.au
15	Sebastion	**Brueck**	ANSTO	s.brueck@unsw.edu.au
16	Stewart	**Campbell**	UNSW Canberra	S.Campbell@adfa.edu.au
17	John	**Cashion**	Monash	john.cashion@monash.edu
18	Qinjun	**Chen**	Wollongong	qc691@uowmail.edu.au
19	Jack	**Clements**	Cryogenic	jack@cryogenicaus.com
20	Jared	**Cole**	RMIT	jared.cole@rmit.edu.au
21	Stephen	**Collocott**	CSIRO	Stephen.Collocott@csiro.au
22	Evan	**Constable**	Wollongong	ec028@uowmail.edu.au
23	David	**Cortie**	ANSTO	davecortie@hotmail.com
24	Geoffrey	**Cousland**	Sydney	g.cousland@physics.usyd.edu.au
25	Jeffrey	**Davis**	Swinburne	JDavis@groupwise.swin.edu.au
26	Guochu	**Deng**	ANSTO	guochu@ansto.gov.au
27	Tim	**DuBois**	RMIT	Timothy.DuBois@rmit.edu.au
28	John	**Dunlop**	CSIRO	john.viv@optusnet.com.au

29	Kate	**Ferguson**	ANU	katherine.ferguson@anu.edu.au
30	Trevor	**Finlayson**	Melbourne	trevorf@unimelb.edu.au
31	Kate	**Fox**	Melbourne	kfox@unimelb.edu.au
32	Xuanwen	**Gao**	Wollongong	xg973@uowmail.edu.au
33	Heike	**Ulrich**	UNSW	
34	Jean	**Goder**	RMIT	s3156057@student.rmit.edu.au
35	Darren	**Goossens**	ANU	goossens@rsc.anu.edu.au
36	Paul	**Graham**	UNSW	p.graham@student.unsw.edu.au
37	Stephen	**Harker**	UNSW Canberra	sjharker@netspace.net.au
38	Marcus	**Hennig**	ANSTO	marcus.hennig@gmx.de
39	Jan	**Herrmann**	NMI	Jan.Herrmann@measurement.gov.au
40	Anita	**Hill**	CSIRO	Anita.Hill@csiro.au
41	Tadahiko	**Hirai**	CSIRO	Tadahiko.Hirai@csiro.au
42	Michael	**Holt**	UNSW	michael.holt@student.unsw.edu.au
43	Jessica	**Hudspeth**	ANU	jessica.hudspeth@anu.edu.au
44	Wayne	**Hutchison**	UNSW Canberra	w.hutchison@adfa.edu.au
45	Paolo	**Imperia**	ANSTO	plo@ansto.gov.au
46	Ian	**Jackson**	ANU	Ian.Jackson@anu.edu.au
47	Jan	**Jeske**	RMIT	jan.jeske@rmit.edu.au
48	Charles	**Johnson**	UTSI	cjohnson@utsi.edu
49	Vedran	**Jovic**	Auckland	vjov001@aucklanduni.ac.nz
50	Sidhar Kumar	**Kannam**	Swinburne	urssrisri@gmail.com
51	Bill	**Kemp**	UNSW Canberra	w.kemp@adfa.edu.au
52	Mustafa	**Keskin**	Erciyes (Turkey)	keskin@erciyes.edu.tr
53	Yakov	**Kulik**	UNSW	ykulik@phys.unsw.edu.au
54	Rakesh	**Kumar**	UNSW	rakesh.kumar@unsw.edu.au
55	Yasar	**Kutuvantavida**	MacDiarmid	y.kutuvantavida@irl.cri.nz
56	Sidney	**Lang**	Ben-Gurion (Israel)	lang@bgu.ac.il
57	Hal	**Lee**	ANSTO	WaiTung.Lee@ansto.gov.au
58	Lucia	**Lepodise**	Wollongong	lml533@uowmail.edu.au
59	Roger	**Lewis**	Wollongong	roger@uow.edu.au
60	Tommy	**Li**	UNSW	tommy.li1@unsw.edu.au
61	Klaus-Dieter	**Liss**	ANSTO	kdl@ansto.gov.au

62	Hua	**Liu**	Wollongong	hua@uow.edu.au
63	Yanyan	**Liu**	UNSW Canberra	Yanyan.Liu@student.adfa.edu.au
64	Zhiqiang	**Liu**	UNSW Canberra	Zhiqiang.Liu@student.adfa.edu.au
65	David	**Maddison**		maddison@connexus.net.au
66	Craig	**Marshall**	Sci-Tek	craig@scitek.com.au
67	Sara	**Marzban**	ANU	sara.marzban@anu.edu.au
68	Philip	**McGill**	Auckland	pmcg027@aucklanduni.ac.nz
69	Garry	**McIntrye**	ANSTO	gmi@ansto.gov.au
70	Chris	**McNeil**	Monash	christopher.mcneill@monash.edu
71	David	**Miller**	UNSW	d.miller@sydney.edu.au
72	Richard	**Mole**	ANSTO	richardm@ansto.gov.au
73	Tapasi	**Mukherjee**	RMIT	s3266761@student.rmit.edu.au
74	Annemieke	**Mulders**	UNSW Canberra	A.Mulders@adfa.edu.au
75	Mallikharjuna	**Mutthavarapu**	Wollongong	mmr716@uowmail.edu.au
76	Naren	**Narayanan**	UNSW Canberra	n.narayanan@ifw-dresden.de
77	Suresh	**Narayanaswamy**	MacDiarmid	s.narayan@irl.cri.nz
78	Jaan	**Oitmaa**	UNSW	j.oitmaa@unsw.edu.au
79	Anna	**Paradowska**	ANSTO	anp@ansto.gov.au
80	Randolph	**Pax**	UNSW Canberra	rpax@uqconnect.net
81	Vitali	**Polonski**	John Morris Sci	vitali@johnmorris.com.au
82	Don	**Price**	CSIRO	Don.Price@csiro.au
83	Andrew	**Princep**	UNSW Canberra	Andrew.Princep@student.adfa.edu.au
84	Fini	**Rafi**	RMIT	nurafiniassila@gmail.com
85	Milos	**Rancic**	ANU	u4395265@anu.edu.au
86	Marlene	**Read**	UNSW	mnr@phys.unsw.edu.au
87	Nicole	**Reynolds**	UNSW	n.reynolds@unsw.edu.au
88	Rob	**Robinson**	ANSTO	robert.robinson@ansto.gov.au
89	Pauline	**Rovillain**	UNSW	p.rovillain@unsw.edu.au
90	Robert	**Saunders**	Nucletron	rob.saunders@au.nucletron.com
91	Jeffrey	**Sellar**	Monash	Jeff.Sellar@monash.edu
92	Igor	**Shvab**	Swinburne	ISHVAB@groupwise.swin.edu.au
93	Jackson	**Smith**	RMIT	s3199683@student.rmit.edu.au
94	Tilo	**Soehnel**	Auckland	t.soehnel@auckland.ac.nz
95	Julian	**Steele**	Wollongong	js598@uowmail.edu.au

96	Jibu	**Stephen**	MacDiarmid	jibustephen@gmail.com
97	Glen	**Stewart**	UNSW Canberra	g.stewart@adfa.edu.au
98	Oleg	**Sushkov**	UNSW	sushkov@phys.unsw.edu.au
99	Lisa	**Thoennessen**	ANSTO	lt063@uowmail.edu.au
100	Heiko	**Timmers**	UNSW Canberra	H.Timmers@adfa.edu.au
101	Gordon	**Troup**	Monash	gordon.troup@monash.edu
102	Clemens	**Ulrich**	UNSW	c.ulrich@unsw.edu.au
103	Lou	**Vance**	ANSTO	erv@ansto.gov.au
104	Tesfaye	**Yigzawe**	Swinburne	TYIGZAWE@groupwise.swin.edu.au
105	Barran	**Yildirim**	UNSW Canberra	Baran.Yildirim@student.adfa.edu.au
106	Mingang	**Zhang**	Wollongong	mingang@uow.edu.au
107	Manjin	**Zhong**	ANU	gxz111@physics.anu.edu.au

WW2012 OVERALL TIMETABLE

Tuesday 31 January

16:00 -	Registration desk open
16:00 – 18:00	*Conference bar open*
18:00 – 19:30	*Dinner*
19:00 -	Posters wp1-wp37 to be mounted

Wednesday 1 February

07:30 – 08:30	*Breakfast*
09:00 – 09:10	Conference opening
09:10 – 10:30	Oral Session: Papers wo1-wo3
10:30 – 11:00	*Morning tea*
11:00 – 12:30	Oral Session: Papers wo4-wo7
12:30 – 14:00	*Lunch*
14:00 – 14:50	Oral Session: Papers wo9, tp3
14:50 – 15:30	Poster Advertisement wp1-wp37
15:30 – 16:00	*Afternoon Tea*
16:00 – 18:00	Poster Session: Papers wp1-wp37
18:00 -	Posters: tp1-tp37 to be mounted
16:30 – 18:00	*Conference bar open*
18:30 – 22:00	Conference Dinner (sponsored by ANSTO)

Thursday 2 February

07:30 – 08:30	*Breakfast*
09:00 – 10:30	Oral Session: Papers to1-to4
10:30 – 11:00	*Morning tea*
11:00 – 12:30	Oral Session: Papers wo8, to6-to8
12:30 – 14:00	*Lunch*
14:00 – 15:00	Oral Session: Papers to9-to10
15:00 – 15:30	Poster Advertisement tp1-tp37
15:30 – 16:00	*Afternoon Tea*
16:00 – 18:00	Poster Session: tp1-tp37
16:30 – 18:00	*Conference bar open*
18:00 – 19:30	*Dinner*
19:30 – 22:00	Trivia Quiz (Lindsay Davis Cup)

Friday 3 February

07:30 – 08:30	*Breakfast*
09:00 – 10:30	Oral Session: Papers fo1-fo4
10:30 – 11:00	*Morning tea*
11:00 – 12:20	Oral Session: Papers fo5-fo7
12:20 – 12:40	Presentations and Closing
12:40 – 14:00	*Lunch*

Specimen Preparation
Biological & Materials
Cell Culturing & Molecular Preparation
Thermomechanical Processing

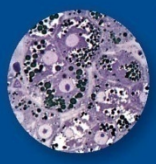

Light & Laser Optics
Confocal & Fluorescence Microscopy
Flow Cytometry & Cell Sorting
Live-cell Imaging
Vibrational & Laser Spectroscopy
Laser Microdissection

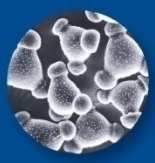

Scanning Electron Microscopy
Imaging & Analytical Spectroscopy
In-situ Imaging & Testing
Cathodoluminescence

Transmission Electron Microscopy
Imaging & Analytical Spectroscopy
Cryo Techniques & Tomography
Phase & Z-contrast Imaging
Diffraction

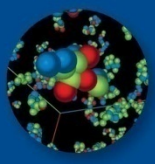

Advanced Ion Platforms
Nanoscale Mass Spectroscopy
Atom Probe Tomography
Ion Milling & Machining
Ion Implantation

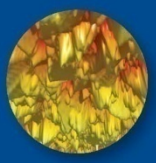

Scanned Probe Techniques
Atomic Force Microscopy
Scanning Tunneling Microscopy
Near-field Scanning Optical Microscopy

X-ray Technologies
X-ray Diffraction
X-ray Fluorescence
X-ray Micro- and Nanotomography

Visualisation and Simulation
Computed Spectroscopy
Computed Diffraction
Image Simulation, Analysis & Data Mining

ammrf

Australian
Microscopy & Microanalysis
Research Facility

ENABLING WORLD-CLASS RESEARCH

The AMMRF is a national grid of equipment, instrumentation and expertise that provides nanostructural characterisation capability and services.

This collaborative facility enables discovery and innovation in fields from engineering to agriculture, healthcare to archaeology.

Our world-class infrastructure is available to all Australian researchers.

With our constant focus on improving access, we are sharing our expertise through online tools.

TECHNIQUE FINDER

An online tool to help you identify the appropriate microscopy technique to answer your research questions. You will find the contact details of the relevant expert staff, who will guide you through the planning, training, data collection and interpretation stages of your experiment.

MYSCOPE

Innovative training for advanced research comprising e-learning modules that help new users progress on our sophisticated instruments.

CONTACT US

AMMRF Headquarters
Madsen Building (F09)
The University of Sydney
NSW 2006 Australia

t: +61 2 9351 2351
f: +61 2 9351 7682
e: info@ammrf.org.au

ammrf.org.au

A4_PressAd_CondMatterConf.indd 1 20/01/12 11:59 AM

WW2012 PROGRAM

Tuesday 31 January

16:00 - Registration desk open
16:00 – 18:00 Conference bar open
18:00 – 19:30 Dinner

Wednesday 1 February

09:00 – 09:10 **Opening:** ***Wayne Hutchison, UNSW Canberra***

09:10 – 10:30 **Chairperson:** ***Annemieke Mulders, UNSW Canberra***

09:10 – 09:40 wo1 Nanostructured Materials for Efficient Performance *INVITED*
Anita Hill, CSIRO Materials Science and Engineering, Clayton

09:40 – 10:00 wo2 Investigating Short-Range Order in Triglycine Sulphate using X-ray and Neutron Diffuse Scattering
Jessica Hudspeth, Australian National University

10:00 – 10:30 wo3 Microstructural-property relations in brittle materials: from A to Z
Jodie Bradby, Australian National University *INVITED*

10:30 – 11:00 **Morning tea**

11:00 – 12:30 **Chairperson:** ***Roger Lewis, University of Wollongong***

11:00 – 11:30 wo4 Superconducting phase qubits and coherent defects: Unravelling the mystery of two-level fluctuators *INVITED*
Jared Cole, RMIT University

11:30 – 11:50 wo5 Fabrication, Characterization and Applications of $Si_{1-x}Ti_xO_2$ (x = 0-1) Inverse Opal Photonic Crystals
Zakiya Al-Azri, University of Auckland

11:50 – 12:10 wo6 The Effects of Optical Intensity and Excited State Quenchers on the Photostability of Electro-Optic Chromophores
Yasar Kutuvantavida, Industrial Research Ltd, New Zealand

12:10 – 12.30 wo7 Photomodulated Reflectance of GaAs and p-type GaAs:Be
Julian Steele, University of Wollongong

12:30 – 14.00 **Lunch**

14:00 – 15:30 **Chairperson:** ***Heiko Timmers, UNSW Canberra***

14:00 – 14:30 wo9 Mapping of Domain Orientation and Molecular Order in Polycrystalline Semiconducting Polymer Films with Soft X-Ray Microscopy
Chris McNeill, Monash University *INVITED*

14:30 – 14:50 tp3 Development of novel visible-light driven photocatalysts for hydrogen production
Vedran Jovic, University of Auckland

14:50 – 15:30 Poster Advertisement wp1-wp37: selected 2 minute talks

15:30 – 16:00 **Afternoon Tea**

16:00 – 18:00 **Poster Session:** wp1-wp37

18:30 – 22:00 **Conference Dinner (sponsored by ANSTO)**
A Brief history of Quasicrystals *INVITED*
Darren Goossens, ANU

Thursday 2 February

09:00 – 10:30		**Chairperson: *John Barthelomew, ANU***
09:00 – 09:30	to1	Advanced materials for lithium rechargeable batteries, supercapacitors and hydrogen storage *Hua Kun Liu, University of Wollongong* *INVITED*
09:30 – 09:50	to2	Positron Annihilation Lifetime Spectroscopy within CAMS *Lou Vance, ANSTO*
09:50 – 10:10	to3	Effect of protein on electrochemical properties of diamond *Kate Fox, University of Melbourne*
10:10 – 10:30	to4	Dynamics of Globular Proteins in Crowded Electrolyte Solutions *Marcus Hennig, ANSTO*
10:30 – 11:00		**Morning tea**
11:00 – 12:30		**Chairperson: *Oleg Sushkov, UNSW***
11:00 – 11:30	wo8	Neutron Scattering Study on the Fe-based High-Tc Superconductors *Wei Bao, Renmin Universit of China* *INVITED*
11:30 – 11:50	to6	Change of the Fermi Surface Topology in the Vicinity of a Magnetic Quantum Critical Point *Michael Holt, UNSW*
11:50 – 12:10	to7	Magnetic Properties of a Cylindrical Spin-1 Core/Shell Ising Nanowire within the Effective-Field Theory *Mustafa Keskin, Erciyes University, Turkey*
12:10 – 12.30	to8	Suppression of the spin spiral in an antiferromagnetic $BiFe_{0.5}Mn_{0.5}O_3$ thin film and powder *David Cortie, University of Wollongong*
12:30 – 14.00		**Lunch**
14:00 – 15:30		**Chairperson: *Klaus Dieter Liss, ANSTO***
14:00 – 14:30	to9	How neutrons support modern materials engineering and helped unravel some historical engineering puzzles *Anna Paradowska, ANSTO* *INVITED*
14:30 – 15:00	to10	Switching between differing magnetic exchange spring states in an $ErFe_2/YFe_2$ multilayer observed by Er X-ray magnetic circular dichroism *Graham Bowden, University of Southampton, UK*
15:00 – 15:30		Poster Advertisement tp1-tp37: selected 2 minute talks
15:30 – 16:00		**Afternoon Tea**
16:00 – 18:00		**Poster Session:** tp1-tp37
18:00 – 19:30		**Dinner**
19:30 – 22:00		**Trivia Quiz, Conference Centre** *Quizmaster: Trevor Finlayson, University of Melbourne*

Friday 3 February

09:00 – 10:30 **Chairperson: *John Cashion, Monash University***

09:00 – 09:30 fo1 Mössbauer measurements on magnetic nanoparticles *INVITED*
Charles Johnson, University of Tennessee, USA

09:30 – 09:50 fo2 Numerical Device Model and Determination of Device Parameters for Organic Light Emitting Diodes (OLEDs)
Tadahiko Hirai, Materials Science and Engineering, CSIRO, Clayton

09:50 – 10:10 fo3 Reinforcing Function of Surface Acetylated Cellulose on Polylactic Acid (PLA) based Biopolymer
Tapasi Mukarjee, RMIT University

10:10 – 10:30 fo4 A study of gas phase and surface formaldehyde polymerisation from first principles
Philip McGill, University of Auckland

10:30 – 11:00 **Morning tea**

11:00 – 12:20 **Chairperson: *Tilo Söhnel, University of Auckland***

11:00 – 11:30 fo5 Orbital Physics in Titanates and Vanadates *INVITED*
Clemens Ulrich, UNSW

11:30 – 11:50 fo6 Thermal and pressure induced spin crossover in a cobalt(II) imide complex
Suresh Narayanaswamy, MacDiarmid Institute

11:50 – 12:20 fo7 Multidimensional Spectroscopy for Revealing Femtosecond Dynamics in Complex Condensed Matter Systems
Jeff Davis, Swinburne University of Technology *INVITED*

12:20 – 12:40 **Awards and Closing: *Wayne Hutchison, UNSW Canberra***

12:40 – 14.00 **Lunch**


scitek
total vacuum solutions
NEW SERVICES
NEW LOCATION
NEW BRANDS
adixen
by PFEIFFER VACUUM
Vacuum Technology including
• Best in class Leak Detection
• Dry Backing Pumps
• Magnetic Bearing Turbomolecular Pumps
• Thin Film Process Pumps
Cambridge NanoTech
Simply ALD
Atomic Layer Deposition for
• Solar
• Nanostructures
• Optical
• Biomedical
diener
Plasma-Surface-Technology
Plasma Solutions for
• Surface Cleaning
• Surface Activation
• Etching
• Coating
• Polymerisation
Gamma Vacuum
Ion Pumps for
• High Energy Physics
• Accelerators
• High Accuracy Instruments
rbd
instruments
Advanced Solutions for
• Surface Analysis
• Ion Sources
• Current Measurement
SEMICORE
Thin Film Tools for
• Innovative R&D
• Pilot Technology
• Production Systems
NOW AT
Unit 4,12 Chaplin Drive
Lane Cove NSW 2066
contact@scitek.com.au
FREE CALL
1800 023 467
www.scitek.com.au

WW POSTER SESSION: Wednesday 1 February

wp1 Muhammad Hamid Ahmed
Relative thermodynamical stability of non-stoichiometric uranium dioxide

wp2 T.J.Bastow, C.R.Hutchinson and A.J.Hill
Strong Interaction of an Intermetallic Platelet with its Boundary

wp3 C.J. Davidson, T.R. Finlayson, J.R. Griffiths, V. Luzin and Q.G. Wang
Neutron Diffraction Determination of Macro and Microstresses in an Al Si Mg Composite and Observed Changes with Plastic Strain

wp4 M. S. Scott, G. I. N. Waterhouse, K. Kato, S. L. Y. Chang, T. Söhnel
XPS, XAS and HRTEM studies of Rh,Pd/CeO2 nanocatalyst activation under conditions relevant to Ethanol Steam Reforming

wp5 L. Thoennessen, K.D. Liss, R. Dippenaar and A. Dehghan-Manshadi
Thermomechanical Processing of Titanium Alloys

wp6 A. Rozario, K. Fox, D. Garrett, S. Lichter, K. Ganesan, H. Meffin, and S. Prawer
Optimizing adhesion of parylene-C to diamond under long-term in vivo conditions

wp7 Jean N D Goder, Nurafini A M Rafi, Gary Bryant, Taavi Hunt, Ben Kent, Chris Garvey
Study of the effect of Penetratin on the gyroid to diamond phase transition in Myverol

wp8 Sidney B. Lang
Pyroelectric, Piezoelectric and Photoeffects in Hydroxyapatite Thin Films on Silicon

wp9 Y.Y. Liu, J.A. Warner, L.G. Gladkis, J.M. Scarvell, P.N. Smith, H. Timmers
Localized Backside Wear Measurement on UHMWPE Prosthesis Insert Using Micro-scratching

wp10 Gordon J. Troup and John F.Boas
An EPR Study of 'Mineral Organic Formula' and 'Vein Eze' Dietary Supplements

wp11 G. J. Bowden, R. C. C. Ward K. N. Martin, and P. A. J. de Groot
^{89}Y NMR-hyperfine relaxation times and transport in MBE grown $REFe_2/YFe_2$ multilayer films

wp12 J. Bertinshaw, R. Maran, N.Valanoor, F.Klose and C. Ulrich
Neutron studies of functional multiferroic BiFeO3 thin films

wp13 S. Brück, M. Paul, H. Tian, A. Müller, K. Fauth, E. Goering, J. Verbeeck, G. Van Tendeloo, M. Sing, R. Claessen
Local Magnetic Structure at the Fe3O4/ZnO Interface

wp14 W.D. Hutchison, N.J. Segal and K. Nishimura
Investigation of Magnetocaloric Effects in $RNiAl_4$

wp15 S. Brazier-Hollins and D. J. Goossens
Time-Dependent Magnetisation in $Fe_{0.5}Ni_{0.5}PS_3$

wp16 R.A. Mole, L.F. Montero, M. Nadeem, V.K. Peterson, R. Piltz and J.A. Stride
Neutron Scattering Studies of Magnetic Coordination Polymers

wp17 P. Rovillain, R. de Sousa , Y. Gallais, A. Sacuto, M-A. Measson, D. Colson, A. Forget, M.Bibes, A. Barthelemy, and M. Cazayous
Electric control of spin wave modes at room temperature in $BiFeO_3$

wp18 P. J. Graham, M. Bartkowiak, A. M. Mulders, M. Yethiraj, E. Pomjakushina and C. Ulrich
Raman Scattering on Multiferroic $TbMnO_3$

wp19 C.J. Hamer and J. Oitmaa
Restoration of Symmetry in the Spectrum of the Bilayer Heisenberg Antiferromagnet

wp20 R.R.P. Singh and J. Oitmaa
Thermodynamic Properties of the Heisenberg Antiferromagnet on the Hyperkagome Lattice: Comparison with $Na_4Ir_3O_8$

wp21 A. J. Princep, A. M. Mulders, E Schierle, E Weschke, J Hester,W D Hutchison, Y Tanaka, N Terada, Y Narumi, U Staub, V Scagnoli, T Nakamura, A Kikkawa, S W Lovesey, E Balcar,
Resonant X-ray Diffraction and the observation of Strange Quantities.

wp22 Y. Kulik and O. P. Sushkov
Hole dispersion in the t-J model in the presence of charge modulation

wp23 F. Bachhuber, J. Rothballer, T. Söhnel and R.Weihrich
A quantum mechanical investigation of the crystal and electronic structures of solid solutions of pyrite-type dipnictides MPn_2 (M = Si, Ge, Ni, Pd, Pt)

wp24 M.N. Read
Self-energy effects and the unbound electronic structure of Cu(111) surface

wp25 Gordon J. Troup, David Paganin, and Andrew Smith
Cutting Entanglement

wp26 J. G. Bartholomew and M. J. Sellars
Optical detection of a single rare earth ion in a solid state host

wp27 J.G. Bartholomew, S. Marzbana M.J. Sellars and R.P. Wang
*Spectroscopic Properties of **Eu3**+: **Y2O3** Thin Films*

wp28 M. Zhong, M. J. Sellars
Extending Hyperfine Coherence Times in $EuCl_3.6H_2O$

wp29 Jan Jeske and Jared H Cole
Quantum decoherence in complex environments

wp30 Timothy C. DuBois, Manolo C. Per, Salvy P. Russo and Jared H. Cole
Delocalised Oxygen model of TLS defects in superconducting phase qubits

wp31 Adurafimihan A. Abiona, William J. Kemp, Mark C. Ridgway, Heiko Timmers
Characterization of a Defect-Pair in Germanium

wp32 G William J. Kemp, Adurafimihan A. Abiona, Patrick Kessler,
Reiner Vianden, Heiko Timmers
First measurements of the quadrupole coupling constant for ^{100}Pd/Rh in antimony, hafnium and rhenium

wp33 L. M. Lepodise and R. A. Lewis
Absorption Lines around 70 Mev in Rubidium Bromide (RbBr)

wp34 Z. Liu and H. Riesen
Photoluminescence and Crystallographic Sites of Sm ions in BaFCl Nanocrystals

wp35 M. M. Rao and R. A. Lewis
Emissivity of Silicon Carbide in THz Spectral Range

wp36 J. S. Smith, D. W. Drumm, A. Budi, M. C. Per, L. C. L. Hollenberg and S. P. Russo
Density functional study of epitaxially-doped nanowires of phosphorus in silicon

wp37 Baran Yildirim, Glen Stewart and Hans Riesen
Structural and Optical Properties of Nanocrystalline $LiGa_5O_8:Fe^{3+}$

scitek
total vacuum solutions

electronic diener
Plasma-Surface-Technology

PLASMA TECHNOLOGY

- Surface Cleaning
- Surface Activation
- Etching
- Coating
- Polymerisation

NOW AT
Unit 4,12 Chaplin Drive
Lane Cove NSW 2066
contact@scitek.com.au

FREE CALL
1800 023 467

www.scitek.com.au

POSTER SESSION: Thursday 2 February

tp1 G.P. Cousland, R. Mole, M. Elcombe, X.Y. Cui, A.E. Smith, C.M. Stampfl and A.P.J. Stampfl
The structure of Yttria-stabilised Zirconia: a combined synchrotron photoemission, neutron scattering and ab-initio investigation

tp2 Xuan-Wen Gao, Chuan-Qi Feng, Shu-Lei Chou, Jia-Zhao Wang, Jia-Zeng Sun, Maria Forsyth, Douglas R. MacFarlane, Hua Kun Liu
5 V $LiNi_{0.5}Mn_{1.5}O_4$ Spinel Cathodes Using Room Temperature Ionic Liquid as Electrolyte

tp3 V. Jovic, G.I.N Waterhouse and T. Soehnel
Development of novel visible-light driven photocatalysts for hydrogen production

tp4 Sridhar Kumar Kannam, B. D. Todd, J. S. Hansen, Peter. J. Daivis
Flow rates of fluids in carbon nanotubes

tp5 I. Shvab and Richard J. Sadus
Hydrogen Bonding and Polarisational Properties of Water: Predictions from MCYna Model

tp6 Tesfaye M. Yigzawe and Richard J. Sadus
Calculation of Thermodynamic Properties of Lennard-Jones Fluid in a Molecular Dynamics Ensemble

tp7 Jan Herrmann, Bakir Babic, Chris Freund, Malcolm Gray, Magnus Hsu and Terry McRae
A metrological scanning probe microscope incorporating a tuning fork sensor and heterodyne laser interferometry

tp8 P Imperia
Sample Environments Updates at the Bragg Institute

tp9 W.T. Lee, F. Klose, D. Jullien and K. Andersen
Polarised ^{3}He based Neutron Polarisers and Analysers for Magnetism Research on ANSTO Instruments

tp10 Guochu Deng, Peter Vorderwisch, Chun-Ming Wu, Garry McIntyre, Wen-Hsien Li
Simulation of Multiple Operation Modes for the Cold Neutron Triple Axis Spectrometer SIKA at Bragg Institute

tp11 Richard A. Mole and Dehong Yu
Pelican: An Inelastic Neutron Scattering Spectrometer With Polarization Analysis

tp12 G.J. McIntyre, H. Kohlmann and B.T.M. Willis
Phonons observed by neutron Laue diffraction

tp13 Klaus-Dieter Liss
X-Rays of the Future: Thinking Energy Recovery Linac

tp14 Theo Hughes and Gordon J.Troup
A Simple Student-made Optical Spectrometer Modified for Gemmology Use

tp15 Gordon J.Troup
A Thermodynamic / Information Theory Analysis of Library Operation

tp16 G D. Wang, A. R. Buckingham, G. J. Bowden, R.C.C. Ward, and P. A. J. de Groot
Meta-stable magnetic exchange spring states with negative coercivity in $DyFe_2/YFe_2$ multilayer

tp17 S. Brück, D. Cortie, J. Brown, T. Saerbeck, C. Ulrich, F. Klose, and J. Downes
Polarized Neutron Reflectometry of Rare-Earth Nitride Thin Films

tp18 J.L. Wang, S.J. Campbell, S.J. Kennedy, P. Shamba, R. Zeng and S.X. Dou
Magnetic Phase Transition and Thermal Expansion in $LaFe_{13-x-y}\ Co_ySi_z$

tp19 S. J. Collocott, X. Tan and H. Xu
Temperature dependence of the coercivity in $Nd_{60-x}Fe_{30}Al_{10}Dy_x$, x = 0, 2 and 4, bulk amorphous ferromagnets: an example of strong pinning of domain walls

tp20 S.J. Harker, G.A. Stewart, H. Okimoto, K. Nishimura and W.D. Hutchison
Magnetic properties of $Nb_{1-X}Hf_XFe_2$

tp21 N.Narayanan, N.Qureshi, H. Fuess and H.Ehrenberg
Charge, magnetization (spin) and spin momentum density studies of the Kagome staircase compound $Co_3V_2O_8$

tp22 N. M. Reynolds, P. Graham, A.M. Mulders, G. McIntyre, S. Danilkin, J. Fujioka, Y. Tokura, B. Keimer, M. Reehuis and C. Ulrich
Inelastic Neutron Scattering in Multiferroic Materials

tp23 A.M. Mulders, M. Bartkowiak, J.R. Hester, E. Pomjakushina, K. Conder
Ferroelectric charge order stabilized by antiferromagnetism in multiferroic $LuFe_2O_4$

tp24 J. Oitmaa and R.R.P. Singh
The Spin-3/2 Heisenberg Antiferromagnet on the Bilayer Honeycomb Lattice : A Model for $Bi_3Mn_4O_{12}\ (NO_3)$

tp25 Rakesh Kumar and Oleg P. Sushkov
Condensation of composite objects in Heisenberg-like models

tp26 O. P. Sushkov
Magnetic properties of lightly doped antiferromagnetic YBCO

tp27 D. Bende T. Söhnel
Exploring structural Oddities in Tin Cluster Compounds $RuMSn_6O_8$ (M = Fe, Co, Mn) with Quantum Mechanical Methods

tp28 J. Stephen and G. V. M. Williams
The Magnetic and Electronic Properties of $FeSr_2YCu_2O_{6+x}$ and $FeSr_2Y_{2-x}Ce_xCu_2O_{8+x}$

tp29 Heather Schijns, Ian Jackson and Douglas R Schmitt
Laboratory Measurements of Frequency-Dependent Seismic Properties of Cracked and Fluid-Saturated Media

tp30 J.D. Cashion, K. Suzuki and E. Murad
Mössbauer Spectra of the Acid Mine Drainage Mineral Schwertmannite from the Sokolov Basin, Czech Republic

tp31 R.A. Pax and G.A. Stewart
Quantitative Determination of Phases using Mössbauer Spectroscopy and X-ray Diffraction: A Case Study Using the Fe-Ti-O System

tp32 R. L. Ahlefeldt and M. J. Sellars
Characterisation of $EuCl_3.6H_2O$ for quantum computation

tp33 K. R. Ferguson, S. E. Beavan and M. J. Sellars
Rephasing Spontaneous Emission in a Rare-Earth Ion-Doped Solid

tp34 Milos Rancic, Sarah Beavan and Matthew Sellars
Optical Imaging and Structure Writing in Rare Earth Ion Doped Crystals

tp35 W.D. Hutchison, S.J Harker, P.G. Spizzirri, F. Hoehne, and M.S. Brandt
Electrically Detected Magnetic Resonance Applied to Near Surface Phosphorus Donors in Silicon

tp36 T. Li, O.P. Sushkov and U. Zuelicke
Spin precession and non-adiabaticity in hole quantum point contacts

tp37 D. J. Miller
Implementation of the PBR protocol using spin-spin interactions

Australian Government

ansto

Nuclear-based science benefiting all Australians

ANSTO's Bragg Institute is a world leader in neutron and X-ray scattering techniques, and houses the region's most comprehensive suite of neutron beam instruments.

Work with us and our specialised facilities to

ask

and answer the

big questions.

www.ansto.gov.au

WW 2012

ABSTRACTS FOR ORAL SESSIONS

wo1

Nanostructured Materials for Efficient Performance

Anita Hill[a,b,c] Cara Doherty[a], Matthew Hill[a], Sang Hoon Han[a], Paolo Falcaro[a], Dario Buso[a], Kris Konstas[a], Aaron Thornton[a], Wei Xian Lim[a], Christopher Hutchinson[a,d], Tim Bastow[a,d]

[a] *CSIRO Materials Science and Engineering, Private Bag 33, S Clayton, Victoria 3169, Australia.*

[b] *CSIRO Process Science and Engineering, Private Bag 33, S Clayton, Victoria 3169, Australia.*

[c] *Monash University School of Chemistry, Wellington Road, Victoria 3800, Australia.*

[d] *Monash University Materials Engineering, Wellington Road, Victoria 3800, Australia.*

Performance properties for materials can often be characterized as having a "tradeoff behaviour" especially when plotted in two dimensions [1]. Examination of the physics underlying these tradeoff relationships can allow materials scientists and engineers to come up with nanostructures that overcome these tradeoffs. In this work we examine tradeoffs that limit our ability to achieve efficient performance and offer some suggestions for methods to model the tradeoffs and to design material architectures that overcome them.

[1] M. F. Ashby, *Materials and The Environment: Eco Informed Material Choice* (Butterworth Heinemann, 2009).

wo2

Investigating Short-Range Order in Triglycine Sulphate using X-ray and Neutron Diffuse Scattering

J.M. Hudspeth[a], D.J. Goossens[b], M.J. Gutmann[c] , A.J. Studer[d] and T.R. Welberry[b]

[a] *Research School of Physics and Engineering, Australian National University, ACT, 0200, Australia.*

[b] *Research School of Chemistry, Australian National University, Canberra, 0200, Australia.*

[c] *ISIS Facility, Rutherford Appleton Laboratory, Chilton, Didcot, Oxon, United Kingdom*

[d] *Bragg Institute, Australian Nuclear Science and Technology Organisation, NSW, 2234, Australia*

Triglycine sulphate (TGS) [$(NH_2CH_2COOH)_3H_2SO_4$] is a hydrogen-bonded ferroelectric with a phase transition temperature of 322K [1]. The phase transition is reversible and second-order, order disorder type, making TGS of fundamental interest in the field of phase transitions [2]. Above the critical temperature, one of the glycine molecules is disordered across a mirror plane. Below the critical temperature, it chooses a side, breaking the symmetry. The ferroelectric state is obtained through the ordering of the glycine orientations on neighbouring sites, but the mechanism for the phase transition is not well understood.
We have investigated the short-range order in TGS by collecting single crystal x-ray and neutron diffuse scattering data on hydrogenous and fully deuterated TGS respectively. Data was collected at temperatures from well below to well above T_C. We have also developed a model for the short-range order using the program ZMC [3].
This has given us some new insight into the behavior of the disordered glycine in TGS. For example, above T_C, the orientations of the disordered glycine appear to be correlated over short range rather than being completely random as suggested by the average structure.

[1] S.G. Zhukov, V.A. Tafeenko, G.V. Fetisov, *Journal of Structural Chemistry* **1999**, *31* 84-90.

[2] K. Itoh, A. Nishikori, H. Yoklomize, E. Nakamura, *Japanese Journal of Applied Physics* **1973**, *24* 235-251.

[3] D.J. Goossens, A.P. Heerdegen, E.J. Chan, T.R. Welberry, *Metallurgical and Materials Transactions A* **2010**, *41* 1110-1118.,

wo3

Microstructural-property relations in brittle materials: from A to Z

J. E. Bradby and J. S. Williams

Department of Electronics Materials Engineering, Research School of Physics and Engineering, Australian National University, Canberra, Australia

Despite being of obvious importance for many applications, the microdeformation of many semiconductors is still not well understood. Indeed, many materials such as silicon and germanium are still considered to display simply brittle characteristics. However under many deformation regimes, such as point loading, a wide range of interesting deformation behaviours, including twinning, defect generation and phase transformation can be displayed. Silicon is an especially interesting material to study under such conditions. The initial response of Si to point loading (via nanoindentation) is the generation of defects along the {111} planes. As loading continues, a transformation from the diamond-cubic phase to a metallic β-Sn structure takes place. On pressure release the β-Sn phase is unstable and transforms to number of phases including an unique amorphous state. While all semiconductors are predicted to display such phase-transformation behaviour, at room-temperature most deform plastically by the generation of slip or dislocations. This talk will outline a landscape of deformation mechanisms across a number of 'brittle' materials from Amorphous silicon to Zinc oxide.

wo4

Superconducting phase qubits and coherent defects: Unravelling the mystery of two-level fluctuators

J. H. Cole[a], T. C. DuBois[a], M. C. Per[a], S. P. Russo[a]
G. Grabovskij[b], J. Lisenfeld[b], P. Bushev[b], C. Müller[c], A. Ustinov[b], A. Schnirman[c]
[a] *Chemical and Quantum Physics, School of Applied Sciences, RMIT University, Melbourne, Victoria 3001, Australia.*
[b] *Physikalisches Institut, Karlsruhe Institute of Technology, D-76128 Karlsruhe, Germany.*
[c] *Institut fu□r Theorie der Kondensierten Materie, Karlsruhe Institute of Technology, D-76128 Karlsruhe, Germany.*

Superconducting phase qubits are one of the most well understood and promising devices for realising controllable qubits in solid-state systems. Unfortunately, they, as well as all other devices based on Josephson junctions, suffer from the presence of two-level defects. These defects appear throughout the operating frequency range and can lead to dephasing, relaxation and imperfect control pulses. Although we know much about these defects, their precise microscopic origin remains a complete mystery. I will discuss recent studies of so-called strongly coupled, coherent two-level fluctuators in superconducting phase-qubits. A number of novel effects are observed in these systems, which are familiar from the field of quantum optics. These include multi-photon transitions, corrections due to higher lying levels and dispersive coupling. Using such techniques, and a strong connection between experiment and theory, helps shed more light on the origin and properties of these two-level defects.

wo5

Fabrication, Characterization and Applications of $Si_{1-x}Ti_xO_2$ (x = 0-1) Inverse Opal Photonic Crystals

Z.H. Al-Azri and G.I.N Waterhouse

School of Chemical Sciences, University of Auckland, Auckland, New Zealand.

The MacDiarmid Institute for Advanced Materials and Nanotechnology, New Zealand.

Photonic crystals are highly ordered materials that possess a periodically modulated refractive index in 1,2 or 3-dimensions with periods typically on the length scale of visible-light (380-750 nm). In this study, we described the fabrication of three-dimensionally ordered macroporous (3DOM) inverse opal materials with composition $Si_{1-x}Ti_xO_2$ (x=0-1) and photonic band gaps (PBG) spanning the visible spectrum. The optical and structural properties of the $Si_{1-x}Ti_xO_2$ inverse opals were characterized by UV-Vis transmittance measurements, SEM, powder XRD, FTIR, XPS, NEXAFS and N_2 physisorption measurements. Results show that optical properties and PBG behavior of the $Si_{1-x}Ti_xO_2$ (x=0-1) inverse opals obey a modified Bragg's law equation, which considers both diffraction and refraction of light in the photonic crystals architectures. The $Si_{1-x}Ti_xO_2$ inverse opal photonic crystals were subsequently exploited in refractive index sensing and dye-sensitized solar cells (DSSCs), and were also suitable bioglass materials. The PBG red-shifted linearly upon filling the macropores in the inverse opals with solvents of progressively higher refractive index. A detection limit of ~0.001-0.002 for refractive index of organic solvents, saline or sucrose solutions range was achievable. The TiO_2 inverse opals films were also very effective for light capture due to their high surface area and dual porosity (both meso and macroporous). A solar conversion efficiency of ~3.2% was reached for a TiO_2 inverse opal thin film of 7 micron thickness. Immersion of $Si_{1-x}Ti_xO_2$ (x = 0-1) inverse opals in a simulated body fluid (SBF), a cocktail of organic salts with composition close to that of human blood plasma, at ~37^oC resulted in the conformal growth of hydroxyapatite [$Ca_{10}(PO_4)_6(OH)_2$] on the walls of the inverse opals. Deposition of hydroxyapatite red-shifted the PBG. The structural features of hydroxyapatite (HAP) coated on the inverted structures were comparable to that of HAP nanopowders prepared independently as a reference material. Results confirmed that inverse opals are promising hybrid bioscaffolds for bone and teeth regeneration.

The Effects of Optical Intensity and Excited State Quenchers on the Photostability of Electro-Optic Chromophores

Y. Kutuvantavida[a], G. V. M. Williams[b], S. Janssens[a], S. G. Raymond[a] and A. Kay[a]

[a]*Photonics, Industrial Research Ltd., PO Box 31310, Lower Hutt 5040, New Zealand*

[b]*MacDiarmid Institute, Victoria University of Wellington, PO Box 600, Wellington 6012, New Zealand*

The development of next generation ultra-fast photonic devices strongly relies on efficient electro-optic (EO) materials. Despite the promise of high EO coefficients in organic compounds compared to their inorganic counterparts one of the significant challenges that have hindered the commercial uptake of organic EO materials is photodegradation. We present the results from optical and photostability measurements on thin films containing amorphous polycarbonate (APC) and an organic EO chromophore, PYR-3 [1].

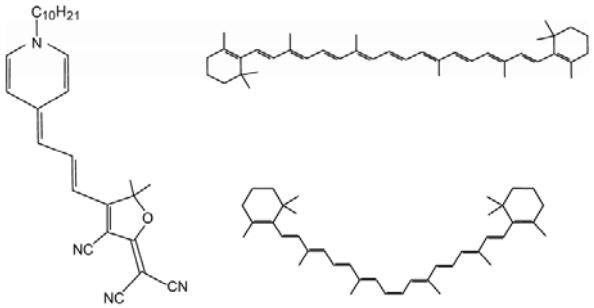

Figure. 1. *Left: Structure of one of the isomers of the PYR-3 chromophore. Right: Structures of trans (top) and cis (bottom) β-carotene.*

The main photodegradation mechanism is through the generation of singlet oxygen when the chromophore relaxes from the excited singlet state to the ground state via the triplet state. Thus, photostability can be enhanced by reducing the oxygen content in the films [2]. There is an increase in the photostability with increasing optical intensity [3]. It can be explained by oxygen-mediated photodegradation that initially reduces the oxygen content in the film. A significant enhancement in photostability can be achieved by adding β-carotene to quench the triplet state and singlet oxygen [3].

[1] A. J. Kay, *et al., J. Mater Chem*. **14**, 1321 (2004).

[2] S. G. Raymond, *et al*., *J. Appl. Phys.* **105**, 113123 (2009).

[3] G. V. M. Williams, *et al*., *J. Appl. Phys.* **110**, 083524 (2011).

Photomodulated Reflectance of GaAs and *p*-type GaAs:Be

J. A. Steele and R. A. Lewis

Institute for Superconducting and Electronic Materials, University of Wollongong, Wollongong, New South Wales 2522, Australia

There are many different methods to characterise semiconductor materials. Optical methods are of great significance because they are contactless, non-destructive and unambiguous. Room temperature photomodulated reflectance (PR) is one such technique.

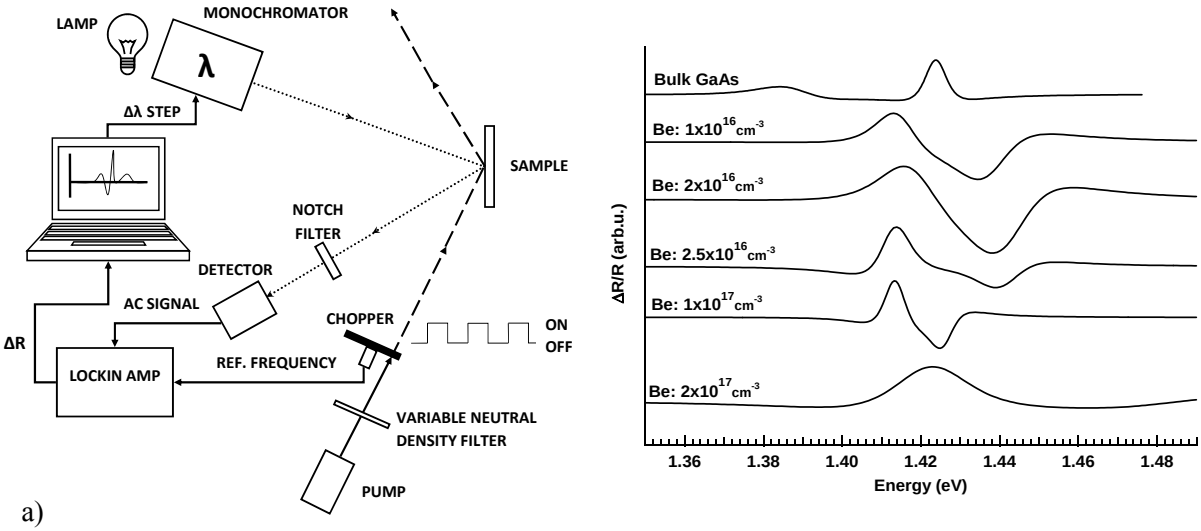

Figure 1: *a) Schematic diagram of photomodulated reflectance spectroscopy, and b) PR spectra of p-type GaAs:Be at the fundamental bandgap for differing Be concentrations*.

PR spectroscopy examines the absolute change in reflectance due to periodic exposure of above bandgap radiation. For photon energies corresponding to critical points in the material's Brillouin zones, the PR spectra yields derivative-like structure. Here we investigate Franz-Keldysh oscillations (FKOs) at the fundamental and split-off bandgaps of *p*-type GaAs:Be samples. The band structure of lightly to heavily doped *p*-type GaAs:Be is seen to undergo a systematic heavy hole-light hole evolution. It is observed that sufficient doping levels revert the semiconductor to a bulk-like PR signal for single band-to-band transitions. We conclude that this direct optical method may serve as a useful means of estimating doping levels.

wo8

Neutron Scattering Study on the Fe-based High-Tc Superconductors

Wei Bao

Department of Physics, Renmin University of China, Beijing 100872, China.

Superconductivity was discovered 100 years ago in elemental metals at a few K. Stimulated by the discovery of cuprate superconductor in doped Mott antiferromagnetic insulator, intense research effort has been devoted to discovery of unconventional superconductors of high transition-temperature (Tc) in magnetic materials. Iron-based superconductors in several related structure families with Tc as high as 56 K have generated much excitement in the last three years, and new discovery continues to appear.Using neutron scattering technique, we have determined crystal and magnetic structure of several families of the new Fe superconductors and their sample composition [1-5], which provide solid foundation for further investigation on electronic structure and processes. Structural and magnetic transitions have been investigated to yield phase-diagrams which show a rich variety of relationship between superconducting and antiferromagnetic orders [6,7]. Such investigation also reveals the shortcoming of widely accepted spin-density-wave theoretic scenario and provides first experimental indication of important role played by the orbital order [2,3]. The symmetry of superconducting order parameter has strong signature in magnetic excitation spectrum. We observed with inelastic neutron scattering method the telltale spin resonance mode of the unconventional s+/- symmetry in the superconducting state of the 11 superconductor [8]. The normal state was shown to exhibit the single-lobed incommensurate excitation continuum of a typical itinerant antiferromagnet, in contrast to spin-wave cone of a localized antiferromagnet [8,9], supporting a Fermi liquid description of the normal state.

[1] Y. Qiu, W. Bao, Q. Huang et al., Phys. Rev. Lett. **101**, 257002 (2008).
[2] Q. Huang, Y. Qiu, W. Bao et al., Phys. Rev. Lett. **101**, 257003 (2008); M. Kofu, Y. Qiu, W. Bao et al., New J. Phys. **11**, 055001 (2009).
[3] W. Bao, Y. Qiu, Q. Huang et al., Phys. Rev. Lett. **102**, 247001 (2009).
[4] W. Bao, Q. Huang, G. Chen et al., Chin. Phys. Lett. **28**, 086104 (2011); P. Zavalij, W. Bao, X. F. Wang et al., Phys. Rev. B **83**, 132509 (2011).
[5] F. Ye, S. Chi, W. Bao et al., Phys. Rev. Lett. **107**, 137003 (2011).
[6] H. Chen et al., EPL. **85**, 17006 (2009); T.J. Liu et al., Nat. Materials **9**, 718 (2010).
[7] W. Bao et al., arXiv:1102.3674 (2011).
[8] Y. Qiu, W. Bao, Y. Zhao et al., Phys. Rev. Lett. **103**, 067008 (2009).
[9] D.N. Argyriou et al., Phys. Rev. B **81**, 220503 (R) (2010).

wo9

Mapping of Domain Orientation and Molecular Order in Polycrystalline Semiconducting Polymer Films with Soft X-Ray Microscopy

C. R. McNeill

Department of Materials Engineering, Monash University, Clayton, Victoria 3800, Australia.

Organic semiconductors that are based on molecules or polymers rather than inorganic materials are an attractive alternative to traditional semiconductors. While they will not likely compete with silicon in terms of charge transport mobility, they are finding use in applications as diverse as efficient solid-state lighting, low-cost solar cells and flexible electronics. State-of-the-art solution-processed organic field-effect transistors typically use polycrystalline organic semiconductor thin films as the active layer. Although it is widely regarded that boundaries between polycrystalline domains are a likely source of charge trapping limiting charge carrier mobility, little is known about the detailed domain structure of such films. In this presentation I will discuss the development of polarised soft x-ray microscopy for imaging the domain structure of polycrystalline conjugated polymer films with < 100 nm resolution.[1] In particular using this technique it is possible to map not only the local polymer backbone orientation, but also the local degree of orientational order and out-of-plane tilt angle. The domain structure of a number of high-mobility systems will be presented and the relationship between domain structure and charge transport discussed.

[1] B. Watts, T. Schuettfort and C. R. McNeill, *Advanced Functional Materials*, **21**, 112-1131 (2011)

to1

Advanced materials for lithium rechargeable batteries, supercapacitors and hydrogen storage

Hua Kun Liu

Institute for Superconducting & Electronic Materials, ARC Centre of Excellence for Electromaterials Science, University of Wollongong, NSW 2522 Australia.

email: hua_liu@uow.edu.au

In order to meet global requirements for clean emissions, it is necessary to develop new materials and better technologies for automotive applications, as well as for other energy storage applications. The Energy Materials Research Program at the Institute for Superconducting & Electronic Materials, the University of Wollongong focuses on developing advanced materials and innovative technologies for obtaining clean energy with high efficiency and low cost.

This talk will highlight our recent efforts in developing new approaches to study the relationship between the structure and the physical, chemical and electrochemical properties of the materials at nano dimensions, and to control the structure, chemistry, shape, and functionality of nanostructures for applications in lithium rechargeable batteries, supercapacitors and hydrogen storage.

Examples presented will include carbon coated Si nanoparticles, self-catalysis-grown SnO_2 nanowires, nanostructured V_2O_5, and high surface area, hollow-structured α-Fe_2O_3/carbon nanocomposite, and $LiFePO_4$-Fe_2P-C nanocomposite as electrode materials with high performances for next generation lithium rechargeable batteries; MnO_2 nanowires, porous VO_x, and highly ordered TiO_2 nanotube arrays as electrode materials for next generation supercapacitors; as well as the catalysts and multicomponent systems to accelerate the dehydrogenation of lightweight metal hydrides (such as magnesium hydride) and complex hydrides (such aslithium borohydride).

to2

Positron Annihilation Lifetime Spectroscopy within CAMS

E. R. Vance

Institute of Materials Engineering, Australian Nuclear Science and Technology Organisation, Kirrawee DC 2232, Australia

and ARC Centre for Antimatter-Matter Studies

The ARC-funded Centre for Antimatter-Matter Studies (CAMS) has been running since 2006 and one of its aims is the study of open volume defects in solid materials. The slow positron beamline constructed at the ANU can interrogate microns-thick films and surface layers and observe nano- and mesopores by the lifetime spectra of the positrons implanted into these layers. In addition, the CAMS project has a number of laboratory, or "desktop", PALS Spectrometers that can detect open volume defects in bulk materials. These defects include cation vacancies in insulating solids (but not anionic vacancies), single vacancies and vacancy complexes in metal alloys, radiation-induced defects and general nano- and mesoporosity and defects, as well as phase separation in polymers.

Examples will be given of the application of positron annihilation lifetime spectroscopy to various materials, notably pores in natural zircons, cation vacancies in oxides and silicates, and alteration
layers on leached candidate glasses for radioactive waste immobilisation.

to3

Effect of protein on electrochemical properties of diamond

E. Slonim[a], K. Fox[a], D. Garrett[a], H. Meffin[c], and S. Prawer[a]

[a] *School of Physics, University of Melbourne, Victoria 3010, Australia.*

[c] *National Information and Communication Technology Australia, Victoria 3010, Australia*

Diamond is a biocompatible and biostable material that is fast becoming a popular material for biomedical applications. However, it is known that when a foreign material such as diamond is placed within the body, proteins in surrounding fluid will readily adsorb to the diamond. This study demonstrates the effect of protein adsorption on a diamond electrode in relation to its electrical stimulation capacity.

Diamond samples were fabricated by microwave chemical vapour deposition to generate electrically conductive nitrogen-doped ultrananocrystalline diamond. Diamond samples were mounted on a flexible circuit cable using conductive epoxy. Samples were connected to an EDAQ electrochemical impedance analyser ERZ100 and impedance was measured. Samples were immersed in a solution of bovine serum albumin at a concentration of 0.1, 0.3 or 0.5mg/ml for 120 minutes. Impedance of samples was measured continually at set intervals of 10 minutes, or only once after the full time. Protein adsorption was determined using depletion measurement via gel staining. X-ray photoelectron spectroscopy was used to characterise protein adsorption.

We have found that the adsorption of protein on diamond electrodes increases electrochemical impedance thereby reducing electrical stimulation capacity. However, the continual application of an electrical current via impedance testing resulted in constant impedance and less protein adsorption.

This research was supported by the Australian research Council (ARC) through its Special Research Initiative (SRI) in Bionic Vision Science and Technology grant to Bionic Vision Australia (BVA).

Dynamics of Globular Proteins in Crowded Electrolyte Solutions

M. Hennig[a], F. Roosen-Runge[b], F. Zhang[b], S. Zorn[b], W. A. Skoda[c], R.M.J. Jacobs[d], M. Sztucki[e], H. Schober[f], T. Seydel[f] and F. Schreiber[b]

[a] *Bragg Institute, ANSTO, Sydney, Australia*

[b] *Institut für Angewandte Physik, Universität Tübingen, Germany.*

[c] *ISIS, Rutherford Appleton Laboratory, Chilton, Didcot, UK*

[d] *Department of Chemistry, CRL, University of Oxford, UK*

[e] *European Synchrotron Radiation Facility, Grenoble, France*

[f] *Institute Laue-Langevin, Grenoble, France.*

We discuss the dynamics of a crowded protein solution depending on the protein volume fraction and the temperature including in particular the denaturing transition. The motivation is to understand proteins under biologically relevant conditions by, *inter alia* utilizing knowledge and methods established in soft condensed matter macromolecular research. To this end, we employ cold neutron high-resolution backscattering spectroscopy to record quasi-elastic and elastic signals. Using this technique we retrieve the short-time self-diffusion coefficient and the total mean-squared displacement of the protein in solution. Furthermore, we investigate the shape of the proteins in solution using small-angle X-ray scattering. We find that the short-time self-diffusion strongly decreases with increasing protein volume fraction. Furthermore, we show that the short-time self-diffusion can be accurately modeled with effective colloid hard-spheres, underlining the importance of hydrodynamic interactions under the condition of crowding [1]. Studying the temperature behavior below and above the denaturing, we observe that the total mean-squared displacement increases monotonically with temperature, but at the denaturing transition it decreases strongly. This observation can be rationalized and quantitatively modeled as a transition from a liquid protein solution to a gel-like state [2].

[1] F. Roosen-Runge et al., *PNAS* **108,** 11815 (2011).

[2] M. Hennig et al., *Soft Matter*, DOI:10.1039/c1sm06609a.

to5

WITHDRAWN

to6

Change of the Fermi Surface Topology in the Vicinity of a Magnetic Quantum Critical Point

Michael Holt[a], Jaan Oitmaa[a] , Wei Chen[b] and Oleg Sushkov[a]

[a] *School of Physics, University of New South Wales, Sydney, 2052, Australia.*

[b]*Max Planck Institute for Solid State Research, Stuttgart, Germany.*

Stimulated by the small/large Fermi surface controversy in the cuprates we study hole dynamics in the bilayer $t-t'-t''-J$ model with strong interlayer coupling $J_\perp$. At $J_\perp/J \approx 2.5$ the system has an $O(3)$ quantum critical point (QCP) separating the magnetically ordered and the magnetically disordered phases. We demonstrate that in addition to the QCP the system has a Lifshitz point (LP) where the topology of the hole dispersion changes from four hole pockets with minima at momenta $\boldsymbol{k} = (\pm\pi/2, \pm\pi/2)$ to a single hole "pocket" with minimum at $\boldsymbol{k} = (\pm\pi, \pm\pi)$. Similar to the $O(3)$ QCP the LP is driven by magnetic quantum fluctuations. The position of the LP, while being close to the position of the QCP is generally different. Dependent on the additional hole hopping integrals t' and t'', the LP can be located either in the magnetically ordered phase and/or in the magnetically disordered phase.

to7

Magnetic Properties of a Cylindrical Spin-1 Core/Shell Ising Nanowire within the Effective-Field Theory*

N. Şarlı[a] and M. Keskin[a,b]

[a] *Institute of Science, Erciyes University, 38039 Kayseri, Turkey.*

[b] *Department of Physics, Erciyes University, 38039 Kayseri, Turkey.*

Magnetic nanowire systems have attracted considerable attention not only because of their academic interest, but also due to the technological applications; in particular, in the areas of magnetic recording media, spin electronics, optics, sensors and thermoelectronics devices [1]. Theoretical studies of magnetic properties of cylindrical spin-1/2 core/shell Ising nanowires have also been investigated by using the effective-field theory (EFT) with correlations [2]. In this work, we investigate the thermal behavior of magnetizations and susceptibilities in a cylindrical spin-1 core/shell Ising nanowire within the EFT with correlations both ferromagnetic and antiferromagnetic exchange interactions between the shell and core. We find that the system undergoes a first- and second-order phase transitions depending on the exchange interactions parameters. For small exchange interactions, the system undergoes two successive phase transitions in which both transitions are a second-order phase transition for the ferromagnetic interaction, and the first one is a first-order and second one is a second-order for the antiferromagnetic interaction. Magnetic susceptibility behaviors versus applied field and hysteresis behaviors are also investigated. The results are in good agreement with the experimental [3] and theoretical results [4].

[1] S. S. P. Parkin, M. Hayashi, L. Thomas, Science **320**, 190 (2008); H. Zhang, A. Hoffmann, R. Divan, P. Wang, Appl. Phys. Lett. **95**, 232503 (2009).

[2] T. Kaneyoshi, J. Magn. Magn. Mater. **322**, 3410 (2010); T. Kaneyoshi, Phys. Stat. Sol. B **248**, 250 (2011); M. Keskin, N. Şarlı, B. Deviren, Solid State Commun. **151,** 1025 (2011).

[3] Y. T. Chong, D. Görlitz, S. Martens, M. Y. E. Yau, S. Allende, J. Bachmann and K. Nielsch, Adv. Mater. **22,** 2435 (2010).

[4] E. Konstantinova, J. Magn. Magn. Mater. **320**, 2721 (2008).

---

* The work was supported by Erciyes University Research Fund, Grand No: FBD-10-3350.

Suppression of the spin spiral in an antiferromagnetic $BiFe_{0.5}Mn_{0.5}O_3$ thin film and powder

D.L. Cortie[a,b], Y. Du[a], Z.X Cheng[a], ,F. Klose[b] and X.L. Wang[a]

[a] *Institute of Superconducting and Electronic Materials, University of Wollongong, NSW*

[b] *The Bragg Institute, Australian Nuclear Science and Technology Organization, NSW.*

Since the advent of the spintronics paradigm [1], there has been a resurgence of interest in materials that simultaneously possess magnetic and ferroelectric ordering [2]. Such materials provide the realistic prospect of manipulating magnet elements using electric fields at room temperature. While electric field control has recently been demonstrated using the interfacial coupling between a multiferroic oxide and a metallic thin film [3], there is still a search to find a suitable single phase ferromagnetic multiferroic [4,5]. Previous work reported that a metastable phase of $BiMnO_3$ was ferromagnetic with a Curie temperature of 99K [5] whereas $BiFeO_3$. is a canted anti-ferromagnetic below 640K with ferroelectric order [2]. We explored the effect on magnetic structure of including high percentages of Mn into a $BiFeO_3$ host in a $La_{0.2}BiFe_{0.5}Mn_{0.5}O_3$ compound. Neutron diffraction was performed on an epitaxial nanoscale film using the instrumentation at ANSTO to obtain the magnetic structure at low temperature, and the results were compared with powders and magnetometry data. The neutron data for the film and powders both indicate a single magnetic transition to a highly collinear G-type antiferromagnetic order where the incommensurate spin spiral present for $BiFeO_3$ appears to be suppressed by the addition of Mn . The Neél temperature is shifted to 225 K. The c/a ratio of the unit cell is found to differ between thin film and the powder suggesting that the epitaxial lattice matching to the $SrTiO_3$ substrate strains the film in the ab plane but preserves the overall unit cell volume leading to a lattice expansion in the c direction and a further reduction in Neel temperature to 130 K. The magnetic properties of the film and powder appear to be dramatically different from the properties of nanoparticles reported for the same compound which showed multiple magnetic transitions to higher temperatures [4].

[1] R. Ramest and Nicola. A. Spaldin, *Nature Materials*, 6, pp 21-40 (2007)

[2] W. Eerenstein, N. D. Mathur & J. F. Scott, *Nature Materials,* 442, 05023(2006)

[3] J. T. Heron et al. Phys. Rev. Lett. 107, 217202 (2011)

[4] Y. Du et al, *App. Phys. Lett.,* 97, 122502 (2010)

[5] E. Montanari et al. *Chem. Mater.* 2005, *17,* 6457-6467

to9

How neutrons support modern materials engineering and helped unravel some historical engineering puzzles

Anna Paradowska,

Bragg Institute, Australian Nuclear Science and Technology Organization, NSW.

to10

Switching between differing magnetic exchange spring states in an $ErFe_2/YFe_2$ multilayer observed by Er X-ray magnetic circular dichroism

G. B. G. Stenning[a], A. R. Buckingham[a], G. J. Bowden[a], R.C.C. Ward[b], G. van der Laan[c], L. R. Shelford[c], F. Maccherozzi[c], S. S. Dhesi[c] and P. A. J. de Groot[a]

[a]*School of Physics and Astronomy, University of Southampton, SO17 1BJ, United Kingdom*

[b]*Clarendon Laboratory, Oxford University, OX1 3PU, United Kingdom*

[c]*Diamond Light Source, Chilton, Didcot OX11 0DE, United Kingdom*

X-ray magnetic circular diochroism (XMCD) studies at Diamond, have been used to examine a complicated double magnetic switching process in an MBE-grown $[ErFe_2(70Å)/YFe_2(150Å)]\times25$ magnetic exchange spring system. Similar studies using bulk-magnetometry reveal only a small magnetic signature of the switching at 200 K [1,2]. By way of contrast, XMCD studies at the Er $M_{4,5}$ edge are characterized by very large magnetic signatures [3]. This is due primarily to the element-specific nature of XMCD which allows one to investigate the Er sub-lattice only, free from masking effects arising from the Fe and Y sub-lattices. Magnetic hysteresis loops for the Er magnetization, at temperatures $T<200$ K, reveal a single irreversible switch between a vertical exchange spring and its reversed state. But experiments at $T>200$ K reveal a crossover to a regime with two irreversible switching processes. Computational modelling for this system gives good agreement with the experiment, revealing that the observed high temperature behaviour is due to transitions between *vertical exchange spring states* and *exchange spring driven spin-flop* states. The origin of the double switching has been traced to instabilities in *both* the spin-flop configuration and vertical spring configuration, at temperatures ~200 K. These, in turn can be associated with the topological shape of the Er^{3+} single-ion anisotropy. De-pinning of exchange spring states is determined primarily by low-energy saddle points which allow the Er magnetic moments to change direction, without riding up over the much larger anisotropy maxima.

[1] K. N. Martin, C. Morrison, G. J. Bowden, and P. A. J. de Groot and R. C. C. Ward, (2008) Phys. Rev.B. **78** 172401

[2] K. N. Martin, K. Wang, G. J. Bowden, A. A. Zhukov, and P. A. J. de Groot J. P. Zimmermann, H. Fangohr and R. C. C. Ward (2006) Appl. Phys. Lett. **89** 132511

[3] G. B. G. Stenning, A. R. Buckingham, G. J. Bowden, R.C.C. Ward, G. van der Laan, L. R. Shelford, F. Maccherozzi, S. S. Dhesi and P. A. J. de Groot (2011) Phys. Rev. B **84** 104428.

fo1

Mössbauer measurements on magnetic nanoparticles

C.E. Johnson

Center for Laser Applications, University of Tennessee Space Institute, Tullahoma, TN 37388, USA.

The phase diagram of nanoparticle alloys is different from that of bulk alloys, and may exhibit lower transition temperatures and different phase boundary compositions compared with bulk crystals [1]. This may enable crystal phases not normally stable at room temperature to be prepared. In addition magnetic nanoparticles are single-domain and exhibit superparamagnetism and decreased magnetization in small applied fields. In superparamagnets the magnetic moments of the particles fluctuate rapidly below the Curie temperature T_C and above a temperature T_B known as the blocking temperature. This produces a reduced magnetization and (in the Mössbauer spectrum) a broadened hyperfine spectrum: below T_B the usual magnetic moment and hyperfine splitting is observed. Since there is a large fraction of atoms on the surface of small particles, there may be surface effects including oxidation. This can lead to a difference in properties of surface atoms in comparison to those deep in the particle. The Mössbauer Effect affords a method of studying these features including detecting the oxidation. Mössbauer spectra of ^{57}Fe in nanoparticles of iron, some iron-cobalt alloys and iron oxides will be presented. Fe and Fe-alloys with diameter 20 nm were not superparamagnetic, but were covered with a nanometer-sized oxide layer which was superparamagentic with a T_B of about 200 K. In 20 nm nanoparticles of Fe_3O_4 (T_c = 858 K) T_B is about 100 K. A surface layer of Fe_2O_3 on the Fe_3O_4 nanoparticles did not show superparamagnetism but its Morin temperature was reduced from 260 K to 220 K. Iron oxide nanoparticles find many applications including biomedicine [2] and in information storage.

[1] M. Wautelet, J.P. Dauchot and M. Hecq, *Mat. Sci. Eng.* **C23**, 187 (2003)

[2] Q.A. Pankhurst, J. Connolly, S.K. Jones and J. Dobson, *J. Phys, D:Appl. Phys.* **36**, R167 (2003)

fo2

Numerical Device Model and Determination of Device Parameters for Organic Light Emitting Diodes (OLEDs)

T. Hirai, K. Weber, J. O'Connell, M. Bown and K. Ueno

Materials Science and Engineering, CSIRO, Clayton, Victoria 3168, Australia.

Recently OLEDs have made significant progress in brightness and lifetime to the extent that they now present themselves as a viable technology for application in large-area flat panel displays (FPD) to compete with (Liquid Crystal Display) LCD and plasma technologies. However, the operating mechanisms such as charge-injection, -transport, -trapping, and -recombination phenomena in organic semiconductors are still unclear and require further investigation. A common approach to estimate the barrier height of an organic-conductor interface is to apply the Richardson-Schottky model [1] with the value of the Richardson Factor (A*) set for a silicon-metal interface. Alternatively, J.C. Scott [2] has proposed that the value of A* for an organic-conductor interface is dependent on the state density and carrier mobility of the organic material.

Several other groups have reported experimental and measurement methods for extraction of device parameters such as carrier mobility, density of state (DOS), barrier height.[3] The impedance spectroscopy (IS) has been shown to be a useful tool for evaluating relaxation, transport and injection in a variety of organic devices.[4-5] In this paper, we propose a novel Schottky and IS numerical models to evaluate carrier injection and transport behavior of organic semiconductor materials. Using temperature dependent current-voltage (I-V) and IS measurements of hole only (HOD), electron only (EOD) devices and OLEDs, we have obtained values for A*, the barrier height, interface trap density, DOS and carrier mobility of organic materials and interfaces as device parameters, in order to understand degradation mechanisms in OLEDs.

[1] O. W. Richardson, *Philos. Mag.* **28,** 633 (1914).

[2] J.C. Scott *J.Vac.Sci.Tech.* **A21,** 521A (2003).

[3] T. Okachi, T. Nagase, T. Kobayashi, and H. Naito: *Jpn. J. Apple. Phys*. **47**, 8965 (2008).

[4] T. Hirai, K. Weber, J. H. Li, M. Bown and K. Ueno, *2011 SID International Symposium* P181.

[5] T. Hirai, K. Weber, J. O'Connell, M. Bown and K. Ueno, *2011 SSDM International Symposium* B-1-6.

fo3

Reinforcing Function of Surface Acetylated Cellulose on Polylactic Acid (PLA) based Biopolymer

T. Mukherjee, N.Kao, Rahul K. Gupta, N.Quazi and S. N. Bhattacharya

School of Civil, Environmental and Chemical Engineering, RMIT University, Melbourne, Victoria 3001, Australia.

Cellulose as available from natural fibers has been much explored as a reinforcing material in biopolymer based matrix like polylactic acid or polylactide (PLA). The property enhancements of such composites for large scale commercial applications like plastics for flexible packaging, is still elusive and pose scientific challenges. Although hydrophilic in nature, PLA is sensitive to hydrolytic degradation under melt processing condition in the presence of small amounts of moisture. Cellulose too has the tendency to form hydrogen bonds with adjacent whiskers due to the high density of hydroxyl groups on their surface, thereby resulting in agglomeration or entanglement. This phenomenon initiates cracks or failure of the composites. Surface modification of cellulose is one way to improve dispersion and thereby enhance the property of such composites for commercial viability. In this study surface modification was carried out on microcrystalline cellulose (MCC) by acetylation technique both at room and high temperature. Acetyl chloride /acetic anhydride was used for esterification reaction on the surface of MCC. Pyridine was used as a catalyst in the medium and dichloromethane was used as a solvent when acetyl chloride was used. Characterization of the acetylated group is performed by FTIR analysis. Acetylated cellulose were subsequently introduced to neat PLA at different loading (1 – 20 wt%). Level of dispersion is characterized by SEM analysis. Change in crystallinity was observed by XRD study. Improvement in elastic modulus, a key property for flexible packaging application is characterized by shear rheology. This improvement in elastic modulus for acetylated MCC in PLA based composite as compared to neat PLA, was primarily attributed to improved dispersion and strong interfacial adhesion between the filler and the matrix. The desired property enhancement aims to evaluate the potential of such composite based bioplastics for packaging applications.

[1] A.N. Frone, S.Berlioz, J.F. Chailan, D.M. Panaitescu, D. Donescu, *Polymer Composites,* vol, 32(6), p, 976 (2011)

[2] T. Mukherjee and N. Kao, *J. Polymers and the Environment.* vol, **19(3)**, p, 714. (2011)

fo4

A study of gas phase and surface formaldehyde polymerisation from first principles

P. R. McGill[a] and T. Söhnel[a,b]

[a] *School of Chemical Sciences, University of Auckland, New Zealand.*

[b] *Centre for Theoretical Chemistry and Physics, The New Zealand Institute for Advanced Study, Massey University Auckland, New Zealand.*

Formaldehyde polymerisation is a key part of formaldehyde's surface chemistry [1] and is also of considerable interest in astrochemistry [2]. Experimental evidence suggests that so-called "gas phase formaldehyde polymerisation" actually occurs on the surface of reaction vessel rather than in the gas phase [3], however thermally driven reaction mechanisms have yet to be examined by computational methods and remain largely conjectural, with studies focusing on radical and ionic mechanisms. Here we present first principles computational studies on both the gas phase and surface formaldehyde polymerisation [4]. Thermally driven gas phase polymerisation is shown to occur by way of neutral species, as opposed to earlier suggestions that a charged species may be involved. Polymerisation is shown to be thermodynamically favourable in the gas phase, but kinetically limited. Derived rate constants are insufficient to account for experimental results, confirming that "gas phase polymerisation" actually occurs on surfaces. The TiO_2 (110) surface is employed as a model surface to study formaldehyde adsorption and polymerisation mechanisms. Formaldehyde monomers are shown to weakly bind by way of coordinate bonding through the carbonyl group to surface Ti. A particularly strong dimerisation configuration is also found where the two ends of paraformaldehyde are terminated by a surface Ti and surface O.

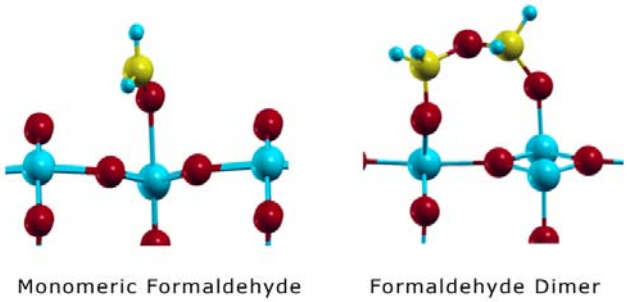

Monomeric Formaldehyde Formaldehyde Dimer

[1] J. Kim, B. D. Kay and Z. Dohnálek, *J. Phys. Chem. C*, **114**, 17017 (2010).

[2] D. E. Woon, *J. Phys. Chem. A*, **105**, 9478 (2001).

[3] J. C. Bevington and R. G. W. Norrish, *Proc. R. Soc. A*, **205**, 516 (1951).

[4] P. R. McGill and T.Söhnel, *Phys. Chem. Chem. Phys.*, (2011), DOI:10.1039/c1cp22887k.

fo5

Orbital Physics in Titanates and Vanadates

Clemens Ulrich

University of New South Wale, School of Physics, Kensington NSW 2052, Australia

ANSTO, The Bragg Institute, Locked Bag 2001, Kirrawee DC NSW 2232, Australia

Spin, charge, and orbital degrees of freedom play an important role in the various phenomena of strongly correlated electron systems like unconventional high-temperature superconductivity in cuprates or colossal magnetoresistance in manganates. In order to obtain a general understanding of the physics of 3d-electron systems, we have focused our research on three model systems with different spin-orbital structure: the titanates, vanadates, and ferrates.

Our extensive neutron scattering experiments on the cubic perovskite systems titanates and vanadates lead to the discovery of a highly unusual magnetic ground state which is in contradiction to the standard Goodenough-Kanamori rules, but indicates the presence of strong orbital fluctuations [1-4]. In particular, our investigations on YVO_3 resulted in an identification of a theoretically predicted but hitherto unobserved 'orbital Peierls state' [3]. Moreover, Raman light scattering experiments and resonant inelastic x-ray experiments allowed the observation of collective orbital excitations (termed ‘orbitons’) in $LaTiO_3$ and $YTiO_3$ [5,6].

[1] C. Ulrich *et al.*, Phys. Rev. Lett. **89**, 167202 (2002).

[2] G. Khaliullin and S. Okamoto, Phys. Rev. Lett. **89**, 167201 (2002).

[3] C. Ulrich *et al.*, Phys. Rev. Lett. **91**, 257202 (2003).

[4] G. Khaliullin *et al.*, Phys. Rev. Lett. **86**, 3879 (2001).

[5] C. Ulrich *et al.*, Phys. Rev. Lett. **97**, 157401 (2006)

[6] C. Ulrich *et al.*, Phys. Rev. B **77**, 113102 (2008).

fo6

Thermal and pressure induced spin crossover in a cobalt(II) imide complex

Suresh Narayanaswamy[a], M.G. Cowan[b], J. Olguin[b], J.L. Tallon[a], and S. Brooker[b]

[a] *MacDiarmid Institute , Industrial Research Limited, Lower Hutt, New Zealand,*

[b] *Department of Chemistry and MacDiarmid Institute, University of Otago, PO Box 56, Dunedin 9054, New Zealand*

The ground state spin state of the transition metal ion compounds can be close to the spin-crossover (SCO) transition in which case subtle structural distortions around the metal ion may favour stabilization in either the high-spin(HS) or low-spin (LS) state [1]. The ground state of these materials may in principle be reversibly interchanged under external stimuli like temperature, pressure, magnetic field or electromagnetic radiation. This bistability attracts sustained research interest due to its potential applications in molecular electronics. A prime objective is to develop SCO materials which display a hysteretic transition at room temperature.

We investigated a new mononuclear cobalt(II) compound $[Co^{II}(dpzca)_2]$ [2] using variable-temperature magnetization measurements using a SQUID, low-temperature Raman spectroscopy at ambient pressure, and high-pressure Raman measurements using a diamond anvil cell at room temperature. Magnetic measurements at ambient pressure show an abrupt, reversible and hysteretic spin crossover with $T_{½}\downarrow$ = 168 K and $T_{½}\uparrow$ = 179 K and thermal hysteresis of ~ 11K. High-pressure Raman measurements at ambient temperature show a reversible pressure-induced HS-LS transition around 0.32 GPa. Both the pressure-induced and thermally-induced transitions are remarkably sharp suggesting a thermodynamic transition rather than a mere crossover. The very large dT_c/dP coefficient suggests a rather large volumetric change in the structure at the transition. A key question is whether structural modification can replicate the pressure effect to achieve a room-temperature SCO material at ambient pressure with a sharp hysteretic transition.

[1] P. Gütlich, H. A. Goodwin, Eds. Spin Crossover in Transition Metal Compounds I. Topics in Current Chemistry; Springer: New York, Vol.**233** (2004)

[2] M.G. Cowan, J. Olguin, S. Narayanaswamy, J.L. Tallon, S. Brooker, J. Am. Chem. Soc. **DOI:** 10.1021/ja208429u (published online) (2011**)**.

fo7

Multidimensional Spectroscopy for Revealing Femtosecond Dynamics in Complex Condensed Matter Systems

G.H. Richards, C.R. Hall, J.O. Tollerud, P. Hannaford and J.A. Davis

Centre for Atom Optics and Ultrafast Spectroscopy, Swinburne University of Technology, Hawthorn, Victoria 3122, Australia.

Resolving electron dynamics in complex condensed matter, such as biological systems and semiconductor nanostructures, presents a significant challenge due to the multitude of closely spaced energy levels. Multidimensional optical spectroscopy provides a means to separate spectrally overlapping states and reveal the pathways and dynamics of electron transfer and relaxation.

This technique, which has its foundations in NMR and IR spectroscopy, is based on transient four-wave mixing experiments, where three incident pulses generate a nonlinear polarization that radiates in the direction which conserves momentum. The three incident pulses required to generate the signal beget three time domains and the conjugate frequency domains. By varying different delays and correlating the frequencies in each time domain the evolution of the system can be carefully followed.

We have developed a set of techniques which extend the capabilities of multidimensional spectroscopy to further isolate different signal pathways and provide access to previously hidden details [1-3]. In this presentation I will describe our approach to multidimensional spectroscopy and the enhancements we have made, and detail some of the insights we have been able to gain into the electron dynamics in semiconductor nanostructures [3] and biological light harvesting complexes [4,5].

[1] J.A. Davis *et al.*, Phys. Rev. Lett. **100** 227401 (2008).

[2] J.A. Davis *et al.* J. Chem. Phys. **134**, 024504 (2011).

[3] C.R. Hall *et al.* J. Chem. Phys.. **135**, 044510 (2011).

[4] J.A. Davis *et al.*, New J. Phys. **12**, 085015 (2010).

[5] G.H. Richards et al., J. Phys. Chem. Lett., (submitted).

POSTER SESSIONS

Wednesday 1.02

Abionaa	*UNSW Canb*	wp31
Ahmed	*RMIT*	wp1
Bachbuber	*Auckland*	wp23
Barthelomew	*ANU*	wp26
Bastow	*CSIRO*	wp2
Bertinshaw	*ANSTO*	wp12
Bowden #2	*UK*	wp11
Bruek #1	*ANSTO*	wp13
DuBois	*RMIT*	wp30
Finlayson	*Melbourne*	wp3
Fox #1	*Melbourne*	wp6
Goder	*RMIT*	wp7
Goossens	*ANU*	wp15
Graham	*ANSTO*	wp18
Hutchison #1	*UNSW Canb*	wp14
Jeske	*RMIT*	wp29
Kemp	*UNSW Canb*	wp32
Kulik	*UNSW*	wp22
Lang	*Israel*	wp8
Lepodise	*UoW*	wp33
Liu yanyan	*UNSW Canb*	wp9
Liu Zhiqiang	*UNSW Canb*	wp34
Marzbanab	*ANU*	wp27
Mole #1	*ANSTO*	wp16
Oitmaa #1	*UNSW*	wp19
Oitmaa #3	*UNSW*	wp20
Princep	*UNSW Canb*	wp21
Rao	*UoW*	wp35
Read	*UNSW*	wp24
Rovillain	*UNSW*	wp17
Smith	*RMIT*	wp36
Soehnel #2	*Auckland*	wp4
Thoennessen	*ANSTO*	wp5
Troup #3	*Monash*	wp10
Troup #4	*Monash*	wp25
Yildirim	*UNSW Canb*	wp37
Zhong	*ANU*	wp28

Thursday 2.02

Ahlefeldt	*ANU*	tp32
Bowden #3	*UK*	tp16
Bruek #2	*ANSTO*	tp17
Campbell	*UNSW Canb*	tp18
Cashion	*Monash*	tp30
Collocott	*CSIRO*	tp19
Cousland	*Usyd*	tp1
Deng	*ANSTO*	tp10
Ferguson	*ANU*	tp33
Gao	*UoW*	tp2
Harker	*UNSW Canb*	tp20
Hermann	*NMI*	tp7
Hutchison #2	*UNSW Canb*	tp35
Imperia	*ANSTO*	tp8
Jackson	*ANU*	tp29
Jovic	*Auckland*	tp3
Kannan	*Swinburne*	tp4
Kumar	*UNSW*	tp25
Lee	*ANSTO*	tp9
Li	*UNSW*	tp36
Liss	*ANSTO*	tp13
McIntyre	*ANSTO*	tp12
Miller	*Usyd*	tp37
Mole #2	*ANSTO*	tp11
Mulders	*UNSW Canb*	tp23
Narayanan	*UNSW Canb*	tp21
Oitmaa #2	*UNSW*	tp24
Pax	*UNSW Canb*	tp31
Rancic	*ANU*	tp34
Reynolds	*UNSW*	tp22
Shvab	*Swinburne*	tp5
Soehnel	*Auckland*	tp27
Stephen	*Wellington*	tp28
Sushkov	*UNSW*	tp26
Troup #1	*Monash*	tp14
Troup #2	*Monash*	tp15
Yigzawe	*Swinburne*	tp6

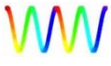

2012

ABSTRACTS FOR POSTER SESSIONS

Relative thermodynamical stability of non-stoichiometric uranium dioxide

Muhammad Hamid Ahmed

School of Applied Sciences, RMIT, Victoria 3000, Australia.

Uranium dioxide is one of the most important compounds in nuclear power industry. Uranium dioxide (UO_2), in nature, exists in hyper-stoichiometric form (UO_{2+x}) with x ranging from 0 to 0.25 [1]. On the oxidation the volume to unit cell shrinks and can possibly cause cracks in the fuel rods and also can cause problems in the handling of nuclear waste.

We determined the relative thermodynamic stability of different stoichiometric phases using the combination of ab-initio and empirical methods. The empirical potential from Twiary et al[2] was validated, for the stoheometric and non-stocheometric phase, against the ab-initio calculations. For our ab initio calculations we used DFT+U [3] formalism as implemented in Vienna Ab Initio Simulation Package. The defect free formation energies of UO_2, U_8O_{17} and U_4O_9 were calculated, which is an indicator of the stability of the structure. Furthermore, the temperature dependence, within the range of 0K to 950K, of the stability of different phases was also determined. U_8O_{17} was found to be the most stable structure through out the range, where UO_2 was the second stable and U_4O_9 was the least stable structure.

[1] Burns, P.C. and R.J. Finch, *Uranium: mineralogy, geochemistry and the environment*1999: Mineralogical Society of America.

[2] Tiwary, P., A. Van De Walle, and N. Gr¯nbech-Jensen, *Ab initio construction of interatomic potentials for uranium dioxide across all interatomic distances.* Physical Review B, 2009. **80**(17): p. 174302.

[3] Dudarev, S., et al., *Electronic Structure and Elastic Properties of Strongly Correlated Metal Oxides from First Principles: LSDA+ U, SIC LSDA and EELS Study of UO2 and NiO.* physica status solidi (a), 1998. **166**(1): p. 429-443.

Strong Interaction of an Intermetallic Platelet with its Boundary

T.J.Bastow [a], C.R.Hutchinson [b] and A.J.Hill[c]

[a] *CSIRO Materials Science and Engineering, Clayton, Victoria 3168*

[b] *ARC COE for Design in Light Metals, Materials Engineering, Monash University, Clayton, Victoria 3800*

[c] *CSIRO Process Science and Engineering, Clayton, Victoria 3168*

^{63}Cu NMR, XRD and TEM experiments have been undertaken to establish the nature of Ω platelets in aluminium alloys containing Cu and Mg and Ag . The platelets, with composition Al_2Cu lie along (111) planes of the Al host lattice, separated from the Al by a one atom thick layer of Mg and Ag atoms. Our results show that for thick platelets, where most of the platelet material is sufficiently distant from the two bounding sides, the dominant structure is exactly tetragonal Al_2Cu θ-phase, but that platelets of order 2 to 4 nm thick have a structure strongly influenced by interaction with the platelet boundary lowering the point symmetry of the Cu atom to non-axial.

NMR is a short range local probe, and a ^{63}Cu nucleus is sensitive to differences in environment up to distances of order 1 nm, so that at more than a few nm distance from the boundary the ^{63}Cu NMR signal is a superposition of the contributions from all the Cu atoms in a platelet, and is thus increasingly dominated by the contribution from Cu atoms more than about 1 nm in from the boundaries as the platelet thickens

The XRD records the (long range) structure of a crystallite (platelet) for which, as the platelet thickens, the boundary contribution becomes less significant.

NMR and XRD observations have shown a smooth transition between these two limits, while TEM observations have confirmed that the platelets remain on the $(111)_\alpha$ during the entire series of individual heat treatments, i.e. up until at least 50 (89.5) hr at 300^{o}C, where the platelets are of order 30 to 50 nm thick.

In summary, Ω Al_2Cu exists only by virtue of its interaction with the boundary which diminishes rapidly with distance into the body of the platelet. There is no phase transition between Ω and θ.

Neutron Diffraction Determination of Macro and Microstresses in an Al-Si-Mg Composite and Observed Changes with Plastic Strain

C.J. Davidson[a], T.R. Finlayson[b], J.R. Griffiths[a], V. Luzin[c] and Q.G. Wang[d]

[a] *CSIRO Process Science and Engineering, P.O. Box 883, Kenmore, Q'ld 4069, Australia.*

[b] *School of Physics, University of Melbourne, Vic 3010, Australia.*

[c] *Bragg Institute, ANSTO, Locked Bag 2001, Kirrawee, NSW 2232, Australia.*

[d] *General Motors, Powertrain Engineering, 823 Joslyn Ave, Pontiac, MI 48340-2920, USA*

Macrostresses in material components include those associated with applied forces and any long-range residual stresses such as those resulting from the component's thermal history. They are independent of the two-phase microstructure of a composite material. Microstresses, on the other hand, are associated with misfit between the phases resulting from differences in thermal expansion coefficients of the composite phases, their different elastic moduli and/or yield stresses [1]. Both macro and microstrain components can be effectively measured using neutron diffraction and the respective stress components determined. Indeed the procedure for separating the two is well documented in the literature [2].
In this presentation such an application of neutron diffraction will be illustrated for an Al-Si-Mg composite, using the Kowari beamline at the OPAL research reactor at the Australian Nuclear Science and Technology Organisation (ANSTO). Macro and microstress components for the axial, radial and hoop directions and as functions of position within cylindrical samples have been measured. In addition, the influences on these components of plastic deformation of samples, deformed by both tension and compression, have been studied. As expected, deformation (to about 1.5% plastic strain for both tension and compression) relieves the macrostress and most of the thermal microstress but sets up new residual microstreses. Experiments to study the effects of smaller plastic strains are planned and the results from these will also be presented and discussed.

[1] R.A. Winholtz, in *Encyclopaedia of Materials: Science and Technology* eds. K.H.J. Buschow, R.W. Cahn, *et al.* (Pergamon Press, 2001) p 8148.

[2] R.A. Winholtz, in *Measurement of Residual and Applied Stress Using Neutron Diffraction* eds. M.T. Hutchings and A.D. Krawitz (Kluver Acad. Pub., 1992) p 131

XPS, XAS and HRTEM studies of Rh,Pd/CeO_2 nanocatalyst activation under conditions relevant to Ethanol Steam Reforming

M. S. Scott [a], G. I. N. Waterhouse [a], K. Kato [b], S. L. Y. Chang [c], T. Söhnel [a]

[a] *School of Chemical Sciences, The University of Auckland, Private Bag 92019, Auckland, New Zealand*

[b] *JASRI, Spring-8, 1-1-1 Kouto, Sayo, Sayou-gun, Hyogo 679-5198, Japan*

[c] *MCEM, and School of Chemistry, Monash University, Victoria 3800, Australia*

Bimetallic Rh,Pd clusters have been identified as the active site in ethanol steam reforming [1]. This study delves the metallic structure by XPS, XAS, HRTEM and XRD (supplementary) to identify a partially pre-activated synthesis technique and identify the key step in reduction of the deposited metal oxides to the bimetallic clusters. Studies on the catalytic activation of Rh,Pd/CeO_2 nanocatalysts during ethanol steam reforming (ex-situ), as well as parallel spectroscopic studies of catalyst activation under reducing H_2 (ex-situ) and CO (in-situ) atmospheres are presented. The studies reveal the catalyst auto-activates under ESR conditions, with metallic Rh and Pd being the dominant noble metal species present after catalyst CO gas activation. By comparison, attempts to activate the catalyst using molecular H_2 proved largely ineffective. HRTEM showed the existence of Rh_2O_3 clusters after H_2 treatment at 400°C. CO was a far more effective reducing agent compared to H_2. The kinetics of the reduction processes depend on the metal, the strength of the metal-support interaction and also the reducing atmosphere. In general palladium is observed to undergo reduction to the metal form more readily than rhodium. Rhodium FCC structure is observed to form almost immediately during in-situ reduction with CO at 400°C (see figure) and 300°C, and more gradually at 200°C. The Pd FCC structure develops at 300°C and 200°C but not at 400°C even at a longer time scale.

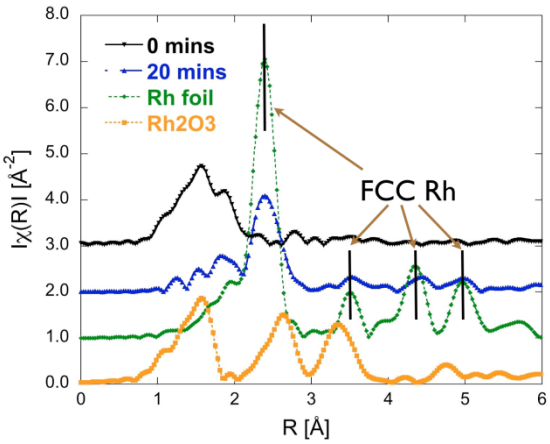

[1] H. Idriss, M. Scott, J. Llorca, S. C. Chan, W. Chiu, P.-Y. Sheng, A. Yee, M. A. Blackford, S. J. Pas, A. J. Hill, F. M. Alamgir, R. Rettew, C. Petersburg, S. D. Senanayake and M. A. Barteau, *ChemSusChem,* **1**, 905 (2008).

[2] M. S. Scott, G. I. N. Waterhouse, K. Kato, S. L. Y. Chang, T. Söhnel, submitted.

Thermomechanical Processing of Titanium Alloys

L. Thoennessen[a,b], K.D. Liss[a], R. Dippenaar[b] and A. Dehghan-Manshadi[b]

[a] *Bragg Institute, ANSTO, New South Wales 2234, Australia.*

[b] *School of Mechanical, Materials and Mechatronic Engineering, University of Wollongong, New South Wales 2522, Australia.*

Fine tuning the properties of titanium alloys will be a major challenge for future light weight structural applications in the aerospace industry [1]. The near-β titanium alloy Ti-5553 of composition Ti-5Al-5V-5Mo-3Cr (mass-%) exhibits excellent harden ability and strength characteristics combined with high fracture toughness and excellent high cycle fatigue behavior [2]. Another alloy which shows a good combination of properties, is the α+β titanium alloy Ti-6242 of composition Ti-6Al-2Mo-4Sn-2Zr (mass-%). The mechanical properties of both kinds of titanium alloys are very sensitive to their microstructure which is strongly influenced by the applied parameters during thermomechanical treatment. To control the microstructure during the processing, it is very important to have knowledge about the thermodynamics and kinetics of the phase transformations taking place under different conditions [3].

The intended research is aimed at unveiling the hot-deformation mechanisms and the development of microstructure in the aforementioned titanium alloys. This will be achieved by the comparison of results from both ex situ experiments (such as Gleeble testing, dilatometry and electron microscopy) and in situ studies. The in situ studies shall be conducted by the use of confocal microscopy and modern diffraction methods such as high intensity neutron diffraction and high energy synchrotron radiation. At the end of the research project we expect to fully understand the thermomechanical processes and precipitation behaviors of those two alloys. This understanding will help us to design new industrial processing routes for aerospace parts with better combination of strength and toughness.

[1] R.R. Boyer, R.D. Briggs, *J. Mater. Eng. Perform.*, 14 (2005).

[2] N.G. Jones et al., *Mat. Sci. Eng.*, A490 (2008).

[3] S.L. Nyakana et al., *J. Mater. Eng. Perform.*, 14 (2005).

Optimizing adhesion of parylene-C to diamond under long-term *in vivo* conditions

A. Rozario[a,b], K. Fox[a], D. Garrett[a], S. Lichter, K. Ganesan[a], H. Meffin[c], and S. Prawer[a]

[a] *School of Physics, University of Melbourne, Victoria 3010, Australia.*

[b] *School of Applied Science, Temasek Polytechnic, 21 Tampines Avenue 1, 529757 Singapore.*

[c] *National Information and Communication Technology Australia, Victoria 3010, Australia*

It is essential that materials implanted into living tissue are biocompatible. One way in which this may be achieved is by treating it or coating in with a known biocompatible material. Diamond is known to be biocompatible, however, its surface roughness and hardness may cause micromechanical tissue damage *in vivo*. To enhance its biocompatibility, it may be encapsulated with a polymeric material called parylene-C. Parylene-C is FDA approved and widely used as a commercial polymer film coating for bio-MEMS. This study aims to determine the ideal combination of treatments that would allow parylene-C to adhere most strongly to a diamond substrate.

Diamond samples were fabricated by microwave chemical vapour deposition using a gas mixture comprising argon, methane and nitrogen to generate electrically conductive nitrogen-doped ultrananocrystalline diamond. Samples were treated using oxygen plasma, a silane adhesion promoter or both. Parylene-C was deposited onto each substrate using a vapour deposition polymerization process, resulting in a thin conformal film. A control diamond substrate was coated for comparison.

The adhesion strength will be measured mechanically by the Scotch Tape test and under chemical stress within an accelerated soaking test where samples are soaked in saline over a range of temperatures and observed for coating delamination. Scanning electron microscopy, x-ray photoelectron spectroscopy, and MTTF (mean time to failure) analysis will be used to ascertain a better understanding of the adhesive or cohesive failure.

This research was supported by the Australian research Council (ARC) through its Special Research Initiative (SRI) in Bionic Vision Science and Technology grant to Bionic Vision Australia (BVA).

Study of the effect of Penetratin on the gyroid to diamond phase transition in Myverol.

Jean N D Goder[1], Nurafini A M Rafi[1], Gary Bryant[1], Taavi Hunt[1], Ben Kent[2], Chris Garvey[2]

[1.] *Applied Physics, School of Applied Sciences, RMIT University*

[2].*Bragg Institute, ANSTO*

Cell-penetrating peptides (CPPs), such as penetratin, have aroused a lot of interest in both the academic and applied research areas for their ability to penetrate cell membranes [1]. Even though there has been much work done, mostly on bilayer membranes, we still do not fully understand the mechanisms involved during this phenomenon.

In our investigation, we are going to focus on the phase transition of Myverol/Saline system from Gyroid to Diamond cubic phase in the presence of penetratin, to get an understanding of how CPPs work in a more complex system. We use a Myverol/Saline system that exhibits these types of phase behaviors at specific compositions [2]. We plan to use a variety of Small Angle Scattering techniques in an attempt to elucidate the transitional phase behavior of the Myverol/Saline system with varying concentrations of penetratin.

From this we hope to develop a model system for investigating the role of a simple peptide in changing the packing of amphiphilic molecules. In this study, we are making the use of 2 complementary techniques, Small Angle X-ray Scattering (SAXS) and small angle neutron scattering (SANS), to investigate the Myverol/Saline system as functions of both temperatures and peptide composition. We also hope to carry out DSC measurements in parallel with the SAXS. We will report on preliminary SAXS experiments carried out at the Australian Synchrotron.

[1] Dupont, E., A. Prochiantz, et al. (2011). "Penetratin story: an overview." Methods in molecular biology (Clifton, N.J.) **683**: 21-29.

[2] Clogston, J., J. Rathman, et al. (2000). "Phase behavior of a monoacylglycerol (Myverol 18-99K)/water system." Chemistry and Physics of Lipids **107**(2): 191-220.

Pyroelectric, Piezoelectric and Photoeffects in Hydroxyapatite Thin Films on Silicon

Sidney B. Lang

Department of Chemical Engineering, Ben-Gurion University of the Negev, 84105 Beer Sheva, Israel

Hydroxyapatite (HA) is the major component of bone and is used in artificial form in many biomedical applications. It was once believed to have a centrosymmetric structure. In theoretical and experimental studies published in 2005, it was shown to have a monoclinic $P2_1$ structure [1,2]. In the work reported here [3], 500-nm films of HA were spin-coated on silicon wafers. The materials were *not poled* but possessed natural polarity. Polarization distributions were determined using the Laser Intensity Modulation Method (LIMM). A true pyroelectric signature was observed by exposing the samples to a laser beam that was turned on and off at a frequency of 0.05 Hz. A pyroelectric coefficient of about 12 $\mu C\ m^{-2}\ K^{-1}$ was found. A piezoelectric coefficient of 16 $pC\ N^{-1}$ was measured by pressing and releasing a Teflon rod against the sample at a frequency of 0.1 Hz. A photoeffect due to the silicon substrate was superimposed on the pyroelectric measurements. In addition to its scientific interest, the HA/Si materials may have useful technological applications as pyroelectric/photoeffect structures.

[1] D. Haverty, S.A.M. Tofail, K.T. Stanton and J.B.McMonagle, *Phys. Rev. B* **71**, 94103 (2005).

[2] S.A.M. Tofail, D. Haverty, K.T. Stanton and J.B. McMonagle, *Ferroelectrics* **319**, 117 (2005).

[3] S.B. Lang, S.A.M. Tofail, A.A. Gandhi, M. Gregor, C. Wolf-Brandstetter, J. Kost, S. Bauer and M. Krause, *Appl. Phys. Lett.* **98**, 123703 (2011).

wp9

Localized Backside Wear Measurement on UHMWPE Prosthesis Insert Using Micro-scratching

Y.Y. Liu[a], J.A. Warner[a], L.G. Gladkis[a], J.M. Scarvell[b], P.N. Smith[b], H. Timmers[a]

[a] *School of Physical, Environmental and Mathematical Sciences, University of New South Wales, Canberra Campus, Canberra, ACT 2600, Australia.*

[b] *Trauma and Orthopaedic Research Unit, The Canberra Hospital, Canberra, ACT 2606, Australia.*

The backside wear has been considered as a potential cause of polyethylene wear particle in LCS RP mobile bearings. Due to multidirectional scratching, the backside wear may be significant. In this paper, we describe a backside wear evaluation by means of micro-scratching on UHMWPE plugs fitted into tibial inserts. Micro-scratching was carried out in four UHMWPE plugs fitted at specified positions of the tibial insert before wear test. In comparison with the depths of the micro-scratches in UHMWPE plugs with Atomic Force Microscopy before and after the wear test, it may be determined how much material was removed. Surface characterisation was also conducted by Scanning Electron Microscopy and Optical Microscopy. Following the wear test, the four plugs show little evidence of the initial micro-scratches and about 4-6 μm depth of material was removed. The results indicate that micro-scratching is a promising method for wear evaluation on UHMWPE tibial inserts.

wp10

An EPR Study of 'Mineral Organic Formula' and 'Vein Eze' Dietary Supplements

Gordon J. Troup and John F.Boas

[a] *School of Physics, Monash University, Victoria 3800, Austr*

The Monash University EPR group has a long history of investigating 'Dietary Supplements' for free radicals and antioxidant metals. 'Vein Eze' contains a grapeseed extract, so should show a free signal from the polyphenols therein. 'Organic Mineral Formula' contains Mn and Cr, which could give EPR signals.

Organic Mineral Formula gives a complex EPR signal at room temperature, in which Mn(2+) is evident, but further analysis is necessary. The 'Vein Eze' capsules contain a bitter tasting viscous brown fluid which is difficult to handle for specimen preparation in the 2mm internal diameter quartz tubes for the Bruker X-band (~ 9.4 GHz) EPR spectrometer used. Work is still in progress, and the final results will be reported at the Conference.

^{89}Y NMR-hyperfine relaxation times and transport in MBE grown $REFe_2/YFe_2$ multilayer films

G. J. Bowden[a], R. C. C. Ward[b] K. N. Martin[a], and P. A. J. de Groot[a]

[a]*School of Physics and Astronomy, University of Southampton, SO17 1BJ, UK,*

[b]*Clarendon Laboratory, Oxford University OX1 3PU, UK*

In a previous communication, ^{89}Y NMR studies of MBE-grown YFe_2, a superlattice [300Å$DyFe_2$/300ÅYFe_2]×40, and bulk powdered YFe_2 samples, at 4.2 K, was reported and discussed [1]. In particular, it was shown that there are significant differences between the ^{89}Y NMR results in bulk and MBE-grown films. In the latter, the NMR frequency (45.85±0.2 MHz) is shifted down in frequency by ~0.1 MHz, with respect to bulk (powdered) YFe_2 (45.94±0.09 MHz). In addition, the NMR line width was found to be broader in the MBE films by about a factor of two. However, more dramatically, the spin-spin lattice relaxation time T_2 was found to be almost ten times longer in the superlattice films (T_2 = 5.1 ms), than in bulk YFe_2 (T_2 = 0.6 ms). The latter was attributed to an increase in inhomogeneous line-width, which inhibits energy-conserving mutual spin-spin-flops, thereby increasing T_2. The increase in NMR-line-width was attributed to the presence of strain within the MBE films, and/or differing dipolar fields particularly near the $DyFe_2/YFe_2$ interfaces. However while the strain may well be responsible for the increase in T_2, in this communication it is argued that there is another much more plausible explanation. In practice, it is difficult to grow $REFe_2$ MBE films with a stoichiometric ratio better than 1-2%. Thus the defect density in MBE grown films is much larger than that in bulk single crystals. The presence of defects will give rise to inhomogeneity in the ^{89}Y NMR line-width. Concomitantly, defects will also affect the resistivity of the MBE-grown films, as a result of 'impurity scattering'. This interpretation is supported by transport measurements on MBE-grown YFe_2, $ErFe_2$, $DyFe_2$ and superlattice films. Despite their single crystal nature, all the films show a surprisingly low residual resistance ratio $R_{4.2K}/R_{300K}$~3-6. Thus the electron mean-free path is very short. This feature could limit the usefulness of MBE-grown $REFe_2$ thin films in spin-transport devices.

[1] G. J., Bowden, P. C. Reidi, G. J. Tomka, R. C. C. Ward, aqnd M. R. Wells (2001) *Hyperfine Interactions* **136/137:** 433–437

Neutron studies of functional multiferroic $BiFeO_3$ thin films

J. Bertinshaw[a,b], R. Maran[c], N.Valanoor[c], F.Klose[a] and C. Ulrich[a,b]

[a] *Bragg Institute, ANSTO, NSW 2234, Australia.*

[b] *School of Physics, University of NSW, NSW 2052, Australia.*

[c] *School of Materials Science and Engineering, University of NSW, NSW 2052, Australia.*

In a multiferroic material, ferromagnetism (FM) and ferroelectricity (FE) coexist, presenting exciting opportunities for research into new phenomena and technological innovation. Bismuth Ferrite ($BiFeO_3$) is among the rare cases where both properties exist at room temperature [1]. As such, its use in functional thin film heterostructures, like multiferroic tunnel junctions or exchange bias systems, which combine multiferroic (MF) and ferromagnetic layers, such as $La_{0.67}Sr_{0.33}MnO_3$ ($LaSrMnO_3$), is of particular interest [2].

In a series of resistivity based measurements [3] and neutron diffraction and polarised neutron reflectometry measurements of $BiFeO_3/LaSrMnO_3$ thin film bilayers we have investigated and found evidence of electromagnetic coupling between the layers. We use these results to provide deeper insight into the complex interplay between the orbital and spin degrees of freedom at the bilayer interface. Neutron experiments were performed at the Bragg Institute, ANSTO in Sydney, Australia, FRM-II in Munich, Germany and NRC-CNBC in Chalk River, Canada.

[1] Catalan, G. & Scott, J. Physics and Applications of Bismuth Ferrite. *Advanced Materials* **21**, 2463 (2009).

[2] Wu, S. et al. Reversible electric control of exchange bias in a multiferroic field-effect device. *Nat Mater* **9**, 756 (2010).

[3] Hambe, M. et al. Crossing an Interface: Ferroelectric Control of Tunnel Currents in Magnetic Complex Oxide Heterostructures. *Advanced Functional Materials* **20**, 2436 (2010).

wp13

Local Magnetic Structure at the Fe_3O_4/ZnO Interface

S. Brück[a,b], M. Paul[c], H. Tian[d], A. Müller[c], K. Fauth[c], E. Goering[e], J. Verbeeck[d], G. Van Tendeloo[d], M. Sing[c], R. Claessen[c]

[a]*School of Physics, University of New South Wales, Sydney NSW 2052, Australia*

[b]*Australian Nuclear Science and Technology Organization, Lucas Heights NSW 2234, Australia*

[c]*Physikalisches Institut and Roentgen Research Center for Complex Material Systems, Universität Würzburg, Würzburg, Germany*

[d]*Electron Microscopy for Materials Science, University of Antwerp, Antwerp, Belgium*

[e]*Max Planck Institute for Intelligent Systems (former Metals Research), Stuttgart, Germany*

Magnetite, Fe_3O_4, is a half-metal with 100% spin polarization of the minority band at the Fermi level. This together with its good conductivity match to standard semiconductors makes it a promising candidate for polarized spin injection into semiconductor materials such as Si, GaAs, or ZnO [1]. An important aspect for such applications is the magnetism directly at the interface between Fe_3O_4 and the semiconductor. Soft x-ray resonant magnetic reflectometry is a technique which is capable of providing structural and magnetic depth profiles with 0.1nm resolution. We present a detailed XRMR and electron energy loss spectroscopy (STEM/EELS) study of an epitaxial Fe_3O_4 thin film grown directly on a semiconducting ZnO substrate [2]. Consistent chemical profiles at the interface between ZnO and Fe_3O_4 are found from XRMR and EELS. The magnetic depth profile of tetragonal Fe^{3+} and octahedral Fe^{2+} ions in Fe_3O_4 is derived with monolayer resolution and reveals a change in the Fe stoichiometry directly at the interface.

[1] A. M Haghiri-Gosnet, T. Arnal, R. Soulimane, M. Koubaa, and J. P Renard, Physica Status Solidi (a) **201**, 1392-1397 (2004).

[2] M. Paul, D. Kufer, A. Muller, S. Bruck, E. Goering, M. Kamp, J. Verbeeck, H. Tian, G. Van Tendeloo, N. J. C. Ingle, M. Sing, and R. Claessen, Appl. Phys. Lett. **98**, 012512 (2011).

wp14

Investigation of Magnetocaloric Effects in $RNiAl_4$

W.D. Hutchison[a], N.J. Segal[a] and K. Nishimura[b]

[a] *School of Physical, Environmental and Mathematical Sciences, The University of New South Wales, Canberra, ACT 2600, Australia*

[b] *Graduate School of Science and Engineering, University of Toyama, 930-8555, Japan.*

The family of metamagnetic compounds $RNiAl_4$ (R = rare earth) exhibit a range of interesting magnetic behaviours. There are multiple magnetic phases, and crystal field driven differences in anisotropy and behaviour for different rare earth ions (R). $TbNiAl_4$ is an illustrative example. It has two phase transitions (three phases) as a function of temperature in low applied magnetic field, and at least three phases as a function of applied magnetic field at low temperature [1]. Coupled with the first of these field driven transitions is a large inverse magneto-caloric effect (MCE) [2]. Recent neutron diffraction studies on single crystal $TbNiAl_4$, in applied magnetic fields, show the onset of an incommensurate antiferromagnetic ordered phase above the first field induced phase transition [3]. The inverse MCE is associated with this reordering.

With a view to establishing the commonality of large inverse MCE across other compounds of the family, $GdNiAl_4$ and $DyNiAl_4$ are studied in this paper. These two compounds are targeted not only because of the large rare earth moments, but also, like the Tb case, they exhibit magnetic multiple phase transitions. Magnetisation data as a function of applied field and temperature is used to estimate the magnetic entropy changes associated with isothermal field sweeps, to various applied fields, and these are compared with $TbNiAl_4$. $DyNiAl_4$ is found to be potentially interesting in terms of the magnitude of the entropy change.

[1] W.D. Hutchison, D.J. Goossens, K. Nishimura, K. Mori, Y. Isikawa, A.J. Studer, *J. Magn. Magn. Mater.* **301,** 352 (2006) and references therein.

[2] L. Li, K. Nishimura and W.D. Hutchison, *Solid State Comm.*, **149**, 932-936 (2009).

[3] W.D. Hutchison, D.J. Goossens, R.E Whitfield, A.J. Studer, K. Nishimura and T. Mizushima, *submitted to PRB* (2011).

Time-Dependent Magnetisation in $Fe_{0.5}Ni_{0.5}PS_3$

S. Brazier-Hollins and D. J. Goossens

Research School of Chemistry, Australian National University, Canberra 0200 Australia.

The MPS_3 family of compounds ($M = Fe^{2+}$, Mn^{2+}, Ni^{2+}, Co^{2+}, Zn^{2+}, Mg^{2+} etc) is a series of layered materials that have potential for use as electrodes in lithium ion batteries, as host lattices for non-linear optical molecules, and as substrates for spintronics. Due to their unusual combination of layered crystal and magnetic structure and flexible substitution chemistry, they are also of considerable fundamental interest in the study of magnetism in two dimensions. Common magnetic ions give rise to a series of antiferromagnets with a range of spin dimensionalities and anisotropy-types ($M = Fe^{2+}$, Mn^{2+}, Ni^{2+} for example). $Fe_{0.5}Mn_{0.5}PS_3$ is a spin glass [1]. We have explored the magnetic properties of $Fe_{0.5}Ni_{0.5}PS_3$ and find that it shows a magnetic state whose relaxation towards equilibrium takes two to three hours. Figure 1 shows magnetisation measured on warming from ~8K (FCW and ZFCW) and on cooling from room temperature to 8K (FCC), all at a field of 1T. The pronounced shift in the critical temperature is due to the rate of change of temperature (3 K min^{-1}) preventing the sample from reaching equilibrium. Neutron diffraction shows the equilibrium magnetic structure to be related to that seen in $NiPS_3$.

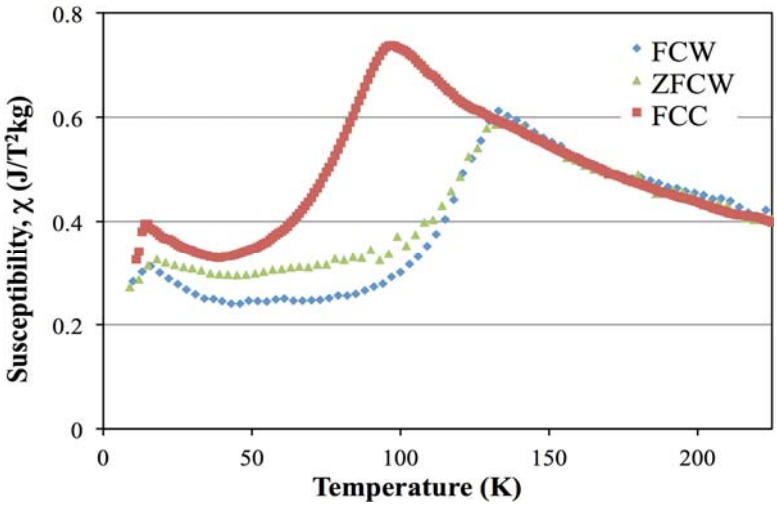

Figure 1: Magnetic susceptibility of $Fe_{0.5}Ni_{0.5}PS_3$ versus temperature at 1T measured while heating and cooling.

[1] Y.Takano, A.Arai, Y.Takahashi, K.Takase, K.Sekizawa, *J. Appl. Phys.* **93** (2003) 8197-8199.

Neutron Scattering Studies of Magnetic Coordination Polymers

R.A. Mole[a], L.F. Montero [a,b], M. Nadeem,[c] V.K. Peterson[a], R. Piltz and J.A. Stride[c]

[a] *The Bragg Institutem, ANSTO, Lucas Heights, Locked Bag 2001, Kirrawee DC, 2232.*

[b] *Institut Laue Langevin, Rue Jules Horowitz, 38042 Grenoble Cedex 9, France*

[c] *School of Chemistry, University of New South Wales, Sydney 2052, Australia*

Porous coordination polymers have been the subject of intense study over the past ten years. The key feature of these materials is a robust framework that remains in tact upon desolvation – the potential uses of these materials range from gas storage to catalysis. The current work focuses on the magnetic behaviour of these frameworks; given the nature of the structures are often low dimensional and low density magnetic topologies and the possibility exists to encorporate frustration, the magnetic properties are often of interest in there own right. If these magnetic properties could be linked to the small changes in structure associated with desolvation, the potential exists for using these materials as magnetic sensors. The material which I will focus on in this contribution, $Co_3(OH)_2(C_4O_4)_2.3H_2O$, shows an unusual three phase magnetic behaviour due to a combination of single ion effects and magnetic frustration, of particular interest is a novel spin idle phase.[1] Recently we have moved on from looking at this spin idle phase and have started to probe the incommensurate phase that proceeds it. Further we have started to study the effect of hydration on the magnetic behaviour. Previous work[2] has shown that there is a large effect on dehydration – with it being hypothesized that a switch from antiferromagnetic to ferromagnetic behaviour is observed. Our recent work has shown that although there is a very clear effect – it is due to small changes in the coordination sphere of the magnetic ion and not the hydrogen bonding pathway as previously suggested. The work has made use of a combination of both single crystal and powder neutron diffraction.

[1] R.A.Mole, J.A. Stride, P.F. Henry, M. Hoelzel, A. Senyshyn, A. Alberola, C.J.Gomez-Garcia, P.R. Raithby, P.T. Wood, *Inorganic Chemistry*, **50**, 2246 (2011)

[2] M. Kurmoo, H. Kumagai, K.W. Chapman, C.J. Kepert, *Chemical Communications*, 2005 (3012).

wp17

Electric control of spin wave modes at room temperature in $BiFeO_3$

P. Rovillain[a,b,c], R. de Sousa[d] , Y. Gallais[a], A. Sacuto[a], M-A. Measson[a], D. Colson[e], A. Forget[e], M.Bibes[f], A. Barthelemy[f], and M. Cazayous[a]

[a] *Laboratoire Matériaux et Phénomènes Quantiques, Université Paris Diderot, France*

[b] *School of Physics, University of New south Wales, Sydney 2052, Australia*

c The Bragg Institute, ANSTO, Kirrawee DC NSW 2234, Australia

[d] *Department of Physics and Astronomy, University of Victoria, Canada*

[e] *Service de Physique de l'Etat Condensé, CEA Saclay, France*

[f] *Unité Mixte de Physique CNRS/Thalès, Université Paris-Sud, France*

Multiferroic materials present the rare case to exhibit simultaneously magnetic and ferroelectric orders in interaction. This interaction corresponds to the magnetoelectric coupling. Thereby, magnetoelectric materials can potentially be used to control spins by an external electric field. This feature seems promising in spintronics and in magnonics that use magnetic excitations (spin wave) for information processing. In $BiFeO_3$, a room-temperature magnetoelectric material, the interaction between the ferroelectric and magnetic orders offers the opportunity to control spins with an electric field. We have detected by Raman scattering two species of spin propagation modes (magnon) in $BiFeO_3$ single crystal: in-plane (phi mode) and modes out of the cycloidal plane (psi mode) [1,2]. The frequencies of these modes have been successfully compared to the results of a Ginzburg-Landau mode [3]. Our result shows that the magnon modes might be interpreted as electromagnon. In order to characterize the magnetoelectric coupling, an external electric field has been applied. We show that in $BiFeO_3$, the spin-wave frequency can be tuned electrically by over 30%, in a non-volatile way and with virtually no power dissipation [4]. These results showed that $BiFeO_3$ is a very promising material for the generation and the control of spin waves in the future magnonic devices.

[1] M. Cazayous, et al. PRL, 101, 037601 (2007).

[2] P. Rovillain et al. PRB, 79, 180411 (2009).

[3] R. de Sousa and J. E. Moore, PRB, 77, 012406 (2008).

[4] P. Rovillain et al. Nature Materials, 9, 975 (2010).

wp18

Raman Scattering on Multiferroic $TbMnO_3$

P. J. Graham[a], M. Bartkowiak[b,c], A. M. Mulders[c], M. Yethiraj[b], E. Pomjakushina[e] and C. Ulrich[a,b]

[a] *School of Physics, University of New South Wales, New South Wales 2052, Australia.*

[b] *The Bragg Institute, Australian Nuclear Science and Technology Organisation, Lucas Heights, New South Wales 2234, Australia.*

[c] *School of Physical, Environmental and Mathematical Sciences, UNSW@ADFA, Canberra, Australian Capital Territory 2600, Australia.*

[e] *Laboratory for Developments and Methods, Paul Scherrer Institute, CH-5232 Villigen, Switzerland.*

Multiferroic materials are promising for their technological potential in next-generation microelectronics. They are materials that possess coexisting ferroelectric polarisation and magnetic order, and in particular cases they exhibit coupling between these parameters. This offers the possibility of manipulating ferroelectric polarisation via magnetic order and vice versa, leading to low-powered, ultra-high-capacity solid-state memory or sensor applications. At present, the physics that underpin magnetoelectric coupling in multiferroics is not entirely understood. Competing theories exist that propose different experimental outcomes. In studying the nature of excitations via Raman scattering, this research intends to provide deeper insight into such behaviour in $TbMnO_3$ and for multiferroic materials in general.

We have performed Raman spectroscopy measurements on a $TbMnO_3$ crystal and two oxygen-isotope-substituted powder samples. Anomalies in oxygen-octohedra stretching modes have been examined in respect to the sinusoidal and multiferroic phases in this material. Anomalies at T_C ~28 K may be ascribed to spin-phonon coupling or to other effects related to the coupled cycloidal-spin and ferroelectric order in the multiferroic phase. Results for anomalies between oxygen-isotope substituted samples indicate that the physical origin for these anomalies is sensitive to oxygen mass. If spin-phonon coupling is responsible for anomalies in the multiferroic phase, our results may suggest that the Dzyaloshinskii-Moriya model, as opposed to the spin-current model, more correctly describes magnetoelectric coupling in $TbMnO_3$. Further experimental and theoretical work is in preparation to explore the implications of our results for magnetoelectric coupling in this material.

wp19

Restoration of Symmetry in the Spectrum of the Bilayer Heisenberg Antiferromagnet

C.J. Hamer and J. Oitmaa

School of Physics, The University of New South Wales, Sydney NSW 2052, Australia.

We study the symmetry properties of magnetic excitations in a model, a square lattice S=1/2 bilayer, which exhibits a Quantum Critical Point (QCP) separating a magnetically ordered Néel phase from a dimer or 'valence bond solid (VBS)' phase.
In the VBS phase the elementary excitations or 'triplons' are triply degenerate S=1 states, which respect the full SU(2) symmetry of the Heisenberg Hamiltonian. On the other hand, in the Néel phase, the SU(2) symmetry is spontaneously broken and the excitations are two degenerate magnons with $S^z = \pm 1$.
As the QCP is approached from within the Néel phase, a third mode, the so-called 'longitudinal mode' [1] must become degenerate with the magnons, so that the full SU(2) symmetry is restored at the QCP. This has been recently observed in the material $TlCuCl_3$ [2]. We explicitly demonstrate this in the bilayer model, using series expansion methods [3]. We also show that the magnon mode becomes degenerate with the triplon mode in the dimerized phase at the critical point, thus showing continuity of the excitation spectrum across the critical point.

[1] A.V. Chubukov and D.K. Morr, Phys. Rev. B**52**, 3521 (1995).

[2] Ch. Ruegg et al., Phys. Rev. Lett. **100**, 205701 (2008).

[3] J. Oitmaa, C.J. Hamer and W. Zheng, *Series Expansions for Strongly Interacting Lattice Models* (Cambridge, 2006) .

wp20

Thermodynamic Properties of the Heisenberg Antiferromagnet on the Hyperkagome Lattice: Comparison with $Na_4Ir_3O_8$

R.R.P. Singh [a] and J. Oitmaa [b]

[a] *Department of Physics, University of California, Davis, CA 95616, U.S.A.*

[b] *School of Physics , The University of New South Wales, Sydney NSW 2052, Australia.*

The hyperkagome lattice is a three-dimensional lattice of corner-sharing triangles. A Heisenberg antiferromagnet on such a lattice will be characterized by strong frustration and strong quantum fluctuations, and is thus a potential candidate for exotic 'quantum spin liquid' behavior [1].

The recent discovery [2] of the material $Na_4Ir_3O_8$, in which the S=1/2 Ir^{4+} ions form a hyperkagome lattice, has led to a flurry of activity and a number of theoretical predictions, which remain unconfirmed. The material shows no long range magnetic order down to 2 K, and a large field-independent low-T specific heat, both suggestive of spin-liquid physics.

In the present work we use high-temperature series expansions [3] to compute the magnetic susceptibility, specific heat and entropy of the model. Comparison with the experimental data yields a value for the exchange constant J ~ 300K. There are discrepancies between the specific heat and entropy data and the measurements, even at high temperatures where our results are well converged. Possible reasons for this are discussed.

[1] M.J. Lawler, A. Paramekanti, Y.B. Kim & L. Balents, Phys. Rev. Lett. **101**, 197202 (2008).

[2] Y. Okamoto, M. Nohara, H. Aruga-Katori & H. Takagi, Phys. Rev. Lett. **99**, 137207 (2007).

[3] J. Oitmaa, C.J. Hamer and W. Zheng, *Series Expansions for Strongly Interacting Lattice Models* (Cambridge, 2006) .

Resonant X-ray Diffraction and the observation of Strange Quantities.

A. J. Princep[a,b], A. M. Mulders[a,b,c] E Schierle[d], E Weschke[d],J Hester[c],W D Hutchison[a] Y Tanaka[e],N Terada[f], Y Narumi[g], U Staub[h], V Scagnoli[h],T Nakamura[i], A Kikkawa[e], S W Lovesey[j,k], E Balcar[l]

[a] *School of PEMS, UNSW, Canberra, ACT, 2600, Australia*

[b] *Department of Imaging and Applied Physics, Curtin University, Perth, WA,845, Australia*

[c] *Bragg Institute, ANSTO, Lucas Heights, NSW, 2234, Australia*

[d] *Helmholtz Zentrum Berlin Mat & Energie GmbH, D-12489 Berlin, Germany*

[e] *RIKEN/SPring-8, Harima Institute, Sayo, Hyogo 679-5148, Japan*

[f] *National Institute for Materials Science, Sengen 1-2-1, Tsukuba, Ibaraki305-0044, Japan*

[g] *Institute for Materials Research, Tohoku University,Sendai 980-8577, Japan*

[h] *Swiss Light Source, Paul Scherrer Institut, CH-5232 Villigen PSI, Switzerland*

[i] *JASRI/SPring-8, Sayo, Hyogo 679-5198, Japan*

[j] *ISIS Facility, Harwell Science and Innovation Campus, Oxfordshire OX11 0QX, U.K*

[k] *Diamond Light Source Ltd., Oxfordshire OX11 0DE, U.K.*

[l] *Vienna University of Technology, Atominstitut,1040 Vienna, Austria*

Condensed matter physics has a growing reputation for providing an opportunity to observe exotic particles and states of matter that have an analogue in other areas of physics. Examples of this include the observation of Dirac strings and magnetic monopoles in spin-ice materials [1], spinon / holon separation in gated nanowires [2], and toroidal moments (anapoles) in the ubiquitous cuprates [3]. Resonant X-ray Diffraction (RXD) is well suited to the observation of a variety of quantities that behave differently under time reversal, coordinate inversion, and rotation [4]. It is possible to distinguish between competing orders and we have determined the orbital order in RB_2C_2, including higer order terms (as illustrated on the cover page) [5,6]

[1] D. J. P. Morris, et.al. *Science* **326** 411 (2009)

[2] Y. Jompol, et.al. *Science* **325** 597 (2009)

[3] V. Scagnoli et.al. *Science* **332** 696 (2011)

[4] S.W. Lovesey, et.al. *Physics Reports* **411** 233 (2005)

[5] A. J. Princep, et.al. *J. Phys.: Condens. Matter*, in print.

[6] A. J. Princep, et.al. *J. Phys.: Condens. Matter* **23** 266002 (2011)

wp22

Hole dispersion in the *t-J* model in the presence of charge modulation

Y. Kulik and O. P. Sushkov

School of Physics, University of New South Wales, Sydney NSW 2052, Australia.

We calculate the dispersion of a single hole injected in the Mott insulator. A novel component is periodic modulation of the external potential. The problem is motivated by the YBCO cuprate, where the periodic potential is generated by oxygen chains.

A quantum mechanical investigation of the crystal and electronic structures of solid solutions of pyrite-type dipnictides MPn_2 (M = Si, Ge, Ni, Pd, Pt)

F. Bachhuber[a,b], J. Rothballer[b], T. Söhnel[a] and R.Weihrich[b]

[a] *School of Chemical Sciences, University of Auckland, Private Bag 92019, Auckland, New Zealand.*

[b] *Institute of Inorganic Chemistry, University of Regensburg, Universitätsstr. 31, 93040 Regensburg, Germany.*

There is a large variety of structure types for MPn_2 (*Pn* = N, P, As, Sb, Bi) compounds with promising properties. Among these structures, a dumbbell-like arrangement of the pnictide atoms is very common. The pyrite-type SiP_2 served as a model compound for DFT calculations on electronic structure in both direct and momentum space as well as IR- and Raman spectra [1, 2]. The calculations were extended to the system $SiP_{2-x}As_x$ where P was successively substituted by As [3]. For SiPAs, an ordering scheme derived from the pyrite structure type according to [4] resulted in hetero- and homoatomic dumbbells with the first clearly preferred over the latter due to dipole momentums from the charges of P (-0.8 e) und As (-0.3 e). There are three different ordering variants for the heteroatomic configuration that slightly differ in stability (few kJ/mol).

Here we present a systematic approach on pyrite-type MPn_2 and related MPn_1Pn_2 compounds for M = Si, Ge, Ni, Pd, Pt with a special focus on the ordering of the mixed dipnictide compounds. In addition, solid solutions were modeled and examined for *Vegard* behavior. Electronic stabilities were calculated particularly for the different ordering variants of the compounds with a 1:1:1 stoichiometry. The crystal structures were analyzed by means of distinctive structural fragments as well as interatomic distances and angles. DOS and band structure plots are given to illustrate the electronic structures. Finally, preferences and tendencies within the groups of the periodic table can be derived and conclusions can be drawn on possible new compounds, which should be experimentally accessible.

[1] F. Bachhuber, J. Rothballer, P. Peter, R. Weihrich, *J. Chem. Phys.* **135**, 124508 (2011).

[2] M. Meier, R. Weihrich, *Chem. Phys. Lett.* **461**, 38 (2008).

[3] F. Bachhuber, J. Rothballer, R. Weihrich, *Z. Anorg. Allg. Chem.* **636**, 2116 (2010).

[4] R. Weihrich, D. Kurowski, A.C. Stückl, S. Matar, F. Rau, T. Bernert, *J. Solid State Chem.* **177**, 2591 (2004).

Self-energy effects and the unbound electronic structure of Cu(111) surface

M. N. Read

School of Physics, University of New South Wales, Sydney 2052, Australia

Over-layered atomic species on metal substrates exhibit surface electronic states that may have technological applications at room temperature [1]. Experimental methods such as (spin) angle-resolved photoemission spectroscopy, (S)ARPES, measure surface and bulk occupied states by utilizing electron transitions to final evanescent (spatially attenuating) states above the vacuum level. A priori knowledge of the bulk and/or surface electronic band structure of these unbound states is required for analysis. There are very few realistic calculations of the bulk band structure and even less calculations of the surface band structure in this energy range.

Here we use a semi-empirical scattering method [2] to calculate the bulk and surface electronic band structure of Cu(111) at the Γ–point for the energy range from 8 eV below the Fermi level to 145 eV above it. Information of the energy variation of the crystal-vacuum potential barrier and the real and imaginary parts of the electron self-energy are required and these are found from an analysis of low-energy electron diffraction (LEED) intensity data. We identify the symmetry of the unbound bulk evanescent states at Γ with respect to the mirror plane of the Cu(111) surface. We find six unbound surface state resonances at 26, 28, 35, 69, 90 and 120 eV above vacuum level. There does not appear to be any other calculations of surface electronic bands in this energy range for Cu(111). As these surface state resonances do not have dispersion with respect to the perpendicular wave vector component as bulk states do they may find use as final states for high-resolution ARPES studies once they are experimentally verified. In particular the predicted unbound first-order image resonance states at 28, 90 and 120 eV with respect to the vacuum level have significantly less broadening (or inverse lifetime) due to inelastic effects than other unbound states and use of these image resonance states may provide a major advantage for ARPES analysis.

[1] J. Hugo Dil, *J. Phys.: Condens. Matter* **21**, 403001 (2009).

[2] M. N. Read, *arXiv*:1104.0977v1[cond-mat.mtrl-sci].

wp25

Cutting Entanglement

Gordon J. Troup, David Paganin, and Andrew Smith
School of Physics, Monash University, Victoria 3800, Australia

This paper is written in the spirit of not unnecessarily complicating things when teaching Quantum Mechanics is concerned. 'Entanglement' can be found in modern research and teaching articles when it is unnecessary. An outline is given of a suggested teaching sequence. Emphasise the fact that the conservation laws of momentum and angular momentum are sufficient to explain the fact that if the values of these in a 'separation' of 'identical' 'twins' is known for one of the twins, then the values for the other twin must be known. Examples are: A Newtonian 'bomb' exploding into two equal parts: 'electron' pair annihilation; and 'electron' pair production, especially when the observation of the spin direction is at an angle to the initial spin direction. The 'two slit' interference experiment is explained by the Heisenberg uncertainly principle, and not by entanglement.

Schrodinger's 'Cat experiment' has to be mentioned for historical reasons, as does the EPR thought experiment, for their errors; Bell inequalities refer to research to detect 'hidden variables'.

So, having said what Entanglement is not, one goes to the theory of q-bits, where entanglement is necessary.

A perhaps loose definition of entanglement ii a situation where, if we look for correlation, it is either greater or less than what we would get with a classical explanation. Think about photon counting. It is well known that if a Bose-Einstein distribution of the photons is observed, the probability of a second photon being observed after a first one is detected, is twice that of the average probability. Does this mean that we have been controlling the entanglement of photons ever since Marconi developed radio, without knowing it? It is called modulation.

Optical detection of a single rare earth ion in a solid state host

J. G. Bartholomew[a] and M. J. Sellars[a]

[a]*Centre for Quantum Computation and Communication Technology, Laser Physics Centre, Australian National University, ACT 2600, Australia*

Despite the wealth of knowledge regarding the physical properties of rare earth ion dopants in crystalline hosts, few researchers have focussed their attention on a single site[1-3]. This has been the case because the very properties which make ensembles of rare earth ions attractive in fields such as quantum communication[4] make them inherently unsuitable for the optical detection of a single emitter[5]. However, via ultra-high frequency resolution and stability, coupled with diffraction limited spatial selectivity it is possible to achieve this feat.

Attempts to detect a single site have been undertaken in a macroscopic crystal of 0.005% Pr^{3+}:Y_2SiO_5 at 4 K where the homogeneous linewidth is on the order of 20 kHz. A ring dye laser operating at 606 nm was externally stabilised producing a sub-kHz linewidth with a drift rate less than 4 kHz over several minutes. This, in conjunction with a home built confocal microscope and a solid immersion lens, allows for a single ion to be isolated within the collection volume. Temporal filtering was used to resolve the the collected emission from the excitation photons, which reduces the background signal to the dark counts of the detecting avalanche photodiode. The excitation pulse sequence and an overall detection efficiency of approximately 1% gave a peak signal on the order of 10 photons per second.

Detection of a single rare earth ion provides future possibilities in several directions. The first is to harness the single ion for applications such as investigations into cavity QED. The second is to utilise the previously unattained resolution to study important processes such as the nature of inhomogeneous broadening of dopant transitions in crystalline host materials.

[1] Schniepp, H., and V. Sandoghdar, *Physical Review Letters,* 89, 1- 4 (2002)

[2] Bartko, A. P. *et al., Chemical Physics Letters,* 358, 459-465 (2002)

[3] Malyukin, Y. V. *et al., Physics Letters A,* 316, 147-152 (2003)

[4] Thiel, C.W., T. Böttger, and R. L. Cone, *Journal of Luminescence,* 131, 353-361 (2011)

[5] Moerner, W. E., *Journal of Luminescence,* 60-61, 997-1002 (1994)

wp27

Spectroscopic Properties of Eu3+: Y2O3 Thin Films

J.G. Bartholomew[ab], S. Marzban[ab], M.J. Sellars[ab] and R.P. Wang[a]

a *Laser Physics Centre, Australian National University, ACT 2600, Australia*

b- Centre for Quantum Computation and Communication Technology, Australian Research Council

A highly efficient and low noise quantum memory for light in a rare earth ion doped crystal has recently been demonstrated [1]. Research now focuses on how to realize a practical device for quantum communication. One area of interest is the construction of rare earth ion doped crystalline waveguides [2]. Among the advantages of such structures is the ability to apply very strong electric fields which would enable the current bandwidth of the memory to be increased significantly.

Through the use of pulsed laser deposition, single crystals have been grown epitaxially onto compatible substrates. Materials including rare earth ion doped Y2O3 and YAG can be grown to a subwavelength thickness. However, the critical issue is determining the growth conditions to preserve the long optical coherence times measured in bulk samples at liquid helium temperatures. Growth conditions include growth temperatures, distance between target and substrates, base pressure in the vacuum chamber, etc. Also, the target and substrate materials need to have good lattice matching in order to get single crystalline thin films.

The characterization of the optical properties of the rare earth ions in the crystalline films can be performed via several techniques including inhomogeneous broadening spectra, holeburning spectroscopy and photon counting-photon echo (PCPE) studies. Of these, the last is the most critical technique for determining whether such films are suitable for waveguide quantum memories. The PCPE technique allows coherent signals to be detected from as few as a thousand optically active ions with minimum signal detection on the order of 30 photons per second. Thus, it is feasible to study the performance of the optical centres in films as thin as 10s of nanometers.

[1] M. P. Hedges, J. J. Longdell, Y. Li, and M. J. Sellars, Nature **465**, 1052-1056 (2010).

[2] N. Sinclair, E. Saglamyurek, M. George, *et al*., *Journal of Luminescence,* **130**(9):1586-1593 (2010).

Extending Hyperfine Coherence Times in $EuCl_3.6H_2O$

M. Zhong, M. J. Sellars

Centre for Quantum Computation and Communication Technology, Research School of Physics and Engineering, The Australian National University, Canberra, Australian Capital Territory 0200, Australia.

Long coherence times are of great significance in quantum computing and quantum information schemes proposed for rare earth ions.

We present a method for extending the coherence times of europium hyperfine ground state transitions in stoichiometric $EuCl_3.6H_2O$ by suppressing the first order Zeeman shift on the transition of interest. We have previously employed this technique to increase the hyperfine coherence time from 550 us to 1.4 seconds in Pr^{3+}:Y_2SiO_5.[1] The principle of the technique is to applying a specific external magnetic field magnitude and direction such that the Zeeman splitting of a hyperfine transition is at a turning point which makes the linear Zeeman shift about this field value vanish, thus reducing the dominant hyperfine dephasing mechanism of nuclear spins fluctuations in the crystal perturbing the target rare earth ions.

With theoretical calculation and a simple model of dephasing mechanism [2], if a magnetic magnitude about 2.5 Tesla along the C_2 axis of the $EuCl_3.6H_2O$ is applied, the hyperfine coherence is expected to be of the order of 10 minutes. We will report on preliminary experimental results.

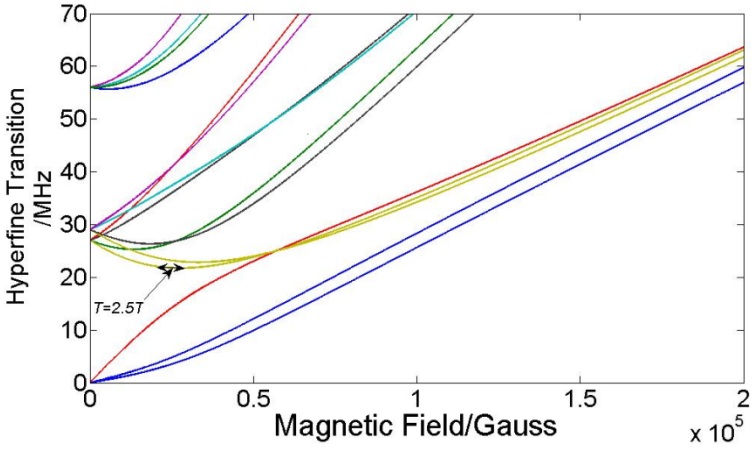

FIG.1
The ground state hyperfine transition with the presence of external magnetic field along the C_2 axis. The magnitude of the field varies from 0 to 2 Tesla.

[1] E. Fraval, M. J. Sellars, J. J. Longdell, Phys. Rev. Lett. 92 (7)(2004) 077601.

[2] J. J. Longdell, A. L. Alexander, M. J. Sellars, Phys. Rev. B74 (19) (2006) 195101-7

wp29

Quantum decoherence in complex environments

Jan Jeske[a] and Jared H. Cole[a]

[a] *Chemical and Quantum Physics, School of Applied Sciences, RMIT University, Melbourne 3001, Australia*

All current realizations of quantum systems experience a rather strong environmental perturbation commonly referred to as decoherence, which destroys all quantum effects after a certain coherence time. A deeper physical understanding of this process is a key component to enable future quantum technology and can be used to infer information about the environment on the nanoscale where the quantum systems act as probes.

We investigate decoherence processes theoretically beyond the standard model of (Markovian) uncorrelated perturbing fluctuations and consider coherent environmental pockets which interact with the system as well as spatially correlated fluctuations. Coherent pockets in the environment can be systems such as two-level fluctuators around superconducting qubits or ^{13}C spins in the diamond lattice around nitrogen-vacancy-centre qubits. These environmental two-level systems can be fully characterized using two qubit-probes due to the unique induced (non-Markovian) oscillating dynamics. Decoherent environments with spatially correlated fluctuations do not induce oscillations. However the spatial correlations can lead to a cancellation of decoherence depending on the environmental correlation length compared to the length of the coherent system dynamics.

The new effects of complex environments (coherent pockets or spatially correlated fluctuations) are discussed and the possibilities of probing such environments with qubits are explored.

.

[1] Jan Jeske, Jared H. Cole et al; Dual-probe decoherence microscopy: Probing pockets of coherence in a decohering environment, arXiv:1110.1945

Delocalised Oxygen model of TLS defects in superconducting phase qubits

Timothy C. DuBois, Manolo C. Per, Salvy P. Russo and Jared H. Cole
Chemical and Quantum Physics, School of Applied Sciences, RMIT University, Melbourne 3001, Australia.

One of the greatest challenges to the realisation of quantum computing is controlling or removing mechanisms that contribute to quantum decoherence in the underlying circuitry. Josephson junctions underpin most quantum circuits (superconducting qubits, single electron transistors & SQUIDS) and are also becoming incredibly useful in the fields of metrology and astronomy. Obtaining long coherence times in superconducting qubits has always been mired by the presence of microscopic two-level systems (TLSs) that cause critical current or charge fluctuations. TLSs have been located in flux, charge, phase and transmon qubits; therefore understanding these systems has become a major field of study. Charge dipoles, Magnetic dipoles and Andreev bound states are the most investigated phenomenological models that attempt to describe TLS behaviour, but are currently indistinguishable as parameters for each model can be fitted to experimental data. In this study, we investigate a microscopic model which focuses on delocalised oxygen atoms in the amorphous layer of the Josephson junction to better describe the TLS.

Characterization of a Defect-Pair in Germanium

Adurafimihan A. Abiona[a,*], William J. Kemp[a], Mark C. Ridgway[b], Heiko Timmers[a]

[a] *School of Physical, Environmental and Mathematical Sciences, The University of New South Wales, Canberra Campus, ACT 2602, Canberra, Australia.*

[b] *Department of Electronic Materials Engineering, Research School of Physics and Engineering, Australian National University, Canberra, ACT 200, Australia.*

Low temperature metal-induced-crystallized germanium is a promising alternative for silicon in Complementary Metal-Oxide-Semiconductor (CMOS) technology [1]. Palladium is one of the suitable metals to induce the low temperature crystallization. It is not clear, how residual Pd-atoms are integrated into the Ge-lattice. Towards answering this question, hyperfine interaction measurements with the ^{100}Pd/^{100}Rh probe in undoped germanium were performed using Time Differential Perturbed Angular Correlation (TDPAC) Spectroscopy.

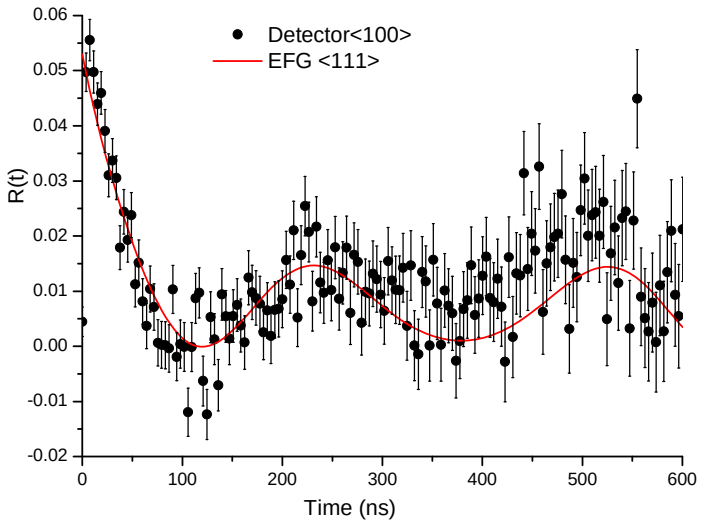

Data from three separate TDPAC measurements show that a substitutional palladium atom tends to pairs with a defect, resulting in a quadrupole interaction frequency of 8.3(2) Mrad/s. This is most pronounced after annealing at 500 °C. The analysis of crystallographic orientation measurements along the <100> (see the ratio function in the figure), <110> and <111> directions of germanium consistently indicate that the palladium pairing orientation could be along a <111> direction, as expected from highly doped n-type silicon [2], or along a <110> direction, but not along a <100> direction.

[1] P *Jin-Hong et al., IEEE International Electron Devices Meeting (IEDM), Technical Digest, 389 (2008)*

[2] R. Dogra et al., *Journal of Electronic Materials* **38,** 623 (2009).

* *On leave from Centre for Energy Research and Development, Obafemi Awolowo University, Ile-Ife, Nigeria.*

First measurements of the quadrupole coupling constant for ^{100}Pd/Rh in antimony, hafnium and rhenium

William J. Kemp[a], Adurafimihan A. Abiona[a,*], Patrick Kessler[b], Reiner Vianden[b], Heiko Timmers[a,c]

[a] *School of Physical, Environmental and Mathematical Sciences, The University of New South Wales, Canberra Campus, ACT 2602, Canberra, Australia*

[b] *Helmholtz-Institut für Strahlen- und Kernphysik, Nußallee 14-16, 53115 Bonn, Germany*

[c] *Department of Nuclear Physics, Research School of Physics and Engineering, Australian National University, Canberra, ACT 200, Australia*

[*] *on leave from Centre for Energy Research and Development, Obafemi Awolowo University, Ile-Ife, Nigeria*

Time differential perturbed angular correlation (TDPAC) spectroscopy in zinc, rhodium, antimony, hafnium and rhenium was performed with the rare ^{100}Pd/Rh probe. The probe was synthesized using the ^{92}Zr(^{12}C,4n)^{100}Pd fusion evaporation reaction, with evaporation residues recoiling into specimens of the metals. TDPAC was performed using four NaI detectors in a standard setup with relative angular orientations of 90° and 180°, respectively. Ratio functions have been obtained by combining the time-differential coincidence spectra from the detectors and subtracting statistical background. The apparent modulations on these ratio functions have been fitted. Results confirm expectations for zinc and rhodium and provide the first measurements of the quadrupole coupling constants for the three other transition metals with measured values of ν_Q = 4.3 MHz, 5.7 MHz, and 3.2 MHz, respectively. These three coupling constants appear to be consistent with published results for zirconium and ruthenium.

wp33

Absorption Lines around 70 Mev in Rubidium Bromide (RbBr)

L. M. Lepodise and R. A. Lewis

Institute for Superconducting and Electronic Materials, University of Wollongong, Wollongong, New South Wales 2522, Australia

The terahertz transmission of rubidium bromide (RbBr) has been measured in the mid- and far-infrared. This material, unlike other alkali halides, displays sharp absorption lines in its transmission spectrum between 550 cm^{-1} and 650 cm^{-1}. At room temperature RbBr exhibits four4 lines at 587.83 cm^{-1}, 609.00 cm^{-1}, 623.70 cm^{-1} and 634.94 cm^{-1}. The position, the width and the strength of these lines are found to be temperature sensitive. As the sample is cooled the line positions shift on average about 0.1 cm^{-1} and the line width reduces by about 0.1 cm^{-1} also on average. The lines also become stronger. The spectra were collected at the temperatures of 50 K to 300 K in 25 K steps. As the temperature is lowered, there is a development of some other lines. For temperatures 300 K to 200 K there were four lines only, while the fifth line started appearing at 175 K at 611.22 cm^{-1}. More lines which are less distinct start appearing at 50 K at 613.43 cm^{-1}, 621.92 cm^{-1}, 629.15 cm^{-1} and 631.85 cm^{-1}. The optical spectrum of rubidium bromide has been measured previously, but in the ranges from 5.5 to 12 eV [1], far from the present spectral region.

[1]. K. Teegarden and G. Baldini, *Physical Review* **155**, 896 (1967).

Photoluminescence and Crystallographic Sites of Sm ions in BaFCl Nanocrystals

Z. Liu and H. Riesen

School of Physical, Environmental and Mathematical Sciences, The University of New South Wales, PO Box 7916, Canberra BC, ACT 2610, Australia.

Nanocrystalline BaFCl:Sm^{3+}, as prepared by co-precipitation from aqueous solutions, is an efficient photoluminescent storage phosphor for ionizing radiation [1,2]. It has potential applications in medical imaging and personal radiation monitoring (dosimetry). Upon X-ray, γ-ray or β-irradiation, the Sm^{3+} ions in the BaFCl host are reduced to Sm^{2+} ions which can be read out efficiently by measuring the narrow ^5D_J-^7F_J *f-f* luminescence lines via excitation into the very intense, parity-allowed $4f^6 \rightarrow 4f^5 5d$ transition in the blue-violet region of the spectrum. In the present work, the photoluminescence properties of nanocrystalline BaFCl:Sm^{3+} before and after X-irradiation were investigated from 2 to 293 K. Upon X-irradiation, significantly different sites of Sm^{3+} ions were identified below 80 K compared with those before X-irradiation, implying a change of the local coordination environment of Sm^{3+} ions by X-irradiation. For the Sm^{2+} ions generated by X-rays, photoluminescence was observed in five inequivalent sites below 120 K whereas two sites were observed at 293 K. In addition, the photobleaching effect on the crystallographic sites of Sm^{3+} and Sm^{2+} ions in nanocrystalline BaFCl were also studied. These results are of significance for a full understanding of the storage mechanism which would lead to the design of other Sm^{3+} activated materials with even higher storage efficiencies.

[1] H. Riesen and W.A. Kaczmarek, *International PCT application WO 2006063409-A1* (2005).

[2] Z. Liu, T. Massil and H. Riesen, *Physics Procedia* **3**, 1539 (2009).

wp35

Emissivity of Silicon Carbide in THz Spectral Range

M. M. Rao and R. A. Lewis

Institute for Superconducting and Electronic Materials, University of Wollongong, Wollongong, New South Wales 2522, Australia

The globar, which is constructed from silicon carbide, is a common radiation source used in far-infrared and terahertz spectroscopy [1]. Often the silicon carbide is considered to be a blackbody of emissivity one. However, a more realistic representation should consider it to be a grey body with an emissivity of less than one. By using a silicon carbide globar as a high temperature source of continuous radiation and a thermopile detector we have attempted to determine a more accurate emissivity of a Globar. The thermopile was calibrated using a number of different radiation sources. The temperature of the globar was varied by applying different electrical currents. The emissivity is deduced from the Stefan-Boltzmann law (the total absolute power of energy radiated being $P = A\varepsilon\sigma T^4$).

[1] M. L. Smith, R. Mendis, R. E. M. Vickers, and R. A. Lewis, *J. Appl. Phys.* **105**, 063109 (2009).

Density functional study of epitaxially-doped nanowires of phosphorus in silicon

J. S. Smith[a], D. W. Drumm[b], A. Budi[b], M. C. Per[a], L. C. L. Hollenberg[b] and S. P. Russo[a]

[a] *Chemical and Quantum Physics, School of Applied Sciences, RMIT University, Melbourne 3001, Australia.*

[b] *School of Physics, The University of Melbourne, Parkville 3010, Australia.*

We present the first *ab initio* calculations of epitaxially-doped phosphorus nanowires in silicon. Density functional theory has been used to investigate the electronic properties of two possible configurations. The configurations reflect what is experimentally achievable with current "bottom-up" epitaxial approaches to fabrication. The nanowires consist of two phosphorus atom rows in the [110] direction with layers of silicon cladding placed perpendicularly to minimise interactions between periodic images. The phosphorus atoms are added substitutionally to bulk Si creating a quasi-one-dimensional wire. They are spaced differently in each configuration, with four and six chemical bonds separating the P donors. We find both configurations to have channels open for conduction and the charge density of the wire to be highly localised around the P donors, decaying sharply with distance into the Si cladding. The results presented here are for nanowires incorporating 40 monolayers of Si cladding. With this level of cladding, the charge density of the wire decays significantly from its maximum value (to less than 0.01%) by the edge of the structure. From our results, we also calculate the effective masses of the conduction electrons and find these to match well to values reported in the literature.

Structural and Optical Properties of Nanocrystalline $LiGa_5O_8:Fe^{3+}$

Baran Yildirim[a], Glen Stewart[a] and Hans Riesen[a]

[a] *School of Physical, Environmental and Mathematical Sciences, The University of New South Wales, ADFA, Canberra, ACT 2600, Australia.*

Detailed Mössbauer, X-ray structural and optical investigations of nanocrystalline Fe^{3+} doped lithium gallate ($LiGa_5O_8:Fe^{3+}$) were carried out. The charge distribution and ground state hyperfine splitting have been analyzed in comparison with Mössbauer and transient spectral hole-burning experiments. We are mainly interested in the coordination state distribution of Fe^{3+} in the Ga rich system as we have previously observed that the luminescent Fe^{3+} ions occupy tetrahedral sites both in the ordered and the disordered phase [1]. The Ga^{3+} ions have slightly higher preference for tetrahedral sites than Fe^{3+} ions, thus site distribution varies compared to Fe rich samples [2]. A similar dependence on the dopant level has been observed also in Co^{2+} doped samples. The phase stabilization of the spinel structure with *Fd3m* space group, that has been reported previously for TM^{2+} doped systems, has been observed for ≥5% doping levels; the structure stays in the face centered phase due to the replacement of Li^{+} ions in the octahedral sites by TM^{2+} ions or with some TM^{3+} doping Li^{+} ions are forced to migrate to the tetrahedral sites [3]. In both cases, ordering in the octahedral sites is disturbed for the mentioned doping levels. Relevant to this observation, the Li ordering in octahedral sites affects the hyperfine parameters [4]. Those parameters are well defined for the isostructural $LiAl_5O_8:Fe^{3+}$system [5]. In addition to Li ordering, the Ga systems have the tendency to form clusters upon doping [6]. In order to elucidate these phenomena, hyperfine parameter values were correlated with the previous findings.

[1] Riesen H., Chem. Phys. Letters 461, 218-221 (2008)

[2] Neto J.M., Domingues P.H., Barros F de S., Guillot M., Barthem V.M.T.S., Jour. Phys. C:Solid State Phys., 19, 5721-5728 (1986)

[3] Rogers D.B., Germann R.W., Arnott R.J., Jour. of Applied Phys., Vol. 34, No. 8 (1965)

[4] Dormann J.L., Tomas A. , Nogues M., Phys. Stat. Sol., 77, 611 (1983)

[5] Viccaro P.J., Barros F. de S., Oosterhuis W.T., Phys. Review B, Vol 5. No 11, 4257-4264 (1972)

[6] Rao E.N., Ghose J., Mat. Res. Bull., Vol. 22, 951-956 (1987)

tp1

The structure of Yttria-stabilised Zirconia: a combined synchrotron photoemission, neutron scattering and ab-initio investigation

G.P. Cousland[a,b], R. Mole[b], M. Elcombe[b], X.Y. Cui[a,c], A.E. Smith[d], C.M. Stampfl[a] and A.P.J. Stampfl[b,e]

[a] *School of Physics, The University of Sydney, Australia.*

[b] *Australian Nuclear Science and Technology Organisation, Lucas Heights, Australia.*

[c] *Australian Centre for Microscopy & Microanalysis, The University of Sydney, Australia.*

[d] *School of Physics, Monash University, Clayton, Australia.*

[e] *School of Chemistry, The University of Sydney, Australia.*

Zirconia-based materials have possible applications in high-temperature fission and fusion environments. Zirconia can be stabilised to room temperature by the addition of yttria to form yttria-stabilised zirconia (YSZ). YSZ is interesting because it retains strength at high temperature and is resistant to neutron bombardment. The structure of YSZ is investigated by comparing results from ab-initio calculations with those from x-ray photoemission and inelastic neutron scattering experiments. This analysis considers two candidate models for YSZ at 9.375 Mol % yttria, one with a supercell of 93 atoms and another with a 186 atom supercell. These structures are constructed using constraints based on findings from first-principles calculations [1] and results from neutron scattering and x-ray measurements [2]. A method is used that studies the shift in Auger and photoemission core-levels. Predicted core-energies are obtained from density functional calculations and are correlated to deconvoluted peaks of zirconium, yttrium and oxygen within photoemission spectra. This is done in order to corroborate the local structure of YSZ at this particular yttria concentration. Attention is also focused on any long range order of yttrium and vacancies. Inelastic neutron scattering experiments are conducted to determine the periodic nature of dopant and vacancy and then results compared to potential model structures. Work will be extended to investigate YSZ samples containing higher yttria concentrations of e.g. 14, 17, 20 and 40 Mol percent.

[1] A. Bogicevic, C. Wolverton, G.M. Crosbie, and E.B. Stechel, *Phys. Rev. B* 64, 014106 (2001).

tp2

5 V $LiNi_{0.5}Mn_{1.5}O_4$ Spinel Cathodes Using Room Temperature Ionic Liquid as Electrolyte

Xuan-Wen Gao [a], Chuan-Qi Feng [b], Shu-Lei Chou [a, f*], Jia-Zhao Wang [a, f*], Jia-Zeng Sun [c, ,f], Maria Forsyth [d, f], Douglas R. MacFarlane [e, f], Hua Kun Liu [a, f]

[a] *Institute for Superconducting and Electronic Materials, University of Wollongong, Wollongong, NSW 2522 Australia*

[b] *College of Chemistry and Chemical Engineering, Hubei University, Wuhan 430062, China*

[c] *Department of Materials Engineering, Monash University, Clayton, Victoria 3800, Australia*

[d] *Institute for Technology Research and Innovation, Deakin University, Geelong, Vic 3217 Australia*

[e] *School of Chemistry, Monash University, Clayton, Victoria 3800, Australia*

[f] *ARC Centre of Excellence for Electromaterials Science, University of Wollongong, Wollongong, NSW 2522, Australia*

In this study, $LiNi_{0.5}Mn_{1.5}O_4$ nanoparticles were prepared as a 5 V cathode material via a rheological phase method. A room temperature ionic liquid (RTIL) with good electrochemical and thermal stability, high ionic conductivity, non-volatility, and non-flammability was used as electrolyte. The electrochemical measurements showed that the $LiNi_{0.5}Mn_{1.5}O_4$ annealed in 750 °C using 1 M lithium bis(trifluoromethanesulfonyl) imide (LiTFSI) in N-butyl-N-methyl-pyrrolidinium bis(trifluoromethanesulfonyl) imide (Py14TFSI) as electrolyte shows comparable capacity to the same material used with conventional electrolyte (1 M $LiPF_6$ in ethylene carbonate: diethyl carbonate (EC:DEC) = 1:2 (v/v)) with improved coulombic efficiency. Electrochemical impedance spectroscopy shows that the RTIL is much more stable as electrolyte for $LiNi_{0.5}Mn_{1.5}O_4$ than the conventional electrolyte.

tp3

Development of novel visible-light driven photocatalysts for hydrogen production

V. Jovic[a], G.I.N Waterhouse and T. Söhnel[a]

[a] *Department of Chemistry, The University of Auckland, Auckland 1142, New Zealand.*

Hydrogen (H_2) powered fuel cells, electrochemical devices that combine H_2 and O_2 to produce electricity, water and heat, are expected to play a key role in both automotive and stationary power applications of the future. This project supports the development of a sustainable H_2 energy economy, and is aimed at the development of efficient visible light driven photocatalysts that can harness sunlight to transform ethanol (CH_3CH_2OH, a renewable biofuel) into H_2 and CO_2. Our approach is based around the fabrication of novel Au/Ce-doped Titania materials with inverse opal structures - materials that possess a 3-dimensioanlly ordered macroporous structure and photonic band gaps (PBG) at visible wavelengths.[1] At the low energy edge of the PBG light propagates with a strongly reduced group velocity, enhancing interaction between incident light and material.[2] Our previous studies have shown that the physical and optical properties of the inverse opals can be selectively tuned and optimized to enhance the efficiency of titania-based photocatalysts under UV irradiation. In the present study, we doped Ce^{3+} (0-4 wt %) into the anatase TiO_2 inverse opal bulk, in order to manipulate the electronic absorption edge of TiO_2 and shift it into the visible region. Surface Au nanoparticles (0.5-10 wt %, diameter 3-6 nm)[3] allow for the reduction of hydrogen protons, formed by the photo-oxidation of ethanol, to molecular hydrogen. Also, fully-vectorial eigenmodes of Maxwell's equations with periodic boundary conditions were computed for each of the inverse opal materials. The simulated structure and resulting dispersion relations showed strong agreement with experimental optical data. Hence, through a coupled manipulation of the electronic and optical absorption bands in these materials, we have developed efficient visible light driven photocatalysts for hydrogen production.

[1] E. Yablonovitch, T.J.Gmitter. *Phys. Rev. Lett.* **18**, 1950-1953 (1989)

[2] J. I. L, Chen, G. von Freymann, S.Y. Choi, V. Kitaev, G.A. Ozin, *J. Mater. Chem,* **18**, 369-373 (2008)

[3] A. Hugon, L. Delannoy, L & C, Louis. *Gold Bulletin.* **41**, 127-138 (2008)

tp4

Flow rates of fluids in carbon nanotubes

Sridhar Kumar Kannam[1+], B. D. Todd[1]*, J. S. Hansen[2], Peter. J. Daivis[3]

[1]*Mathematics Discipline, Faculty of Engineering and Industrial Science and Centre for Molecular Simulation, Swinburne University of Technology, Melbourne, Australia.*

[2]*DNRF centre "Glass and Time", IMFUFA, Roskilde University, Roskilde, Denmark.*

[3]*School of Applied Sciences, RMIT University, Melbourne, Australia.*

The hydrodynamic boundary condition (BC) is now a subject of greater significance than ever before, though the problem has existed from the beginning of the 19th century.[1,2] Since then, many researchers have attempted to formulate a general BC at a fluid-solid interface. The 21st century has seen revolutionary advancements in nanoscience and nanotechnology, which in turn, poses many fundamental questions about the nature of fluid flow in nanometric pores such as carbon nanotubes (CNTs) and aquaporins. Among them the most important is the BC.[3,4] Recently we proposed a method to calculate the interfacial friction coefficient between fluid and solid which determines the BC.[5,6] We apply the method to methane and water flow in CNTs of various diameters. Using equilibrium molecular dynamics (EMD) simulations, we first calculate the friction coefficient between the fluid and solid adjacent to it. The ratio of shear viscosity of the fluid to this friction coefficient gives the slip length, which is a measure of the flow enhancement, defined as the observed flow rate either in simulation or experiment to that predicted from classical hydrodynamic theories with no-slip boundary conditions. We then use direct non-equilibrium molecular dynamics simulations (NEMD) to calculate the slip length from the streaming velocity profiles obtained from Poiseuille flow type simulations. Our model predictions are found to be in excellent agreement with the NEMD simulation results. Our model therefore enables one to calculate the intrinsic friction between fluid and solid used to calculate the limiting or minimum slip length for a given fluid and solid, which is otherwise difficult to calculate using direct NEMD at experimentally accessible fields/shear rates.

[1] H. Lamb, Hydrodynamics (Cambridge University Press, New York, 1993) .

[2] G. K. Batchelor, An Introduction to Fluid Dynamics (Cambridge University Press, 2000).

[3] E. Lauga, M. P. Brenner, and H. A. Stone, Experimental Fluid Dynamics (Springer, 2007).

[4] W. Sparreboom, A. v. d. Berg, and J. C. T. Eijkel, New J. Phys. **12**, 015004 (2010).

[5] J. S. Hansen, B. D. Todd, & P. J. Daivis, Phy. Rev. E. **84**, 016313 (2011).

[6] S. K. Kannam, J. S. Hansen, B. D. Todd, P. J. Daivis, J. Chem. Phys. **135,** 144701 (2011).

tp5

Hydrogen Bonding and Polarisational Properties of Water: Predictions from MCYna Model

I. Shvab and Richard J. Sadus

Center for Molecular Simulation, Faculty of Information Communication Technologies, Swinburne University of Technology, Melbourne, Victoria 3122, Australia.

Temperature and density dependence of structural and polarizational properties of bulk water have been systematically investigated using the *ab initio* MCYna potential [1]. Molecular dynamics simulations [2] were conducted along the isochores 1, 0.8, and 0.6 g/cm^3 in the temperature range 278-750K. Special attention has been paid to the structural change of water in the range from boiling up to the critical temperature. Radial distribution functions in general show good agreement with the neutron diffraction experiment using the isotopic substitution technique [3] with exception of smaller first oxygen-oxygen and oxygen-hydrogen peaks. Our study indicates the collapse of tetrahedral water structure at temperatures higher than the normal boiling temperature along the isochore 1g/cm^3. At the given density water‘s structure changes from a tetrahedral ice-like structure at room temperature to the simple liquid-like structure at higher temperatures. Significant collapse of the hydrogen bond network at temperature 650K was observed. Tetrahedral structure and number of hydrogen bonds gradually decrease with decreasing density.

The static dielectric constant and average dipole moment as functions of temperature gradually decrease along all isochores. Dielectric constants calculated for water at normal density and temperatures less than 450K show agreement within 5% from experimental data. Dielectric constants along the isochors 0.8 and 0.6g/cm^3 are in qualitative agreement with available experimental data. Average dipole moments for water at ambient conditions are also in good agreement with the *ab initio* calculations of Dyer [3].

[1] J. Li, Z. Zhou, and R. J. Sadus, *J. Chem. Phys.* **127**, 154509 (2007).

[2] R. J. Sadus, *Molecular Simulation of Fluids: Theory, Algorithms and Object-Orientation* (Elsevier, Amsterdam, 1999) p 523.

[3] A. K. Soper, *Chem. Phys.* **258**, 121 (2000)

[4] P. J. Dyer, P. T. Cummings, *J. Chem. Phys.* **125**, 144519 (2006).

tp6

Calculation of Thermodynamic Properties of Lennard-Jones Fluid in a Molecular Dynamics Ensemble

Tesfaye M. Yigzawe and Richard J. Sadus

Centre for Molecular Simulation, Swinburne University of Technology, Victoria 3122, Australia.

We have calculated the thermodynamic properties at different state points of a Lennard-Jones (LJ) fluid [1] employing statistical mechanical methods developed by Lustig [2], Ray and Zhang [3], Cagin and Ray [4] and Meier and Kabelac [5] in a molecular dynamics ensemble [3] near the critical point following the recently work of Mausbach and Sadus [6] on a Gaussian Core model potential. In order to investigated the effect of finite system size and finite cutoff length we setup the simulation for two different sets of particle number and cutoff length. We report our simulation results for a system consisting of 2000 particles with a cutoff radius of 6.5σ. Energy, pressure and isothermal pressure coefficient (γ_v) are smooth near or at the critical point. Isobaric heat capacity (C_v), isentropic compressibility (β_s), the Joule-Thomson coefficient (μ_{jt}) and speed of sound (ω_0) exhibited fluctuations along the isotherm near or at the critical point, whereas the isobaric heat capacity (C_p), isothermal compressibility (β_T) and thermal expansion coefficient (α_p) diverge near or at the critical point caused by the finite system size. We used the results from the LJ simulation to calculate the state variables in Argon. By comparing the results with the experimental data of Younglove [7] we have checked the validity of our simulation. We have also simulated a repulsive and short ranged Weeks-Chandler-Anderson potential [8]. All the simulated thermodynamic state variables were smooth in a region where the LJ potential showed fluctuation and discontinuity. We have compared the results with Hess et al. [9].

[1] J. E. Lennard-Jones, Proc. Phys. Soc., **43** (1931) 461.

[2] R. Lustig, J. Chem. Phys., **109** (1998) 8816.

[3] J. R. Ray and H. Zhang, Phys. Rev. E, **59** (1999) 4781.

[4] T. Cagin and J. R. Ray, Phys. Rev. A, **37** (1988) 247.

[5] K. Meier and S. Kabelac, J. Chem. Phys., **124** (2006) 064104.

[6] P. Mausbach and R. J. Sadus, J. Chem. Phys., **134** (2011) 114515.

[7] B. A. Younglove, J. Phys. Chem. Ref. Data, **11** (1982) Supp. 1.

[8] J. D. Weeks, D. Chandler and H. C. Anderson, J. Chem. Phys., **54** (1971) 5237.

[9] S. Hess, M. Kroger and H. Voigt, Physica A, **250** (1998) 58.

tp7

A metrological scanning probe microscope incorporating a tuning fork sensor and heterodyne laser interferometry

Jan Herrmann, Bakir Babic, Chris Freund, Malcolm Gray, Magnus Hsu and Terry McRae
National Measurement Institute, PO Box 264, Lindfield NSW 2070, Australia.

The design, construction and preliminary evaluation of a metrological scanning probe microscope (mSPM) are currently underway at the National Measurement Institute (NMI). The mSPM is the key instrument in NMI's SPM metrology facility, traceably linking dimensional measurements at the nanometre scale with NMI's realisation of the SI metre. This traceability will be achieved by measuring the displacement of the sample translation stage with respect to a fixed probe using laser interferometry with a frequency stabilised laser that is referenced to NMI's optical frequency comb.

The instrument incorporates a quartz tuning fork (QTF) mounted tip for operation in non-contact frequency modulation atomic force microscopy (FM AFM) mode, a flexure-hinged, piezoelectrically actuated three-axis nanopositioning stage, and a plane mirror differential heterodyne interferometry system. To achieve a target total uncertainty of less than 1 nm for the position measurement within the measurement volume of 100 μm × 100 μm × 25 μm, the mSPM is designed to minimise uncertainties caused by thermal expansion and distortion, alignment errors and environmental vibrations. The instrument is well shielded against thermal fluctuations as well as seismic and acoustic vibrations.

The nanopositioning stage can provide sample motion suitable for AFM imaging with the planned load of intereferometry mirrors, sample platform and sample. A reliable method to attach AFM tips to QTFs, developed at NMI, allows the use of QTFs as non-contact FM AFM sensors when operating with a suitable set of oscillation parameters as illustrated by the acquisition of preliminary sample images with the mSPM operating in FM AFM mode.

The displacement sensitivity of the heterodyne plane mirror interferometry system is 1 pm $Hz^{-1/2}$ above 5 Hz and 0.1 pm $Hz^{-1/2}$ above 50 Hz. Using a tunable synthetic heterodyne laser source, polarisation control and signal processing, the configuration has been optimised to enable operation of the mSPM interferometers with less than 140 pm of cyclic error.

When commissioned, NMI's SPM facility will be used for calibrating transfer artifacts, for characterisation of nanoparticles and other nanomaterials, and for research and development requiring high-accuracy nanoscale measurements and imaging.

tp8

Sample Environments Updates at the Bragg Institute

P Imperia

The Bragg Institute, ANSTO, Lucas Heights, NSW Australia

The Sample Environment (SE) Group of the Bragg Institute is in charge of the development and maintenance of SE equipment ranging from ultra low temperature inserts to furnaces, cryocoolers, gas rig and high pressure equipment for a range of experiment in non ambient conditions to be performed with the Bragg neutron scattering instruments. The SE group also provides user support and develops, together with the users, ad-hoc new SEs for specific experiments.

Equipment in advanced testing, manufacturing or conceptual phases includes: a new magnet, dilution insert, gas mixing and sorption system (static and dynamic), new innovative vapor systems for static and dynamic delivery, standard and non standard new cryogenic equipment, rapid quencher, high pressure rig for gas delivery and a new hydrothermal cell.

In this presentation, together with the newest projects, a review of scientific cases and scientific results obtained with recently commissioned equipment will be presented. The details of the new equipment, time lines and examples of scientific applications at the neutron scattering facility, made possible by the acquisition of high level equipment as well as example of ad-hoc developments for specific experiments, will be discussed.

tp9

Polarised ^{3}He based Neutron Polarisers and Analysers for Magnetism Research on ANSTO Instruments

W.T. Lee[a], F. Klose[a], D. Jullien[b] and K. Andersen[c]

[a] *Australian Nuclear Science and Technology Organisation, Lucas Heights, NSW 2234, Australia.*

[b] *Institut Laue-Langevin, Grenoble, France.*

[c] *European Spallation Source, Lund, Sweden.*

Polarised ^{3}He based neutron polariser and polarization analyser [1] have become a matured technology for polarised neutron experimental works. A joint project of the Australian Nuclear Science and Technology Organisation (ANSTO) and the Institute Laue Langevin (ILL) is underway to provide 6 OPAL neutron scattering instruments with these important research capabilities. The instruments include SANS Quokka, diffractometer Wombat, thermal triple-axis spectrometer Taipan, reflectometer Platypus, Taipan's cold-neutron counterpart Sika, and cold neutron time-of-flight spectrometer Pelican. Discussions are underway to further expand the use to more instruments, including the Laue diffractometer Koala and new instruments that are being designed and constructed.

The project will produce a ^{3}He gas polarizing station that uses the Metastable Exchange Optical Pumping method [2]. Silicon-window polarised ^{3}He cells will polarize the incident neutron beam on several instruments and analyse the scattered neutrons on Platypus and Quokka. Wide-angle analyser "Pastis" cells [3] will be used for Wombat and Pelican. The polarizers and analysers are housed in magnetio-static cavities "Magic Box" and "Pastis" uniform field coils. The polarizing station has passed major performance requirements. The equipment for use on instruments are being built and tested for ^{3}He polarisation lifetime, and infrastructural changes are being incorporated on ANSTO instruments.

This presentation will provide examples illustrating the use of polarised neutrons to study magnetic materials and explain the methodology for using this technique. The latest status of the polarizing station and test results of the instrument components will be presented.

[1] Tasset, et. al., *Physica* **B 180** & **181**, 896 (1992).

[2] G. K. Walters, et. al., *Phys. Rev. Lett.* **8**, 429 (1962).

[3] K.H. Andersen, et. al., *Physica* **B 404**, 2652 (2009).

Simulation of Multiple Operation Modes for the Cold Neutron Triple Axis Spectrometer SIKA at Bragg Institute

Guochu Deng[1*], Peter Vorderwisch[1,2,3], Chun-Ming Wu[3], Garry McIntyre[1], Wen-Hsien Li[3]

[1]*Bragg Institute, ANSTO, Lucas Heights, NSW 2234, Australia*

[2]*Hahn-Meitner Institut - Berlin, Germany*

[3]*Department of Physics, National Central University, Jhongli 32054, Taiwan*

The coming high flux cold-neutron triple axis spectrometer, SIKA at Bragg Institute, is built with an unconventional design, equipped with a multi-strip analyzer array of 13 PG(002) blades (see Fig. 1), a linear position-sensitive detector and a separate diffraction detector. Such a design allows SIKA to run in a traditional step-by-step mode or various mapping (or dispersive) modes by changing the configuration of analyzers and detectors. In this study, several typical mapping modes are analyzed and simulated using Monte Carlo ray-trace package SIMRES of RESTRAX. [1] The performance of different mapping modes are demonstrated and evaluated, providing the dispersion relations of these operation modes as references for experimental studies. The simulation shows the flexibility and fast data-collecting potential of SIKA as a new generation of triple axis spectrometer. The simulated data could be compared with the experimental data in the future and as a reference to the selection of effective operation modes.

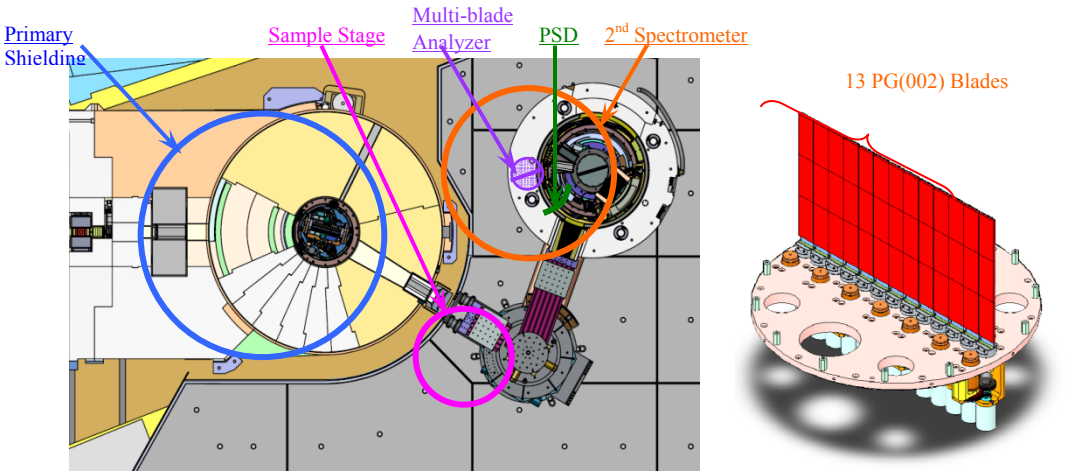

Fig. 1. Left: top view of SIKA; Right: the SIKA analyzer stage consisting of 13 pieces of freely controlled PG(002) blades.

[1] J. Šaroun, J. Kulda, "RESTRAX - a program for TAS resolution calculation and for scan profile simulation", Physica B 234-236 (1997) 1102-1104.

* Corresponding author: guochu.deng@ansto.gov.au

tp11

Pelican: An Inelastic Neutron Scattering Spectrometer With Polarization Analysis

Richard A. Mole[1] and Dehong Yu[1]

[1]*Bragg Institute, ANSTO, Locked Bag 2001, Kirrawee DC, 2232, Australia*

A new time of flight inelastic neutron scattering instrument, Pelican, is currently under construction at the OPAL research reactor at ANSTO. The instrument is designed to be of broad use with applications ranging from superconductivity and condensed matter physics, through to polymer science and soft condensed matter. The use of large PSD detectors (Fig 1) will allow a large fraction of reciprocal space to be measured simultaneously allowing the study of single crystals as well as powders and liquids. The instrument is also designed to allow polarization analysis with a large detector coverage. A supermirror transition polarizer will be utilized, while the neutron polarization will be determined using ^{3}He and a PASTIS coil setup [1]. The utilization of polarization analysis further extends the potential use of Pelican to allow the study of magnetic excitations in a wide range of materials. In the current poster I will present the scientific background behind the instrument along with potential scientific applications.

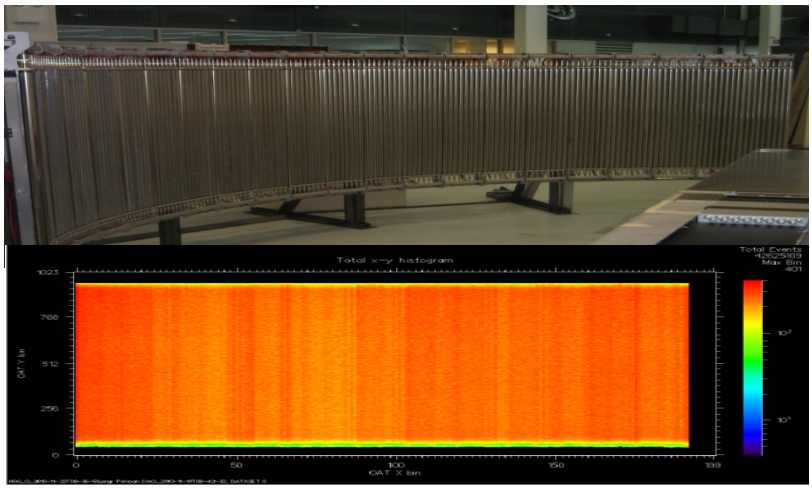

Fig 1: (Top) The pelican detector array, (bottom) readout of the pelican detector array.

[1] J.A. Stride, K.H. Andersen, A.P. Murani, H. Mutka, H. Schober and J.R. Stewart, **Physica B**, 2005, **356**, 146

tp12

Phonons observed by neutron Laue diffraction

G.J. McIntyre[a], H. Kohlmann[b] and B.T.M. Willis[c]

[a] *The Bragg Institute, ANSTO, Lucas Heights 2234, NSW, Australia.*

[b] *Universität des Saarlandes, Anorganische Festkörperchemie, Saarbrüken, Germany.*

[c] *Chemistry Research Laboratory, University of Oxford, Oxford, UK.*

After languishing for many decades as a technique mainly for aligning single crystals, neutron Laue diffraction has been reborn thanks to the success of X-ray Laue diffraction for protein crystallography at synchrotrons and to the development of efficient large-area image-plate detectors. The Laue technique with thermal neutrons is proving very successful for small-molecule crystallography on crystals frequently no larger than 0.1 mm^3, first on VIVALDI at the ILL in France [1], and now on KOALA on the OPAL reactor at ANSTO [2], and is opening neutron diffraction to fields of structural chemistry previously deemed impossible. The volumetric view of reciprocal space, such a strength in the detection of phase changes, incommensurability and twinning, does come at a price though: all scattering, inelastic as well as elastic, contributes to the observed Laue patterns. Can we turn this to our advantage? The geometry of the projection of the four-dimensional dispersion surfaces of coherent inelastic neutron scattering [3] onto the two dimensions observed by neutron Laue diffraction is derived. The scattering from low-energy acoustic phonons dominates, resulting in a 'bow-tie' of thermal diffuse scattering symmetric about the plane of diffraction for each Laue spot. Simple analysis of the shapes of the 'bow ties' for different Laue spots permits direct and rapid determination of the sound velocities, with no need for particular alignment of the crystal on modern Laue diffractometers with large-solid-angle detectors. Experimental Laue patterns for Al_2O_3 from VIVALDI illustrate several geometrical aspects of the manifestation of thermal diffuse scattering, and yield values of the sound velocities in good accord with values obtained by ultrasound attenuation measurements.

[1] G.J. McIntyre, M.-H. Lemée-Cailleau and C. Wilkinson *Physica B* **385-386**, 1055 (2006).

[2] P.D.W. Boyd *et al*. *Angew. Chem.* **49**, 6315 (2010).

[3] C.J. Carlile and B.T.M. Willis *Acta Cryst. A* **45**, 708 (1989**)**.

tp13

X-Rays of the Future: Thinking Energy Recovery Linac

Klaus-Dieter Liss

The Bragg Institute, Australian Nuclear Science and Technology Organisation, Australia.

X-ray and neutron radiations are the salient tools to investigate matter all the way from a sub-atomic scale of the size of a nucleus through nano and micrometer extensions to macroscopic entities, like engineering devices or tree dimensional whole human body mapping. A similar huge span of magnitude is valid on the time scale, where these techniques allow to track oscillations of a single electron to processes lasting hours, days or years.
X-Ray sources, in particular, grow in their brilliance faster than Moore's Law, and open un-thought opportunities for future investigations. Next generation concepts are based on the Free Electron Laser and the Energy Recovery Linac. Both sources can be characterized by enhanced beam properties, as coherence and time resolution, affecting directly the length and time scales accessible for investigations. The Energy Recovery Linac, is the next generation after 3rd generation synchrotron radiation and opens unique opportunities to advance the fields of research as established by the latter.
Novel and un-precedented applications can be sought in fields of research throughout the Asutralian community, such as in quantum nanoscience, where opto-mechanical nano resonators will be probed by X-rays; macroscopic quantum states investigated, such as a Bose Einstein Condensate structurally analyzed; in solid state physics, where coherent optical and acoustic phonons are followed directly in phase space and time; in materials characterization such as structural changes in amorphous and nano-crystalline materials; and in the field of coherent imaging and diffraction into the nanometer and atomic resolution.
It is proposed that Australia moves to the forefront of technology and science in this field, which would not only boost the research opportunities but also the economic and social benefits of our country.

[1] Klaus-Dieter Liss: *"OZ-ERL - X-Rays of the Future: An Australian Energy Recovery Linac"*, White Paper, Physics Decadal Plan, Australian Academy of Science & Australian Institute of Physics (2011).
http://www.physicsdecadalplan.org.au http://tinyurl.com/ERL-in-Oz
http://liss.freeshell.org/kdl/papers/Decadal_Plan_for_Physics_2011_ERL_Klaus-Dieter_Liss.pdf

tp14

A Simple Student-made Optical Spectrometer Modified for Gemmology Use

Theo Hughes and Gordon J.Troup

[a] *School of Physics, Monash University ,Clayton, Victoria, Australia.*

A simple optical spectrometer, made from cardboard, foam plastic and a holographic grating, is assembled and used to view spectra by first year physics students for a laboratory exercise. Its cheapness and lightness is in contrast with those of the short metal handheld spectrometers used in gemmology and mineralogy as aids to specimen identification.

The student spectrometer has been modified for gem/mineral identification. The interior of the box was white from the cardboard and foam plastic used to make it. Black paper has been used, very easily, to render the inside black, thus removing annoying reflections of the spectra. Other improvements have also been made.

It is proposed to demonstrate the operation of the modified spectrometer as a collage arrangement on the poster.

tp15

A Thermodynamic / Information Theory Analysis of Library Operation

Gordon J.Troup

[a] *School of Physics, Monash University, Clayton 3800,, Victoria, Australia.*

A library is certainly composed of condensed matter! In the early days of CMM Wagga, the week was shared with librarians doing courses. This is no longer the case, and neither are the libraries of today the same as the model treated here, the Science library at Monash University of the early 1990's. The clue to this analysis is that the ordered library is when it is closed with all books, etc., in their proper places, and the disordered one is when it is in full swing, with books etc. all over the place and students and library staff all present.

To our former librarians at Wagga, and to the library staff at the Science library at Monash University, this paper is dedicated

tp16

Meta-stable magnetic exchange spring states with negative coercivity in $DyFe_2/YFe_2$ multilayers

D. Wang[a], A. R. Buckingham[a], G. J. Bowden[a], R.C.C. Ward[b], and P. A. J. de Groot[a]
[a]*School of Physics and Astronomy, University of Southampton, SO17 1BJ, United Kingdom*
[b]*Clarendon Laboratory, Oxford University, OX1 3PU, United Kingdom*

It is known that YFe_2 dominated exchange spring $DyFe_2/YFe_2$ multilayers can exhibit a negative coercivity [1]. In the presence of a high magnetic field, directed along an easy in-plane Dy [001]-axis, magnetic exchange springs form in the soft YFe_2 layers. Here the net magnetic moment is maximized because the Dy magnetic moments and those of the Fe atoms in the YFe_2 springs act in unison. However as the field is reduced, the YFe_2 springs unwind leading to a man-made net AF state with a negative magnetic moment.

Recent measurements on a $[DyFe_2(40\text{Å})/YFe_2(160\text{Å})]\times 40$ multilayer with a one to four ration, at 50-100 K, with the field applied along a nominally hard $[\bar{1}10]$ in plane axis, show remarkably similar magnetization curves to those obtained along the easy in-plane [001]-axis [1], despite out-of-plane behaviour. This can be understood in terms of a local minimum in the anisotropy surface of the Dy^{3+} atom. Such an interpretation is supported by (i) neutron studies [2] and (ii) micro-magnetic simulations of the exchange spring system [3]. Although the magnetization curves are almost identical, the spin-configurations for the two spin-configurations are very different.

[1] Goodeev S. N., Beaujour J-M. L., Bowden G. J., de Groot Raindfor B. D., Ward R. C. C., and Wells M. R. (2001) J. App. Phys. **89** 6828-6830.
[2] M. J. Bentall, R. A. Cowley, W. J. L. Buyers, Z. Tun, W. Lohstroh R. C. C. Ward and M. R. Wells (2003) J. Phys.: Condens. Matter **15** 4301–4330
[3] G J Bowden, K N Martin, B D Rainford and P A J de Groot (2008) J. Phys.: Condens. Matter **20** 015209

tp17

Polarized Neutron Reflectometry of Rare-Earth Nitride Thin Films

S. Brück[a,b], D. Cortie[a], J. Brown[c], T. Saerbeck[a], C. Ulrich[b], F. Klose[a], and J. Downes[c]

[a]*Australian Nuclear Science and Technology Organization, Lucas Heights NSW 2234, Australia*

[b]*School of Physics, University of New South Wales, Sydney NSW 2052, Australia*

[c]*Department of Physics, Macquarie University, NSW 2109, Australia*

Rare-earth monopnictides like HoN, DyN, or ErN are semiconductors with typical band gaps between 0.73 and 1.3eV. The fact that they exhibit ferromagnetic ordering at low temperatures makes them possible candidates for an intrinsically ferromagnetic semiconductor [1]. Thin, polycrystalline rare-earth nitride films of 15 – 40nm thickness were grown onto c-plane sapphire substrates using low-energy ion assisted deposition. A temperature- and field-dependent polarized neutron reflectometry study in combination with SQUID magnetometry was carried out to characterize the magnetic properties of these films in a depth resolved way. The investigated samples show a homogeneous distribution of the magnetic moment throughout the film with ferromagnetic ordering temperatures comparable to the bulk materials. ErN and HoN films do not show an opening of the magnetic hysteresis loop even for the lowest measured temperature of T=2K. DyN on the other hand clearly shows a coercive field and remnant magnetization at 5K.

[1] Chun-Gang Duan, R F Sabirianov, W N Mei, P A Dowben, S S Jaswal, and E Y Tsymbal, J. Phys.: Condens. Matter **19**, 315220 (2007).

Magnetic Phase Transition and Thermal Expansion in $LaFe_{13-x-y}Co_ySi_z$

J.L. Wang[a,b,c], S.J. Campbell[c], S.J. Kennedy[b], P. Shamba[a], R. Zeng[a] and S.X. Dou[a]

[a]*Institute for Superconductivity and Electronic Materials, University of Wollongong, Wollongong, NSW 2522*

[b]*Bragg Institute, ANSTO, Lucas Heights, NSW 2234*

[c]*School of Physical, Environmental and Mathematical Sciences, The University of New South Wales, Canberra ACT 2600*

The structural and magnetic properties of a series of $LaFe_{13-x-y}Co_ySi_x$ compounds have been investigated by X-ray diffraction, thermal expansion, magnetic and Mössbauer effect measurements. As is evident from the thermal expansion curves of Fig. 1(a), the Curie temperatures of $LaFe_{13-x}Si_x$ compounds increase with increasing Si content from T_C~219 K for x=1.6 to T_C~250 K for x=2.6. Further enhancement in the Curie temperature from T_C~250 K to T_C~281 K is obtained on substitution of Co for Fe in $LaFe_{10.4}Si_{2.6}$ to $LaFe_{9.4}CoSi_{2.6}$. A pronounced positive spontaneous volume magnetostriction has been observed below the Curie temperature T_C (see Fig. 1(a)). The anomalous thermal expansion can be attributed to the volume dependence of the magnetic energy.

Both the magnetization and Mössbauer spectroscopy studies (e.g. Fig. 1(b)) indicate that the type of the magnetic phase transition at T_C changes from first order for $LaFe_{11.4}Si_{1.6}$ to second order for $LaFe_{10.4}Si_{2.6}$ and $LaFe_{9.4}CoSi_{2.6}$. The different natures of the magnetic transitions in $LaFe_{13-x-y}Co_ySi_x$ are discussed in terms of the classical model for itinerant ferromagnets and the volume dependence of the magnetic energy which is very sensitive to the distance between first-neighbor transition-metal atoms.

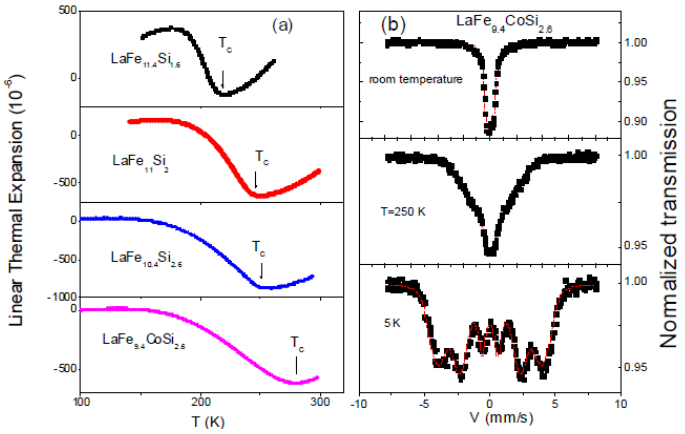

Fig. 1 (a) Temperature dependence of the linear thermal expansion of $LaFe_{13-x-y}Co_ySi_x$.
(b) ^{57}Fe Mössbauer spectra of $LaFe_{9.4}CoSi_{2.6}$ at room temperature, 250 K and 5 K. The dashed lines show fits to the Mössbauer spectra.

tp19

Temperature dependence of the coercivity in $Nd_{60-x}Fe_{30}Al_{10}Dy_x$, x = 0, 2 and 4, bulk amorphous ferromagnets: an example of strong pinning of domain walls

S. J. Collocott[a], X. Tan[b] and H. Xu[b]

[a]*CSIRO Materials Science and Engineering, Lindfield, NSW, Australia 2070.*

[b]*Laboratory for Microstructures, School of Materials Science and Engineering, Shanghai University, Shanghai 200072, China*

The realization that certain alloys, of a particular composition, in ternary alloy systems based on RE-Fe-Al (RE = Nd, Pr or Sm), form a bulk amorphous material with hard magnetic properties, termed bulk amorphous ferromagnets, has created much interest. The formation of glassy or amorphous metallic alloys by the process of melt spinning, with cooling rates of 10^6 K/s, is well known. This process results in a metallic ribbon which may be only a few microns in thickness. Unlike glassy metal ribbons, "bulk amorphous alloys" or "bulk metallic glasses" can be cast into rods, some millimetres in diameter. Structural studies of bulk amorphous alloys, using techniques such as high-resolution transmission electron microscopy, reveal the existence of small nanocrystalline clusters, which form ordered regions, embedded in a magnetically-soft amorphous matrix. Bulk amorphous alloys with hard magnetic properties based on RE-Fe-Al (RE = Nd, Pr or Sm) alloy systems typically exhibit, at room temperature, an intrinsic coercivity ($\mu_0 H_c^i$) of order 0.4 T and a remanence of order 100 mT.
Bulk amorphous ferromagnet alloys of composition $Nd_{60-x}Fe_{30}Al_{10}Dy_x$, x = 0, 2 and 4, have been prepared by arc-melting and suction casting into a copper mould. At room temperature all the alloys exhibit hard magnetic properties, and the intrinsic coercivity is seen to increase with increasing dysprosium content i.e. from 0.337 T, x = 0, to 0.537 T, x = 4. Measurements of the intrinsic coercivity as a function of magnetic field sweep rate are made, and from these measurements the fluctuation field, H_f, for each alloy, is determined. Measurements of the intrinsic coercivity were made from 300 K to 10 K, and with decreasing temperature the intrinsic coercivity increases, reaching a maximum at 44 K, 57 K and 72 K, for x = 0, 2, and 4, respectively, before decreasing rapidly. For each alloy, in the temperature region above its peak to 300 K, the temperature dependence of the intrinsic coercivity is well explained by the strong pinning model of domain walls of Gaunt [1].

[1] P. Gaunt, Philos. Mag. B **48** 271 (1983).

tp20

Magnetic properties of $Nb_{1-X}Hf_XFe_2$

S.J. Harker[a], G.A. Stewart[a], H. Okimoto[b], K. Nishimura[b] and W.D. Hutchison[a]

[a] *School of Physical, Environmental and Mathematical Sciences, The University of New South Wales, Canberra, ACT 2600, Australia*

[b] *Graduate School of Science and Engineering, University of Toyama, 930-8555, Japan.*

The intermetallic series $Nb_{1-x}Hf_xFe_2$ ($0 < x < 0.8$) forms with the hexagonal C14 Laves phase structure with space group $P6_3/mmc$ and exhibits an unusual range of magnetic properties. Stoichiometric $NbFe_2$ is a weak itinerant antiferromagnet with a spin-density-wave transition at $T_{sdw} \approx 10$ K [1]. More recently, considerable interest has been directed at the existence of ferromagnetic quantum criticality for a small excess of Nb ([2] and references therein). In its unannealed form, $HfFe_2$ exhibits a minor C14 phase component (the preferred phase is cubic C15) that orders ferromagnetically at $T_C \approx 427$ K.

The main thrust of this work is the use of ^{57}Fe-Mössbauer spectroscopy to monitor the magnetism at the atomic level via the magnetic hyperfine fields (B_{hf}) acting at the 2a- and 6h-Fe sites. To this end, Mössbauer spectra have been recorded as a function of temperature and hafnium concentration ($0 < x < 0.8$). In apparent contradiction of bulk magnetic data, the low temperature Fe 6h-site magnetic hyperfine field increases monotonically across the series while the saturation magnetisation exhibits a minimum at $x = 0.4$. Furthermore the Mössbauer data indicate generally higher transition temperatures. The former is consistent with the existence of an antiferromagnetic phase while the latter needs to be explored further. In addition, the magnetisation data reveal spin glass behaviour at low temperatures in the region $x = 0.45$ to 0.79, which may be partly responsible for the suppression of the bulk moment through this region [3].

[1] Y. Yamada, H. Nakamura, Y. Kitaoka, K. Asayama, K. Koga, A. Sakata and T. Murakami, *J. Phys. Soc. Japan* **59** (1990) 2967.

[2] B.P. Neal, E.R. Ylvisaker and W.E. Pickett, *Phys. Rev. B* **84** (2011) 085133 (1-7).

[3] S.J. Harker, G.A. Stewart, H. Okimoto, K. Nishimura and W.D. Hutchison, *Hyperfine Interactions,* DOI 10.1007/s10751-011-0445-y

tp21

Charge, magnetization (spin) and spin momentum density studies of the Kagome staircase compound $Co_3V_2O_8$

N.Narayanan[a,b,*], N.Qureshi[a], H. Fuess[a] and H.Ehrenberg[c]

[a]*Structural Research, Darmstadt University of Technology, Darmstadt, Germany.*

[b]*IKM, IFW Dresden, Dresden, Germany*

[c]*Karlsruhe Institute of Technology (KIT), Karlsruhe, Germany*

[*]*Now at UNSW Canberra.*

In recent times compounds with Kagome structure are extensively studied due the variety of states exhibited ranging from a proposed spin liquid in γ-$Cu_3Mg(OH)_6Cl_2$, orbital ordering in $Cu_3(V_2O_7)(OH)_2 2H_2O$, five magnetic phase transitions in $Co_3V_2O_8$ (CVO) and multiferroicity in $Ni_3V_2O_8$ [1-3]. The ferromagnetic ground state structure (FM) of CVO reveals two strongly different magnetic moments for the crystallographically distinct cross tie Co_c and spine Co_s of 1.54 μ_B and 2.73 μ_B respectively, despite the fact that both Co^{2+} ions apparently present in high-spin configurations [3]. Experimental magnetization density reveals different shapes around Co_c and Co_s, that may lead to interesting orbital physics and to the role of electron correlation in CVO. The experimental spin density in momentum space on the other hand gives hints about the dominant exchange interactions in FM CVO, that are until now assumed to be the intralayer nearest neighbor (NN) interactions, although several other next NN and interlayer exchange paths were proposed. In order to get better understanding and newer insights into the observed phenomena density functional (DFT) based electronic structure calculations with different levels of correlation corrections are carried out and the calculated densities together with the projected density of states (PDOS) are compared to the experimental ones. The charge and magnetization (spin) densities together with PDOS reveal the possibility of a correlation driven orbital occupation of the "e_g" electrons in the paramagnetic phase and of the "t_{2g}" hole in the FM phase and strong coupling between the correlation driven orbital occupation and the band gap problem of CVO. From the calculated and experimental spin momentum density it could be concluded that it is very sensitive to the level of correlation and the magnetic phase. Electron correlation enhances the spin population between the Kagome layers and thus enhancing the interlayer couplings.

[1] R. H. Colman, A. Sinclair, and A. S. Wills, *Chem. Mater.* **23**, 1811 (2011).

[2] O. Janson, J. Richter, P. Sindzingre, and H. Rosner, *Phys. Rev. B* **82**, 104434 (2010).

[3] N.Qureshi et al., *Phys. Rev. B* 79, *094417* (2008).

tp22

Inelastic Neutron Scattering in Multiferroic Materials

N. M. Reynolds[a,b], P. Graham[a], A.M. Mulders[c], G. McIntyre[b], S. Danilkin[b], J. Fujioka[d], Y. Tokura[d], B. Keimer[e], M. Reehuis[f] and C. Ulrich[a,b]

[a]*School of Physics, University of New South Wales, Sydney, Australia.*
[b]*The Bragg Institute, Australian Nuclear Science and Technology Organization, Lucas Heights, New South Wales 2234, Australia.*
[c]*School of Physical, Environmental and Mathematical Sciences, UNSW@ADFA,Canberra*
[d]*Department of Applied Physics, University of Tokyo, Tokyo 113-8656, Japan.*
[e]*Max-Planck-Institute for Solid State Research Stuttgart, Germany*
[f]*Helmholtz-Zentrum for Materials and Energy Berlin, Germany*

Magnetism and ferroelectricity are both exciting physical properties and are used in everyday life in sensors and data storage. Multiferroic materials are materials where both properties coexist. They offer a great potential for future technological applications like the increase of data storage capacity or in novel senor applications. The coupling mechanism between both antagonistic effects, electrical polarization and magnetic polarization, is not fully understood yet. The aim of the project is the systematic study of multiferroic materials such as $TbMnO_3$ and related materials by inelastic neutron scattering (INS) in order to obtain a deeper insight into the interplay between the two interacting effects.

We have started our investigations with $TbVO_3$, which is isostructural to $TbMnO_3$, but has a collinear antiferromagnetic spin arrangement [1] instead of a cycloidal spin structure [2]. By using inelastic neutron scattering (INS) we have obtained the spin wave dispersion relation and the crystal field excitations of the Tb-ions in $TbVO_3$. These data will be compared with previously obtained data of D. Senff on $TbMnO_3$ [3]. Experiments were performed at the ILL in Grenoble, France and at the research reactor OPAL at ANSTO, Australia.

[1] M Reehuis et al., *Phys. Rev. B* **73**, 094440 (2006).
[2] N. Aliouance et al., *Phys. Rev. Lett.* **102**, 1 (2009).
[3] D. Senff et al., *Phys. Rev. B* **77**, 1 (2008).

tp23

Ferroelectric charge order stabilized by antiferromagnetism in multiferroic $LuFe_2O_4$.

A.M. Mulders[a], M. Bartkowiak[a,b], J.R. Hester[b], E. Pomjakushina[c], K. Conder[c]

[a]*School of Physical, Environmental and Mathematical Sciences, UNSW@ADFA, Canberra ACT 2600, Australia.*

[b]*The Bragg Institute, Australian Nuclear Science and Technology Organisation, Lucas Heights, NSW 2234, Australia*

[c]*Laboratory for Development and Methods, Paul Scherrer Institut, 5232 Villigen PSI, Switzerland.*

Neutron diffraction measurements on multiferroic LuFe2O4 show changes in the antiferromagnetic (AFM) structure characterized by wavevector q = (1/3 1/3 ½) as a function of electric field cooling procedures. The increase of intensity from all magnetic domains and the decrease in the 2D magnetic order observed below the Neel temperature are indicative of increased ferroelectric charge order. The AFM order changes the dynamics of the CO state, and stabilizes it. It is determined that the increase in electric polarization observed at the magnetic ordering temperature is due to a transition from paramagnetic 2D charge order to AFM 3D charge order.

[1] A.M. Mulders, M. Bartkowiak, J.R. Hester, E. Pomjakushina, K. Conder, Phys. Rev. B 84, 140403(R) (2011)

tp24

The Spin-3/2 Heisenberg Antiferromagnet on the Bilayer Honeycomb Lattice : A Model for $Bi_3Mn_4O_{12}(NO_3)$

J. Oitmaa [a] and R.R.P. Singh [b]

[a] *School of Physics,The University of New South Wales, Sydney NSW 2052, Australia.*

[b] *Department of Physics , University of California, Davis, CA 95616, U.S.A.*

The bismuth manganese oxynitrate material $Bi_3Mn_4O_{12}(NO_3)$ [1] has a Curie-Weiss constant of order 250K but shows no long-range magnetic order at least down to 0.4K. Structurally, the material consists of S=3/2 Mn ions forming honeycomb layers, with adjacent layers forming bilayers, and the bilayers separated by nitrate layers at much larger separations.
The simplest model for the material is thus a honeycomb bilayer with antiferromagnetic exchange J, $J_\perp$ between nearest neighbours within and between layers, respectively.
We have used series expansion methods [2] to study the properties of this model, and find the quantum phase transition between Néel and dimerized phases to occur at $J_\perp / J = 9.3 \pm 0.2$, which is in good agreement with recent Quantum Monte Carlo results [3]. However this is a value much larger than expected in the real material. To explain the absence of Néel order we include frustrating second neighbour interactions J', and show that the critical value of $J_\perp / J$ can be greatly reduced in this way. We also compute excitation spectra in the disordered phase, which will be able to provide a more stringent test of the model, when neutron scattering results become available.

[1] O. Smirnova et al., J. Am. Chem. Soc. **131**, 8313 (2009).

[2] J. Oitmaa, C.J. Hamer and W. Zheng, *Series Expansions for Strongly Interacting Lattice Models* (Cambridge, 2006) .

[3] R. Ganesh et al., Phys. Rev. B **83**, 144414 (2011).

tp25

Condensation of composite objects in Heisenberg-like models

Rakesh Kumar and Oleg P. Sushkov

School of Physics, University of New South Wales, Sydney 2052, Australia.

In the present work, we focus our study for the Heisenberg antiferromagnet on bilayer square lattice. The model itself has been extensively studies in past by various means. Sushkov *et al.* [1,2] studied this model by Brueckner theory and quantum Monte-Carlo simulations. The results show a quantum phase transition between Neel order and dimer phase at $g_c\approx 2.5$. In Brueckner theory framework, they found the quantum critical point by formulating this theory in disordered (dimer) regime. So far no satisfactry theory has been developed in the ordered side to get the same critical point. Vojta *et al.* [3,4] proposed unitary transformed bond-operators which give qualitatively correct physics but with a different quantum critical point, i.e., $g_c\approx 4$ which is equivalent of considering no constraint in disordered phase. Motivated by these works, we are trying to develop a theory in the magnetically ordered phase which gives the correct physics as well as the same critical point. We are restricted our study close to critical point. In our study, we are using the Belyaev diagrammatic technique and assuming the condensation of longitudinal triplet bosons in magnetically ordered phase.

[1] V. N. Kotov, O. Sushkov, Zheng Weihong, and J. Oitmaa, Phys. Rev. Lett. **80**, 5790 (1998).

[2] P. V. Shevchenko, A. W. Sandvik, and O. P. Sushkov, Phys. Rev. B **61**, 3475 (2000).

[3] Matthias Vojta and Klaus W. Becker, Phys. Rev. B **60**, 15201 (1999).

[4] T. Sommer, M. Vojta and K.W. Becker, Eur. Phys. J. B **23**, 329 (2001).

tp26

Magnetic properties of lightly doped antiferromagnetic YBCO

O. P. Sushkov

School of Physics, University of New South Wales, Sydney 2052, Australia.

The present work addresses YBCO at doping below x=0.06 where the compound is a collinear antiferromagnet. In this region YBCO is a normal conductor with a finite resistivity at zero temperature. The value of the staggered magnetization at zero temperature is $0.6\mu_B$, the maximum value allowed by spin quantum fluctuations. The staggered magnetization is almost independent of doping. On the other hand, the Neel temperature decays very quickly from T_N=420K at x=0 to practically zero at x = 0.06.

The present work explains these remarkable properties and demonstrates that the properties result from the physics of a lightly doped Mott insulator with small hole pockets.

Nuclear quadrupole resonance data are also discussed. The data shed light on mechanisms of stability of the antiferromagnetic order at $x < 0.06$.

Exploring structural Oddities in Tin Cluster Compounds $RuMSn_6O_8$ (M = Fe, Co, Mn) with Quantum Mechanical Methods

D. Bende[a,b], T. Söhnel[a],

[a] *School of Chemical Sciences, The University of Auckland, New Zealand.*

[e] *Faculty of Chemistry, Philipps-Universität Marburg, Germany.*

The compound $RuFeSn_6O_8$ has been the focus of recent research [1]. It is among the very few known substances where Fe^{2+} is explicitly located in a tetrahedral oxygen surrounding. This causes the iron d_{eg} valence band to be filled with three electrons, which should result in strong (dynamic) lattice distortions. Usually the latter effect is so strong that an octahedral coordination is preferred for the iron sites, which is the reason why substances with tetrahedrally coordinated Fe^{2+} are so rare. Surprisingly, the phase $RuFeSn_6O_8$ is a very stable paramagnetic semiconductor.

In this work the electronic structure of the compounds $RuMSn_6O_8$ (M = Fe, Co, Mn) were explored and a variety of different approaches (LDA/GGA+U, magnetic ordering, spin-orbit-coupling) with different methods (TB-LMTO- ASA, LAPW) has been tested on their impact on the description of the electronic structure. Discrepancies in the experimental results of Mössbauer (indicating a structural distortion below 57 K) and scattering experiments (no structural distortion observed) had already indicated a complex relationship between electronic and spatial symmetry [1]. One attempt to explain those findings was postulating a dynamic Peierl's distortion at the FeO_4 tetrahedra, which could be promoted by the very unusual d-configuration (d^6) of the Fe-atoms for the tetrahedral surrounding. The presence of a dynamic Peierl's distortion assumes lowered underlying lattice symmetry than the cubic one that was found in scattering experiments. The symmetry of the lattice has been lowered and optimised to explore the relations between nucleic ordering and electronic structure. All these investigations have additionally been performed for the isostructural compounds $RuMnSn_6O_8$ and $RuCoSn_6O_8$ to eventually come across certain trends or properties that are characteristic for the electron configuration of iron.

[1] T. Söhnel, P-Z. Si, C. Rohmann, L. Kienle, M. Ruck, N. Sharma; C. Ling, M. Avdeev, B. Johannessen, *Proceedings of the 3rd International Symposium on Structure-Property Relationships in Solid Stet Materials* (Max-Planck Institute for Solid State research, Stuttgart, Germany, 2010) p. 55.

tp28

The Magnetic and Electronic Properties of $FeSr_2YCu_2O_{6+x}$ and $FeSr_2Y_{2-x}Ce_xCu_2O_{8+x}$

J. Stephen[a] and G. V. M. Williams[a]

[a] *MacDiarmid Institute, Victoria University of Wellington, PO Box 600, Wellington 6012, New Zealand*

$FeSr_2YCu_2O_{6+d}$ and $FeSr_2Y_{2-x}Ce_xCu_2O_{8+x}$ are an interesting class of compounds that contain 2D CuO_2 planes and oxygen deficient FeO_x planes [1,2]. They are structurally very similar to the well-studied ruthenocuprates $RuSr_2RCu_2O_8$ and $RuSr_2R_{2-x}Ce_xCu_2O_{10-x}$ (R is a rare earth) that display magnetic order arising from the RuO_2 planes and superconductivity arising from the CuO_2 planes [3-5]. The magnetic order in the ruthenocuprates is not fully understood. It is believed to be antiferromagnetic at low magnetic fields and a spin-flop transition occurs as the magnetic field is increased [1]. The iron-cuprates have not been as well studied and little is known about the electronic and magnetic properties and if they can be electronically doped.

In this presentation we report the results from magnetization, resistivity and thermopower measurements on $FeSr_2YCu_2O_{6+d}$ and $FeSr_2Y_{2-x}Ce_xCu_2O_{8+x}$. $FeSr_2YCu_2O_{6+d}$ is superconducting and we show that it can be hole or electron doped and there is evidence for a Stoner enhancement arising from the slightly oxygen-deficient FeO_x planes. $FeSr_2Y_{2-x}Ce_xCu_2O_{8+x}$ is not superconducting but it can be made with a wide Ce concentration range. There is evidence for antiferromagnetic spin fluctuations and a spin-glass occurs at low temperatures. We also observe a large magnetoresistance at low temperatures.

[1] H. Fuji, Y. Mihara, T. Mochiku, Y. Hata, and K. Kadowaki, *Physica C* **415**, 85 (2004).

[2] M. Pissas, C. Christides, G. Kallias, D. Niarchos, and R. Sonntag, *J. Phys.: Condens. Matter* **10**, 3929 (1998)

[3] A. Felner, U. Asaf, Y. Levi, and O. Milio, *Phys. Rev. B* **55**, 3374 (1997).

[4] G. V. M. Williams and S. Krämer, *Phys. Rev. B* **62**, 4132 (2000).

[5] G. V. M. Williams and M. Ryan, *Phys. Rev. B* **64**, 094515 (2001).

tp29

Laboratory Measurements of Frequency-Dependent Seismic Properties of Cracked and Fluid-Saturated Media

Heather Schijns[a], Ian Jackson[b] and Douglas R Schmitt[a]

[a] *Department of Physics, University of Alberta, Edmonton, Alberta, Canada.*

[b] *Research School of Earth Sciences, Australian National University.*

An understanding of the frequency-dependent seismic properties expected of cracked and fluid-saturated rocks of the Earth's upper crust underpins applications as diverse as earthquake forecasting, geothermal power extraction, enhanced oil recovery, and CO_2 sequestration. The capability to perform laboratory measurements with both low-frequency forced-oscillation and high-frequency wave-propagation methods, under conditions of independently controlled confining and pore-fluid pressure, is therefore critical. An important step in the development of such broad-band capability has been the modification of existing laboratory equipment to newly allow flexural, as well as torsional, forced-oscillation testing of cylindrical rock specimens. Flexural oscillation tests on an experimental assembly containing a fused silica control specimen yield results indistinguishable from those of numerical modelling with both finite-difference and finite-element methods – demonstrating the viability of the method [1]. Both torsional and flexural oscillation methods along with complementary high-frequency wave propagation methods have been applied to specimens of dense polycrystalline alumina and quartzite, each thermally cracked to generate an interconnected network of cracks of low aspect ratio, and tested dry, and saturated with either argon or water. The shear and flexural moduli vary systematically with effective pressure – providing clear evidence of pressure-induced crack closure. Similarities and differences between effective moduli measured under different conditions of pore-fluid saturation are tentatively interpreted in terms of the timescales for stress-induced redistribution of pore fluid.

[1] I. Jackson, H. Schijns, D.R. Schmitt, J. Mu and A. Delmenico, *Rev. Sci. Instrum.* **82**, 064501 (2011).

tp30

Mössbauer Spectra of the Acid Mine Drainage Mineral Schwertmannite from the Sokolov Basin, Czech Republic

J.D. Cashion[a], K. Suzuki[b] and E. Murad[c]

[a] *School of Physics, Monash University, Victoria 3800, Australia.*

[b] *Department of Materials Engineering, Monash University, Victoria 3800, Australia.*

[c] *Departamento de Química, ICEx, Universidade Federal de Minas Gerais, 31270-901 Belo Horizonte, Minas Gerais, Brazil*

Mankind has been mining sulphidic ores for at least 5000 years (the copper age) and the effects of the subsequent acid sulphide oxidation can be seen in many areas. The minerals which are precipitated depend on the local conditions (Eh, pH, $[SO_4^{2-}]$ and $[Fe^{2+}]$). and the principal ones are jarosite, $KFe_3(SO_4)_2(OH)_6$, goethite, α-FeOOH, schwertmannite, approximately $Fe_8O_8(OH)_6SO_4$,and ferrihydrite, $Fe_5HO_8.4H_2O$. The last two are always poorly crystalline, producing broad, poorly-defined XFD lines, and Mössbauer spectroscopy is one of the best means of identification together with their characteristic colours [e.g.1]. The schwertmannite sample studied here was a particularly well-formed sample from the Lomnice pit in the Sokolov Basin, Czech Republic [2].

The room temperature Mössbauer spectrum comprised a broadened quadrupole split doublet as do most poorly crystalline ferric oxyhydroxides, although this was more asymmetric than is common. Surprisingly, by 78 K the spectrum had split out into a magnetically ordered form although still with a considerable contribution from the doublet for which the asymmetry had now reversed. This indicated that there was a range of particle sizes and/or crystallinities present, so that part of the sample was now below the superparamagnetic blocking temperature and part above. By 5 K, the doublet had disappeared and the resulting sextet was asymmetric, with very broad lines.

The ordering temperature of such samples is strongly dependent on the crystallinity so a zero velocity thermal scan was carried out to determine the onset of magnetic ordering. These results will be compared with those from magnetic susceptibility.

[1] E. Eneroth and C. Bender Koch, *Hyperfine Interact.* **156/157**, 423 (2009).

[2] E. Murad and P. Rojík, *Clay Min.* **40,** 427 (2005).

Quantitative Determination of Phases using Mössbauer Spectroscopy and X-ray Diffraction: A Case Study Using the Fe-Ti-O System

R.A. Pax and G.A. Stewart

School of PEMS, UNSW Canberra, PO Box 7916, Canberra BC ACT 2610

Commercial processes involving minerals that naturally contain iron are amenable for study using Mössbauer spectroscopy (for example, refer to [1] and references therein). Furthermore, if the process's purpose is to alter the oxidation state of the Fe to facilitate its removal, then Mössbauer spectroscopy becomes a very powerful tool to investigate the process itself. However, the traditional tool for on-site phase analysis is x-ray powder diffraction (XRD). This is despite the fact that the interpretation of XRD patterns is not a trivial process when the number of phases present in the sample is large, especially when the structures of some of the phases are not well known or are compromised by the presence of impurities.

This paper will consider the relative advantages and disadvantages of XRD and Mossbauer spectroscopy for the investigation of processes involving the Fe-Ti-O system. Particular emphasis will be directed at issues related to the quantitative determination of the constituent phases.

[1] E. Murad and J. Cashion, *Mössbauer Spectroscopy of Environmental Materials and their Industrial Utilization* (Kluwer Academic Publishers, 2004).

tp32

Characterisation of $EuCl_3.6H_2O$ for quantum computation

R. L. Ahlefeldt and M. J. Sellars

Centre for Quantum Computation and Communication Technology, Research School of Physics and Engineering, The Australian National University, Canberra ACT 0200, Australia

$EuCl_3.6H_2O$ is a crystal of interest for quantum computing because of its very low optical linewidth and high concentration of optical centres. A multi-bit ensemble based quantum computer could be created in $EuCl_3.6H_2O$ by doping it with a rare earth such as Ce. The optical transitions of Eu ions around the dopant are shifted due to the strain caused by the dopant, resulting in satellite lines in the spectrum. Two hyperfine ground states of the Eu ions in each satellite line can be used as qubit levels.

As part of an initial characterisation of $EuCl_3.6H_2O$ for quantum computing we have assigned many of the satellite lines to crystallographic sites by measuring the hyperfine splitting of satellite lines in 0.1% Ce:$EuCl_3.6H_2O$ as a magnetic field is rotated about the sample. This technique is very similar to EPR.

One limitation on the use of $EuCl_3.6H_2O$ for quantum computing is the short optical coherence time. We show that this can be substantially increased, from 77 us to 740 us, by fully deuterating the crystal.

tp33

Rephasing Spontaneous Emission in a Rare-Earth Ion-Doped Solid

K. R. Ferguson[a], S. E. Beavan[a] and M. J. Sellars[a]

[a] *Centre for Quantum Computation and Communication Technology, Laser Physics Centre, RSPE, Australian National University, Canberra, Australia*

Extending the range and versatility of current quantum communication links requires the development of a quantum repeater; a device comprised of single photon sources and quantum memories that enables entanglement to be generated and stored across distant memory nodes. One way to efficiently map the 'flying qubits' (photons) onto atomic states for storage is to use collective states within ensembles of atoms, where interference effects give rise to an enhanced directionality as compared to single atoms [1].

Experimental work to date has largely employed Alkali gases for proof of principal demonstrations of quantum repeater elements. However, the storage times in such systems are fundamentally limited by atomic diffusion.

Here we present a proposal for generating entangled pairs of photons using a rare-earth ion doped crystal. This can be achieved using photon echo techniques to re-phase coherence in an ensemble of Pr^{3+} ions in a crystal of Pr^{3+}:Y_2SiO_5, which was created when a photon was spontaneously emitted. This scheme is referred to as "rephased amplified spontaneous emission" (RASE), and was originally proposed by Ledingham *et. al.* [2].

RASE has been demonstrated in a solid state ensemble of rare-earth ions, but we have been unable to prove the non-classical nature of the correlations due to insufficient signal to noise. The proposed experiment is to use an optical cavity to enhance the quantum efficiency of the transition of interest, and reduce the level of noise.

If entangled photon pairs can be efficiently generated, this will enable us to distribute entangled states across remote crystals and demonstrate basic operations of a discrete variable quantum repeater. Being an easy-to-implement solid state system, this is a promising platform for scalable quantum information processing devices.

[1] L. M. Duan, M. D. Lukin, J. I. Cirac, and P. Zoller, *Long-distance quantum communication with atomic ensembles and linear optics*, Nature, 141, 413-148 (2001).

[2] P. M. Ledingham, W. R. Naylor, J. J. Longdell, S. E. Beavan and M. J. Sellars, *Nonclassical photon streams using rephased amplified spontaneous emission*, Phys. Rev. A., 81 (2010) .

tp34

Optical Imaging and Structure Writing in Rare Earth Ion Doped Crystals

Milos Rancic[a], Sarah Beavan[a] and Matthew Sellars[a]

[a] *Research School of Physics and Engineering, Australian National University, ACT 0200, Australia*

Nuclear Magnetic Resonance (NMR) imaging, is a well-known technique that achieves sub-wavelength imaging resolution in bulk materials.

In this work we apply the concepts of NMR imaging[1] to optical transitions in order to image density of dopant Rare Earth ions in crystals. The aim of the work was to achieve sub-wavelength imaging of the ion density at optical frequencies[2], with possible applications of active waveguide fabrication.

The major obstacle in achieving high resolution imaging using the techniques of NMR was found to be the inhomogeneous broadening of the optical transitions. This is a not an issue for regular liquid phase NMR, as the transitions are homogeneously broadened. To circumvent the resolution limit imposed by the inhomogeneous broadening, an imaging pulse sequence that re-phased the inhomogeneous broadening was proposed and demonstrated.

Although only relatively low one-dimensional resolution (10^{-3} m) was demonstrated, the possibility of achieving sub-wavelength resolution was investigated theoretically. As a secondary goal, the creation of one-dimensional sub-wavelength optical structures in rare earth crystals was also investigated, through the use of similar pulse techniques. The highest resolution one dimensional grating created had a resolution of $\lambda = 30 \pm 1$ μm. Once again, higher frequency gratings are theoretically possible.

[1] P. T. Callaghan, Principle of Nuclear Magnetic Resonance Microscopy, Oxford publishing, 1993

[2] A. L. Alexander, Investigation of Quantum Information Storage in Rare Earth Doped Materials, Ph.D thesis, Australian National University, 2007

tp35

Electrically Detected Magnetic Resonance Applied to Near Surface Phosphorus Donors in Silicon

W.D. Hutchison[a], S.J Harker[a], P.G. Spizzirri[b], F. Hoehne[c], and M.S. Brandt[c]

[a]*School of PEMS, University of New South Wales, ADFA, Canberra, ACT 2600, Australia.*

[b]*School of Physics, The University of Melbourne, Parkville, Victoria 3010, Australia.*

[c]*Walter Schottky Institute, Technical University of Munich, D-85748 Garching, Germany.*

The magnetic resonance of donors in semiconductors via their electron spin resonance (ESR) is well established. However, the sensitivity of conventional ESR is limited, requiring samples with 10^{10} donor spins or more. More sensitivity can be achieved through the detection of magnetic resonance via the effects of spin selection rules on other observables, such as charge transport.

Electrically detected magnetic resonance (EDMR) is a transport technique which measures the change in dc conductivity due to donor resonances. EDMR has the sensitivity to detect as few as 50 spins[1]. It is also particularly useful for the study of semiconductor interface defects and their influence on donors which are located in proximity. Previously, we presented comparisons of EDMR results for implanted Si:P devices with a range of surface preparations [2]. We not only found a strong correlation between P and P_b charge trap signal strengths matching the postulated recombination mechanism requiring both of these species[3,4], but also the surprising result of larger signal strengths from thermal oxides having lower areal trap densities. In this work, we further explore the underlying reasons for this counter intuitive signal enhancement as a function of trap density and present new data which shows continuing degradation of the silicon interface with time.

[1] D.R. McCamey, H. Huebl, M.S. Brandt, W.D. Hutchison, J.C. McCallum, R.G. Clark and A.R. Hamilton, Applied Physics Letters, **89** 182115-1 - 182115-3 (2006).

[2] W.D. Hutchison, P.G. Spizzirri, F. Hoehne and M.S. Brandt, paper 8**,** Proceedings of the 34rd ANZIP Condensed Matter and Materials (Wagga) Meeting, Waiheke 2010. http://www.aip.org.au/wagga2010/

[3] D. Kaplan, I. Solomon and N.F. Mott, *Journal de Physique – Lettres* **41** 159 (1976).

[4] F. Hoehne, H. Huebl, B. Galler, M. Stutzmann and M.S, Brandt, Phys. Rev. Lett. **104**, 046402 (2010)..

tp36

Spin precession and non-adiabaticity in hole quantum point contacts

T. Li[a], O.P. Sushkov[a] and U. Zuelicke[b]

[a] *School of Physics, University of New South Wales, Sydney 2052, Australia.*

[b] *School of Physical and Chemical Sciences, Victoria University of Wellington.*

Zeeman splitting in one-dimensional hole systems has been the subject of several recent experimental investigations. Due to the intrinsic spin-orbit interactions present in hole systems, dynamics is highly nontrivial even in the simplest situations and the experimental result has not been reconciled with previous theory. Notably, the evidence of strongly anisotropic suppression of the Zeeman splitting for the in-plane direction in quantum point contacts grown in the high symmetry direction has been baffling, as the theory, being based on the spherical approximation, predicts axial symmetry. We argue that the experimental result is evidence of non-adiabatic spin dynamics in the wire induced by the Dresselhaus interaction and present general qualitative comments regarding the possibility and physical implications of an anisotropic spin susceptibility.

tp37

Implementation of the PBR protocol using spin-spin interactions

D. J. Miller

Centre for Time, University of Sydney, Sydney 2006 and

School of Physics, University of New South Wales, Sydney 2052.

Pusy, Barrett and Rudolph (PBR) [1] have recently shown that the statistical interpretation of the quantum state is inconsistent with the predictions of quantum theory. It has been said that "this result may be the most important general theorem relating to the foundations of quantum mechanics since Bell's theorem" [2]. PBR show how their protocol could be implemented experimentally by a quantum circuit involving a unitary rotation on each qubit, followed by the operation of an entangling gate and finally a Hadamard gate applied to each qubit.

The main result of the present work is to show that the PBR protocol can be implemented by a Hamiltonian operating on spin-half systems in the solid state representing the qubits. After the interaction of the spins and a suitable time evolution the necessary states can be distinguished by an energy measurement.

It is also shown that the state-dependent rotation [3] that can be achieved by a weak measurement of one of the spins sheds further light on the PBR result.

[1] M. F. Pusey, J. Barrett and T. Rudolph, arXiv:1111.3328v1 [quant-ph].

[2] E. S. Reich, *Nature News*, 17 November 2011.

[3] D. J. Miller, *Phys. Rev. A* **83**, 032121 (2011).

WW2012 AUTHOR INDEX

Tuesday 31.01	Wednesday 1.02		Thursday 2.02		Friday 3.02	
	900 Opening Wayne Hutchison		900 Hua Kun Liu (invited)	chair: John Barthelomew	900 Charles Johnson (invited)	chair: John Cashion
	910 Anita Hill (invited)	chair: Anna Mulders	930 Lou Vance		930 Tadahiko Hirai	
	940 Jessica Hudspeth		950 Kate Fox		950 Tapasi Mukarjee	
	1000 Jodie Bradby (invited)		1010 Marcus Hennig		1010 Philip McGill	
	1030 Morning tea		1030 Morning tea		1030 Morning tea	
	1100 Jared Cole (invited)	chair: Roger Lewis	1100 Wei Bao (invited)	chair: Oleg Sushkov	1100 Clemens Ulrich (invited)	chair: Tilo Soenel
	1130 Zakiya Al-Azri		1130 Michael Holt		1130 Suresh Narayanaswamy	
	1150 Yasar Kutuvantavida		1150 Mustafa Keskin		1150 Jeff Davis (invited)	
	1210 Julian Steele		1210 David Cortie		1220 Awards and Closing Wayne Hutchison	
	1230 Lunch		1230 Lunch		1240 Lunch	
	1400 Chris McNeill	chair: Heiko Timmers	1400 Anna Pardowska (invited)	chair: Klaus Dieter Liss		
	1430 Vedran Jovic		1430 Graham Bowden			
	1450 2 min poster adds		1500 2 min poster adds			
	1530 Afternoon tea		1530 Afternoon tea			
1600 Registration	1600 Posters and Drinks		1600 Posters and Drinks			
1800 Dinner 1920	1830 Conference Dinner		1800 Dinner			
	After Dinner Talk Darren Goossens		1930 Trivia Quiz Trevor Finlayson			
	2200		2200			